AD-A247 927

||||||||||||||||||||||||

THE RELATIONSHIP BETWEEN FUEL LUBRICITY AND DIESEL INJECTION SYSTEM WEAR

INTERIM REPORT
BFLRF No. 275

DTIC
S ELECTE
MAR 27 1992
D
D

By

P.I. Lacey
Belvoir Fuels and Lubricants Research Facility (SwRI)
Southwest Research Institute
San Antonio, Texas

Under Contract to

U.S. Army Belvoir Research, Development
and Engineering Center
Logistics Equipment Directorate
Fort Belvoir, Virginia

Contract No. DAAK70-87-C-0043

January 1992

92-07792

||||||||||||||||||||

REPORT DOCUMENTATION PAGE

1a. REPORT SECURITY CLASSIFICATION Unclassified	1b. RESTRICTIVE MARKINGS None

2a. SECURITY CLASSIFICATION AUTHORITY N/A	3. DISTRIBUTION / AVAILABILITY OF REPORT
2b. DECLASSIFICATION / DOWNGRADING SCHEDULE N/A	Approved for public release; distribution unlimited

4. PERFORMING ORGANIZATION REPORT NUMBER(S) Interim Report BFLRF No. 275	5. MONITORING ORGANIZATION REPORT NUMBER(S)

6a. NAME OF PERFORMING ORGANIZATION Belvoir Fuels and Lubricants Research Facility (SwRI)	6b. OFFICE SYMBOL (If applicable)	7a. NAME OF MONITORING ORGANIZATION

6c. ADDRESS (City, State, and ZIP Code) Southwest Research Institute 6220 Culebra Road San Antonio, Texas 78238-5166	7b. ADDRESS (City, State, and ZIP Code)

8a. NAME OF FUNDING / SPONSORING ORGANIZATION U.S. Army Belvoir Research, Development and Engineering Center	8b. OFFICE SYMBOL (If applicable) STRBE-FL	9. PROCUREMENT INSTRUMENT IDENTIFICATION NUMBER DAAK70-87-C-0043; WD 7 and 27

8c. ADDRESS (City, State, and ZIP Code)

Fort Belvoir, VA 22060-5606

10. SOURCE OF FUNDING NUMBERS

PROGRAM ELEMENT NO.	PROJECT NO.1L263001	TASK NO.	WORK UNIT ACCESSION NO.
63001	D150	07(1)	

11. TITLE (Include Security Classification)

The Relationship Between Fuel Lubricity and Diesel Injection System Wear (U)

12. PERSONAL AUTHOR(S)
Lacey, Paul I.

13a. TYPE OF REPORT Interim	13b. TIME COVERED FROM 1 Sep 90 TO 1 Nov 91	14. DATE OF REPORT (Year, Month, Day) 1992 January	15. PAGE COUNT 127

16. SUPPLEMENTARY NOTATION

17. COSATI CODES			18. SUBJECT TERMS (Continue on reverse if necessary and identify by block number)
FIELD	GROUP	SUB-GROUP	Low-Lubricity Fuel Fuel Lubricity
			Fuel Injection Pump Wear
			BOCLE Wear Maps

19. ABSTRACT (Continue on reverse if necessary and identify by block number)

Use of low-lubricity fuel may have contributed to increased failure rates associated with critical fuel injection equipment during the 1991 Operation Desert Storm. However, accurate quantitative analysis of failed components from the field is almost impossible due to the unique service history of each pump. This report details the results of pump stand tests with fuels of equal viscosity, but widely different lubricity. Baseline tests were also performed using Reference No. 2 diesel fuel. Use of poor lubricity fuel under these controlled conditions was found to greatly reduce both pump durability and engine performance. However, both improved metallurgy and fuel lubricity additives significantly reduced wear. Good correlation was obtained between standard bench tests and lightly loaded pump components. However, high contact loads on isolated components produced a more severe wear mechanism that is not well reflected by the Ball-on-Cylinder Lubricity Evaluator.

20. DISTRIBUTION / AVAILABILITY OF ABSTRACT [X] UNCLASSIFIED/UNLIMITED ☐ SAME AS RPT ☐ DTIC USERS	21. ABSTRACT SECURITY CLASSIFICATION Unclassified
22a. NAME OF RESPONSIBLE INDIVIDUAL Mr. T.C. Bowen	22b. TELEPHONE (Include Area Code) (703) 664-3576 22c. OFFICE SYMBOL STRBE-FL

DD Form 1473, JUN 86 Previous editions are obsolete.

EXECUTIVE SUMMARY

Problems and Objectives: The U.S. Army is using highly refined aviation turbine fuels in its ground tactical fleet. Such fuels commonly have both decreased viscosity and lubricity when compared to diesel. Currently, no recognized standard exists to define the lubricity requirements of the injection systems on compression ignition equipment. However, increased failure rates reported during Operation Desert Shield/Storm, as well as the results of previous bench wear tests, indicate that a problem may exist.

Importance of Project: The fuel injection system is central to the reliable operation of compression ignition engines. However, effective comparison between failed pumps returned from the field is difficult, as each unit has a unique service history. The present study details the effect of lubricity on the durability of a fuel-sensitive injection system under carefully controlled conditions.

Technical Approach: Full-scale pump stand tests were performed with fuels of similar viscosity but varying lubricity. The degree of pump wear was then compared with both standard and nonstandard bench-scale wear tests, included in previous reports. The effects of fuel viscosity on the lubrication of a critical area prone to failure were mathematically modeled, and the results confirmed using a modified pump stand test procedure.

Accomplishments: It is predicted that slightly reduced fuel viscosity will not, by itself, promote premature pump seizure. However, severe injection pump wear was produced with low-lubricity fuels. The standard Ball-on-Cylinder Lubricity Evaluator (BOCLE) test was found to be directionally correct in predicting the level of wear observed. However, the BOCLE test has some inherent weaknesses and is not universally accurate, particularly for more highly loaded contacts or possibly high-sulfur fuels.

Military Impact: The results of this study indicate that continuous use of low-lubricity fluids, such as some Jet A-1 fuels, will produce appreciable injection pump wear and a severe decrease in engine performance. However, lubricity additives and hardware modifications successfully reduce wear under the operating conditions tested. No durability problems are expected to occur with JP-8.

FOREWORD/ACKNOWLEDGMENTS

TABLES OF CONTENTS

TABLES OF CONTENTS (CONT'D)

LIST OF ILLUSTRATIONS

LIST OF TABLES

I. INTRODUCTION

Many fuels provide a limited range of contact conditions in which successful lubrication is possible. Fuel systems are designed to reflect these needs; however, seemingly minor changes in fuel composition or equipment design may significantly alter component durability. During the mid 1960s, improvements in the refining and treatment processes removed many of the compounds in aviation kerosene required for effective lubrication. Since that time, considerable effort has been expended in the study of the wear mechanisms present with low-lubricity fuels. Most of this effort has been directed towards aviation turbine fuels such as Jet A-1 (1)* and JP-8 (2), using the Ball-on-Cylinder Lubricity Evaluator (BOCLE).(3) A standard procedure to measure fuel-related wear using the BOCLE has been produced (4); nonetheless, no minimum lubricity requirement for aviation fuels currently exists.

The U.S. Department of Defense is currently procuring aviation turbine fuels for ground equipment that previously operated on diesel.(5) In addition, increasingly strict emissions regulations pertaining to compression ignition engines is causing production of more severely refined diesel fuels. Both developments are producing increased interest in the wear resistance of fuel-lubricated components. However, relatively little research has been conducted in this area, and the lubricity requirements of the diesel fuel injection system are largely undefined.

JP-8 has successfully undergone testing in both the laboratory and in field trials.(6-12) However, increased failure rates were reported for fuel-sensitive rotary injection pump components operating on Jet A-1 in Operation Desert Shield/Storm. Although Jet A-1 and JP-8 have similar viscosity and physical properties, Jet A-1 does not contain a corrosion inhibitor and has lower lubricity under most test conditions.(13) Post-failure disassembly and examination of pumps returned from the field did not allow quantitative correlation between fuel lubricity and pump durability, as each pump had a unique service history. A systematic evaluation of pump performance and fuel lubricity was required under carefully controlled laboratory conditions.(14)

---

* Underscored numbers in parentheses refer to the list of references at the end of this report.
NOTE: In the present study, the term "lubricity" is used according to the broad definition provided by Appeldoorn and Dukek (15): "If two liquids have the same viscosity, and one gives lower friction, wear, or scuffing, then it is said to have better lubricity."

1

II. OBJECTIVE

The primary objective of the program is to develop bench tests that reflect the lubricity requirements of the fuel injection system. The current report details the results obtained from carefully regulated pump stand tests performed in a laboratory. These results are then compared with data from both standard and nonstandard bench wear test procedures, and a minimum lubricity requirement is defined.

III. BACKGROUND

Following the conversion of JP-4 to JP-8 for use in U.S. and North Atlantic Treaty Organization (NATO) aircraft, the U.S. Department of Defense (DOD) has adopted the single fuel for the battlefield concept. As previously stated, JP-8 was evaluated in compression ignition engines in a range of laboratory and field tests. The engines used to evaluate the effects of JP-8 fuel included the 6V-53T and the NHC-250 engines, neither of which was adversely affected.(7,8) Indeed, the highly refined aviation kerosenes demonstrated a number of advantages (16) in that they produced less combustion chamber deposits and lubricant degradation while increasing thermal efficiency. In addition, JP-8 would eliminate winter waxing, filter plugging, and other problems associated with ground equipment operating with diesel fuel. Selected fuel specification requirements related to diesel and turbine engine performance are provided in TABLE 1.

However, a number of possible disadvantages with JP-8 compared to DF-2 were also apparent: the lower average net energy content of the light aviation fuel marginally increased fuel consumption and decreased maximum power on engines not equipped with fuel density compensation. In addition, increased wear of the rotary fuel injection pump was observed during an engine test performed with a GM 6.2L engine.(9) Subsequently, however, an engine test (10) and vehicle tests performed over approximately 10,000 miles using similar equipment demonstrated no decrease in pump durability with JP-8.(11) Similarly, JP-8 was successfully used in a large-scale demonstration in all military diesel fuel-consuming ground vehicles and

TABLE 1. Comparison of Selected Fuel Specification Requirements Related to Diesel and Turbine Engine Performance

Properties	VV-F-800D DF-A	DF-1	DF-2	DF-2 (OCONUS)*	MIL-T-5624N JP-5/NATO Code F-44	MIL-T-83133C JP-8/NATO Code F-34	ASTM D 1655 Jet A-1/NATO Code F-35
Flash Point, °C, min	38	38	52	56	60	38	38
Cloud Point, °C, max	-51	**	**	13	NR†	NR	NR
Pour Point, °C	Rpt	Rpt	Rpt	18	NR	NR	NR
Freezing Point, °C, max	NR	NR	NR	NR	-46	-47	-47
Kinematic Viscosity at 40°C, cSt	1.1 to 2.4	1.3 to 2.9	1.9 to 4.1	1.3 to 5.0(A)	NR(1.50)(B)	NR(1.25)(B)	NR(1.25)(B)
Kinematic Viscosity at -20°C, cSt, max	NR	NR	NR	NR	8.5	8.0	8.0
Distillation, °C							
10% recovered, max	NR	NR	NR	NR	205	205	205
20% recovered, max	NR	NR	NR	NR	Rpt	Rpt	Rpt
50% recovered, max	Rpt	Rpt	Rpt	NR	Rpt	Rpt	Rpt
90% recovered, max	288	288	338	357	Rpt	Rpt	Rpt
End Point, max	300	330	370	370	290	300	300
Residue, vol%, max	3	3	3	3	1.5	1.5	1.5
Carbon Residue on 10% Bottoms, wt%, max	0.10	0.15	0.35	0.2	NR	NR	NR
Sulfur, mass%, max	0.25	0.50	0.50	0.30	0.40	0.30	0.30
Cu Corrosivity							
3 hr at 50°C, max	3	3	3	1	NR	NR	NR
2 hr at 100°C, max	NR	NR	NR	NR	1	1	1
Ash, wt%, max	0.01	0.01	0.01	0.02	NR	NR	NR
Accelerated Stability, mg/100 mL, max	1.5	1.5	1.5	1.5	NR	NR	NR
Neutralization Number, mg KOH/g, max	0.05	NR	NR	0.1	0.015	0.015	0.015
Particulate Contamination, mg/L, max	10	10	10	10	1.0	1.0	1.0
Cetane Number, min	40	40	40	45	NR(42.3)(B)	NR(44.9)(B)	NR(44.9)(B)
Net Heat of Combustion							
MJ/kg, min	NR	NR	NR	NR	42.6	42.8	42.8
Btu/gal	NR	NR	NR(130,575)(B)	NR(127,776)(B)	NR(125,965)(B)	NR(123,138)(B)	NR(123,138)(B)
Corrosion Inhibitor, mg/L	NR	NR	NR	NR	QPL-25017	QPL-25017	NR
Antiicing Additive, vol%	NR	NR	NR	NR	0.15 to 0.20	0.10 to 0.15	NR
Electrical Conductivity, pS/m	NR	NR	NR	NR	NR	150-600	NR/50-450

* Meets all requirements of NATO Code F-54 Guide Specifications.
** Specified according to anticipated low ambient temperature at use location.
† NR = No Requirement.
(A) Kinematic Viscosity values given are equivalent to NATO requirement of 1.8 to 9.5 cSt at 20°C.
(B) Average value from Reference No. 17 shown for comparison purposes.

3

equipment at Fort Bliss, TX.(16) It is also noted that Jet A-1/Arctic Diesel Fuel has been used year-round in diesel-powered equipment in Alaska for many years. No immediate explanation for discrepancy between the different test programs is apparent. The relatively short test duration/average vehicle milage in each instance may have been a contributing factor.

Jet A-1 was used in diesel-fueled ground materiel assets involved in Operation Desert Shield. However, increased maintenance associated with the Stanadyne rotary fuel injection pump was again reported in this action.(18,19) During these actions, 12 Stanadyne rotary fuel injection pumps returned from the field were disassembled, and the cause of failure determined. Three additional pumps that had operated on commercial diesel were also disassembled as a baseline for comparison.(20,21) However, direct comparison is not possible between these failures with Jet A-1 and the previous studies performed using JP-8. Jet A-1 contains no lubricity additives and consists solely of kerosene fractions, while use of a corrosion inhibitor as a lubricity enhancer is now mandatory in JP-8. This corrosion inhibitor is commonly a dimeric organic acid, usually dilinoleaic acid (DLA), which curtails the high material removal rates associated with oxidative wear.

The results of the post-failure analysis indicate that most of the failures in the field may be attributed to causes other than poor fuel lubricity. Observed pump failure modes ranged from normal wear, to contamination, to catastrophic pump seizure. However, the cause of failure in three of the pumps was not evident. As a result, the possibility that low lubricity or low viscosity has a deleterious effect could not be conclusively eliminated. Furthermore, decreased wear was present in both pumps that had operated on diesel fuel or contained an improved metallurgy specifically designed for use on low-viscosity fuels. This modification is commonly known as an "arctic" kit, as it was originally designed for use with diesel fuel arctic grade (DF-A) in cold climates. However, in the present context, it would be more appropriately referred to as a low-lubricity/low-viscosity kit and is most beneficial under high ambient temperature conditions. These field results are significant in that they indicate that the durability of the standard Stanadyne pump may be lubricity dependent. As a result, the Stanadyne pump was singled out as the basis for the present study. However, it is likely that other commercially available systems may be adversely affected by low-lubricity fuels.

IV. APPROACH

A.   Summary of Technical Approach

Endurance tests were performed using a motorized pump stand to define the effects of fuel lubricity on pump durability. The test series included both standard pumps and arctic pumps that contain an improved metallurgy to allow effective comparison. Preliminary tests and calculations indicate that pump seizure was not primarily due to the decreased viscosity of the aviation fuels. As a result, the test series was designed to highlight the effects of pump degradation due to corrosive/oxidative wear and failure of the boundary film in low-lubricity fuels. To eliminate the effects of hydrodynamic/elastohydrodynamic lift, the tests were performed with fuels of varying lubricity but similar viscosity. Clay-treated Jet A-1 was used as the base fuel, and selected additives were included to provide the level of lubricity required. Baseline tests were also performed with diesel fuel for comparison. The lubricity of each fuel was carefully monitored throughout the test using the BOCLE.

Pump performance was continuously monitored so that the test could be terminated prior to catastrophic failure. Overall degradation in performance was defined by operating each pump on an engine test and a pump calibration stand both before and after each test. Pretest and post-test measurements were also taken with an unused pump to ensure that the test equipment is self consistent. Finally, each pump was completely disassembled, and qualitative and quantitative wear measurements performed. The results obtained from these measurements were correlated with both standard and nonstandard bench wear tests.

B.   Test Equipment

For this project, five standard (Model No. DB2829-4524) and five arctic fuel pumps (Model No. DB2829-4523) were procured. The arctic component corresponds to that currently used on the High Mobility Multipurpose Wheeled Vehicle (HMMWV). Both pump models are identical in configuration, but the arctic pump contains an improved metallurgy in certain critical components. A more complete description of the Stanadyne pump and a schematic diagram are

5

given in Appendix A. It should be noted that these pumps do not contain the elastomeric flex ring retainer assembly (Part No. 22940, NSN 2910-01-188-3386) that promoted many of the failures observed during Operation Desert Shield/Storm (ODS).(18,20,21) A parts changeover request was issued in June to July 1985, changing the configuration of the elastomeric flex ring assembly. Many of the failures in ODS would have been lessened if that changeover had been completed.

For ease of reference, a code number was assigned to each pump. The code number corresponding to each serial number is provided in TABLE 2.

TABLE 2. Fuel Injection Pump Code Sheet

Code No.	Pump Type	Serial No.
1	Standard	6627504
2	Arctic	6624985
3	Standard	6627505
4	Arctic	6624984
5	Standard	6627506
6	Arctic	6624983
7	Standard	6627507
8	Arctic	6624981
9	Standard	6627499
10	Arctic	6624980

The pumps were not disassembled prior to testing, and no quantitative pretest dimensional measurements were taken on individual pump components. A number of previous studies in this area have attempted to record the weight loss of parts subject to wear.(22) However, previous work at BFLRF with Stanadyne pumps has indicated that accurate post-test measurements are possible using surface profilometry.(20,21)

Prior to testing, each pump was placed on a test stand, and the fuel delivery and injection timing were precisely calibrated in accordance with the manufacturer's specifications.(23) Complete descriptions of the calibration procedure, results, and manufacturer's tolerances are provided in Appendix B. The operating characteristics of each pump were then precisely recorded, as some tolerance is built into the manufacturer's specifications. These results were maintained for comparison with similar measurements taken after completion of the pump stand tests. Ultimately, however, engine performance is the definitive test of pump operation. Injection timing, fuel delivery, and well-defined cut-off points in the injection cycle, all combine to produce an efficient combustion process. These characteristics were evaluated on a GM 6.2L engine both before and after each pump stand test.

The parameters measured included fuel consumption, brake horsepower, and exhaust temperature. A more complete description of the engine test procedure is provided in Appendix C.

Each of the pumps produced very similar engine power curves prior to testing, as depicted in Figs. 1a and 1b for the standard and arctic pumps, respectively. The engine power produced with Jet A-1 (conforming to ASTM D 1655 (1), Lab No. AL-19346-F) in the new pumps is approximately 12 percent lower than with diesel fuel (VV-F-800D) (24) over the complete speed range. The net heat of combustion for the Jet A-1 fuel is 34 MJ/L compared with 36 MJ/L for the diesel fuel, corresponding to a 5-percent decrease. In addition, fuel delivery for each pump on Jet A-1 is reduced by approximately 6 percent compared to diesel, as shown in Figs. C-9 to C-27 in Appendix C. The decrease in pump delivery is probably caused by increased leakage around the pumping plungers, due to the relatively low viscosity of Jet A-1.

After these initial measurements were taken, no modifications or adjustments were made to the pumps until completion of the test series and subsequent evaluation on both the calibration stand and engine.

An arctic and a standard pump were tested simultaneously on a Unitest stand with a common fuel supply as depicted in Fig. 2. To ensure a realistic test environment, the mounting arrangement and drive gear duplicate that of the GM 6.2L engine. For this study, 250 gallons of test fuel were maintained in an enclosed reservoir and were continuously recirculated throughout the duration of each test. A centrifugal supply pump provided a positive head of 3 psi at the inlet to the test pumps. A primary (sock) filter (AC Part No. T935) and a cartridge filter corresponding to that used on the 6.2L engine in the HMMWV (GM Part No. 14075347) were used to remove wear debris and particulate contamination. Finally, a 5-kW explosion-resistant circulation heater produced the required fuel inlet temperature. The heater has a relatively low watt density of 15 W/in.^{2} to minimize fuel degradation due to flash heating, and a 40-liter (11-gal.) reservoir was placed in line after the heater to ensure that the fuel supply temperature remained stable as the thermostat cycled. Each pump was fully insulated using rockwool to ensure that the temperature of the complete unit is similar to that of the incoming fuel.

a. Standard Pump

b. Arctic Pump
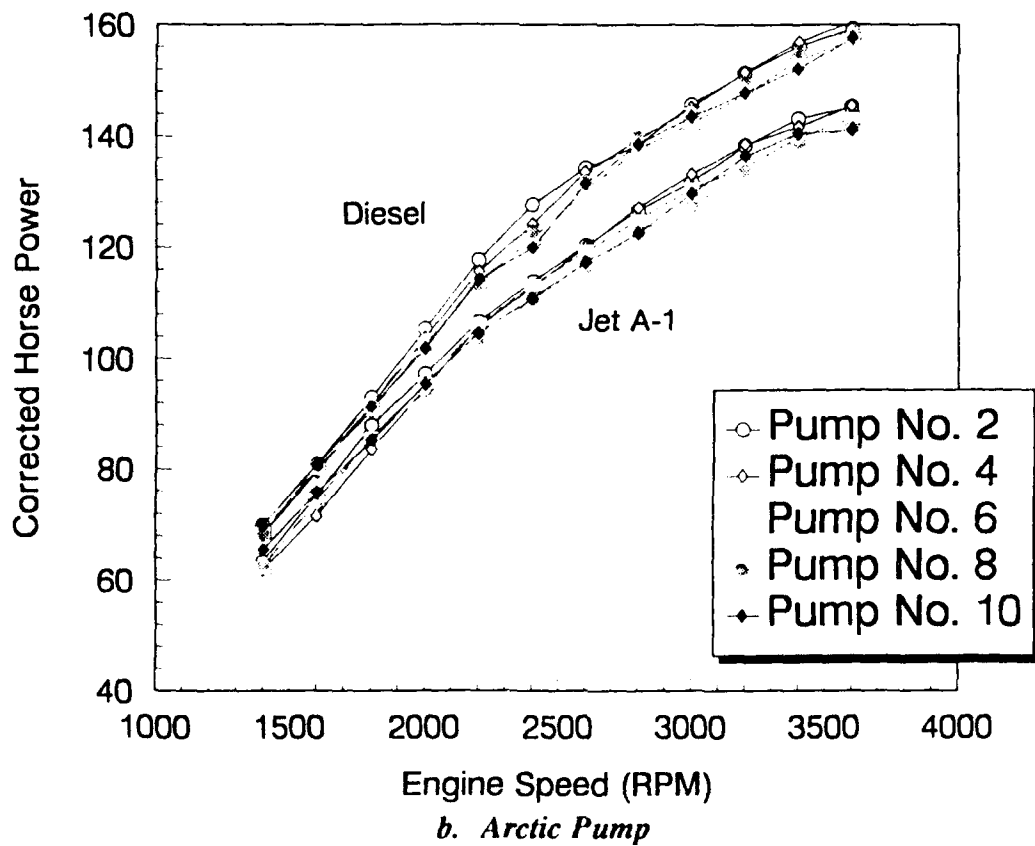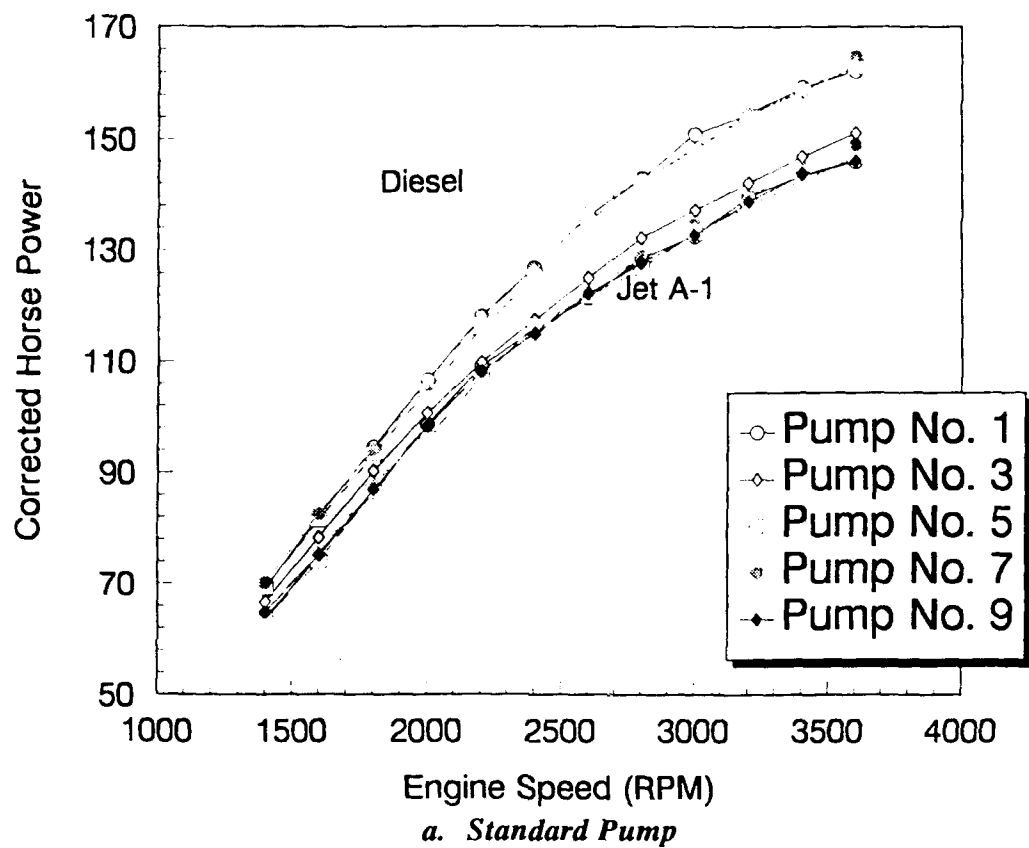
Figure 1. <u>Brake horsepower with test pumps prior to testing</u>

8
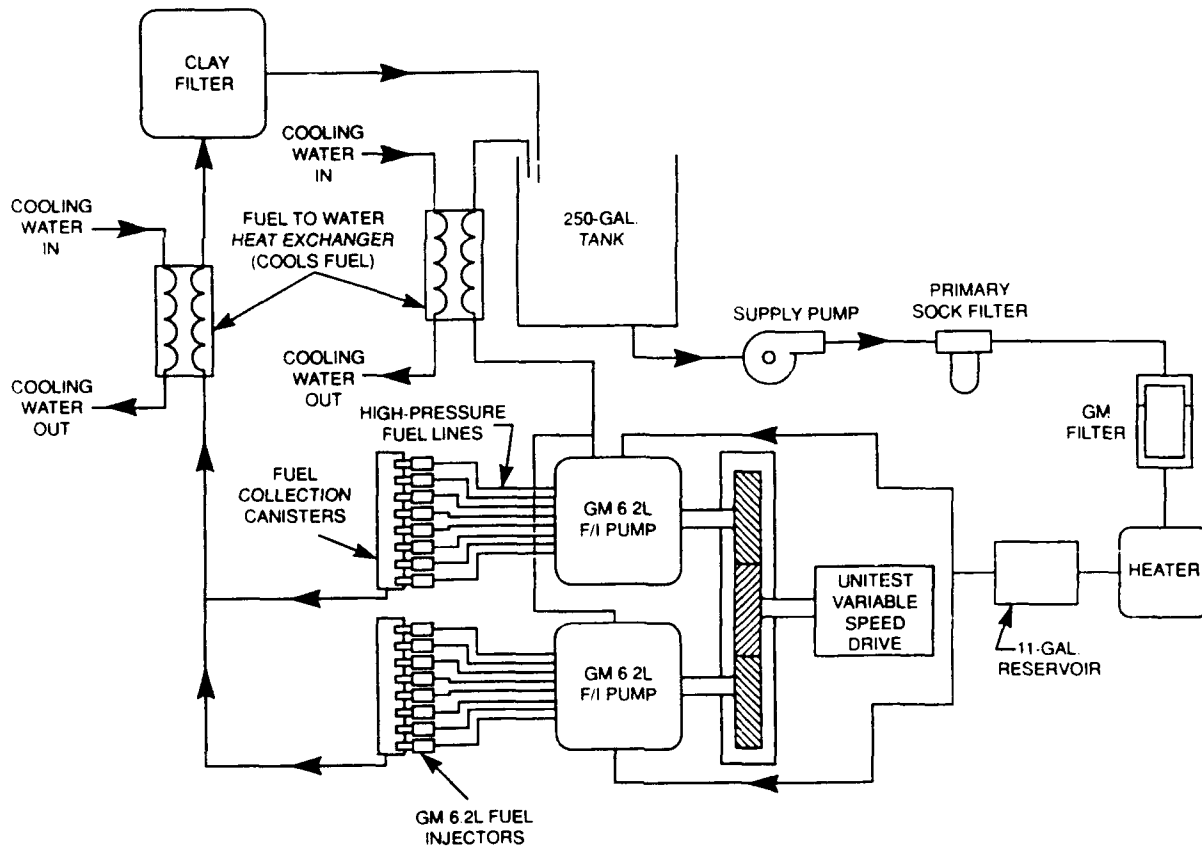
Figure 2. Fuel system schematic

The high-pressure outlets from the pumps were connected to eight NA52X fuel injectors from a GM 6.2L engine, assembled in a collection canister. Fuel from both canisters was then returned to the bulk storage tank via a common return line. A separate line to the bulk storage tank was used to carry excess fuel from the governor housing. Fuel-to-water heat exchangers on both the return lines from the injector canisters and the governor housing controlled the temperature of the fuel. J-type thermocouples were placed at the inlet side of each pump and in the bulk storage tank. The temperature of the fuel reservoir was maintained below the minimum flash point of Jet A-1 (given in Appendix D) to minimize evaporation of the lighter fractions in the fuel. A pressure gauge was placed at the inlet to each pump, and a separate tool was manufactured to allow continuous measurement of the internal transfer pump pressure during normal operation.

C. Test Fuels

The test fuels and their treatment are the single most important aspect of the test methodology. Fuel viscosity, chemical composition, cleanliness (both particulate and chemical), and moisture content will each affect the test results. Jet A-1 conforming to ASTM D 1655 (1) was used as the base fuel, and selected additives were used to provide the required level of lubricity. This highly refined fuel is similar to DF-A diesel used in arctic conditions and, in many ways, reflects the reformulated diesel fuels expected to appear on the commercial market in the near future, i.e., the fuel contains both low sulfur and low aromatics.

A more complete description of the physical and chemical properties of the fuel used is included in Appendix D. The results of a previous world survey to define the effective viscosity range available in aviation kerosene fuels are given in Fig. 3.(17) The fuel selected has a viscosity of only 1.07×10^{-6} m^2/s at 40°C, which is close to the minimum available. This value corresponds to approximately 0.68×10^{-6} m^2/s at 76°C and is well below the minimum fuel inlet viscosity of 1.2×10^{-6} m^2/s (at pump inlet temperature) recommended by the pump manufacturer.(25) As a result, hydrodynamic and elastohydrodynamic bearing lift should be minimized, thereby producing increased metallic contact and boundary wear.

The theoretical lubricity of each fuel/additive combination was defined using the BOCLE wear test, with the results provided in TABLE 3. In this test, the average wear scar diameter (WSD) formed between counterformal specimens is taken as an indicator of fuel lubricity. It should be noted that a number of different procedures for the BOCLE have been used through the years, which will provide different and possibly contradictory test results.(3) The BOCLE results provided in the present study were derived in accordance with the procedure detailed in ASTM D 5001-89.(4) The Jet A-1 base fuel produces a wear scar of 0.72 mm in diameter, which is believed to be representative of this fuel type. However, some commercially available highly refined Jet A-1 fuels produce a wear scar of up to 0.8 mm. The DCI-4A additive was previously shown to improve lubricity (26) and reduces the diameter of the BOCLE wear scar produced with

---

NOTE: The viscosity of many diesel fuels interchanged under NATO Code No. F-54 will also be less than 1.2×10^{-6} m^2/s at 76°C.
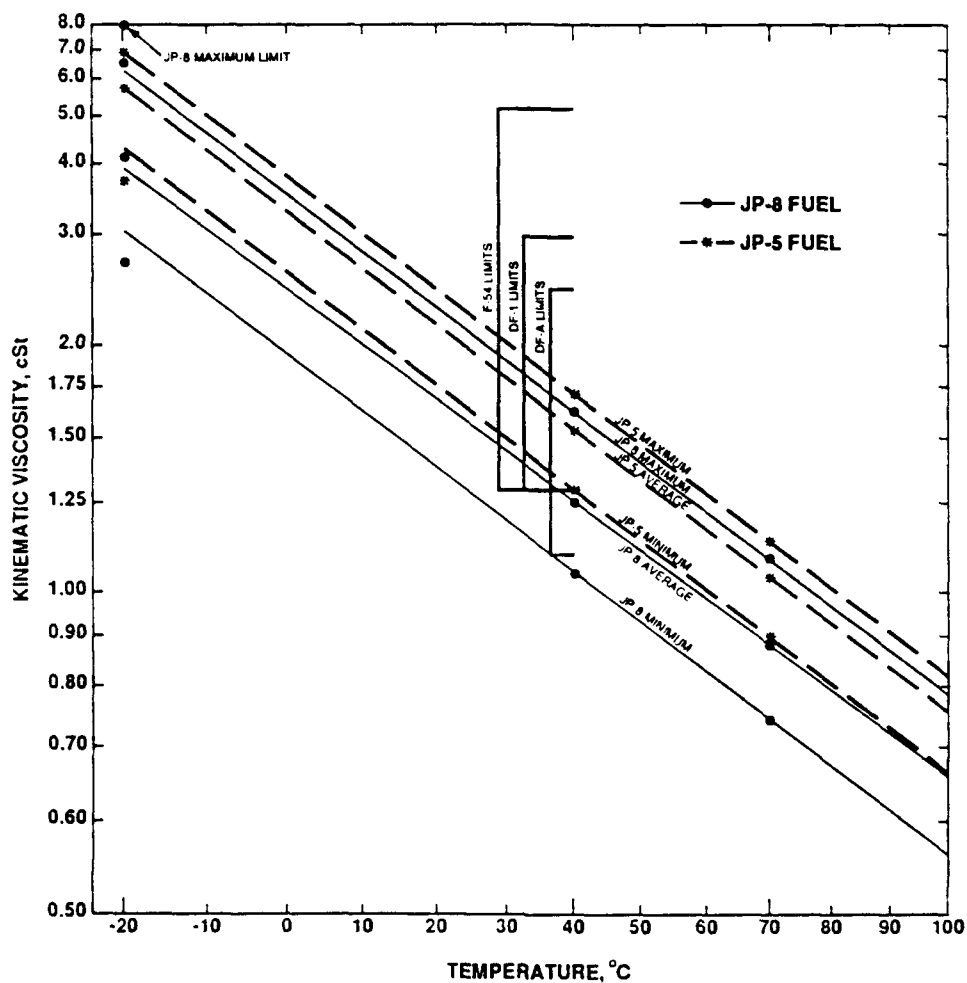
[Derived from a survey of 91 fuel samples from around the world.(17)]

Figure 3. Viscosity temperature relationships of JP-8/Jet A-1/DF-2

TABLE 3. Additives Used in Pump Stand Tests

Pump No.	Fuel	Additive	Concentration, mg/L	BOCLE Result, Average WSD (mm)
1	Jet A-1	None	--	0.72
2	Jet A-1	None	--	0.72
3	Jet A-1	MIL-I-25017—DCI-4A	15	0.58
4	Jet A-1	MIL-I-25017—DCI-4A	15	0.58
5	Jet A-1	MIL-S-53021—BIOBOR-JF/FOA-15	227/71	0.37
6	Jet A-1	MIL-S-53021—BIOBOR-JF/FOA-15	227/71	0.37
7	Ref. No. 2 DF*	None	--	0.56
8	Ref. No. 2 DF*	None	--	0.56

* Test fuel used in Caterpillar 1-H2 lubricants test.

11

clay-treated Jet A-1 to 0.58 mm from its original value of 0.72 mm.* The BIOBOR-JF/FOA-15 additive combination was shown to greatly reduce wear under **lightly loaded conditions** to a level similar to that seen with formulated engine lubricants.(13) This additive combination produces a BOCLE wear scar diameter of only 0.37 mm; however, nonstandard wear tests indicate that it may be less effective under more severe contact conditions. Baseline tests were also performed with Reference No. 2 diesel fuel (Cat 1-H), conforming to Federal Specification VV-F-800D.(24) This fuel has a kinematic viscosity of 3×10^{-6} m^2/s at 40°C, which is appreciably greater than that of the Jet A-1 fuel previously described. The remaining physical and chemical characteristics of the diesel fuel are provided in Appendix D.

V. PRELIMINARY TESTS AND CALCULATIONS

A. Requirement for Preliminary Tests

The surface protection provided by a fuel is not a unique characteristic, but rather is highly dependent on the test environment and mechanical configuration. The selection of the optimum laboratory test to accurately, yet rapidly, simulate field conditions is necessarily a compromise among competing variables.

The pump manufacturers routinely perform pump stand tests under both continuous and intermittent conditions.(27) They also indicate that the effects of poor lubricity on boundary lubricated wear are most likely to be highlighted by continuous operation at maximum rated pump speed, i.e., maximum sliding distance. However, the fuel pump and injection components perform under a variety of contact geometries, pressures, and velocities to cover lubrication conditions from boundary to fully developed hydrodynamic film. Formation of such a film is a dynamic process and depends on continuous relative motion, correct clearances, and sufficient viscosity to prevent excessive fluid flow. Furthermore, catastrophic failure commonly occurs due

---

* Jet A-1 containing the DCI-4A corrosion inhibitor additive conforms to MIL-I-25017 (28) and is effectively similar to JP-8, as defined in MIL-T-83133C, without the antistatic and antiicing additives.(2) BIOBOR-JF/FOA-15 is qualified under MIL-S-53021 (29), as a biocide for use in diesel fuels meeting the requirements of VV-F-800 intended for intermediate or long-term storage.(30)

to rupture of the hydrodynamic film around the pump rotor with subsequent seizure close to the transfer pump section.(20,21) Such seizures may be attributed to a number of causes, including excessive side loading in the transfer pump, insufficient viscosity of the Jet A-1 fuel, or rapid changes in pump temperature.(31) The relative importance of this failure mechanism and its relationship to fuel lubricity are presently undefined.

B. Evaluation of the Hydrodynamic Film Supporting the Pump Rotor

The pump rotor is suspended by a hydrodynamic film and effectively forms a journal bearing within the pump housing. The hydrodynamic film thickness is a function of the Sommerfeld number for the contact, which may be derived from the bearing geometry and conditions as provided in Equation 1 below. Bearing eccentricity may then be obtained by consulting appropriate tables.(32,33)

$$ S = \left(\frac{r}{c}\right)^2 \left(\frac{\mu N}{P}\right) \qquad \text{(Eq. 1)} $$

Where: r = Journal radius (0.0115 m)

c = Radial clearance (2.54 × 10⁻⁶ m)

μ = Viscosity of fuel **inside** bearing $\left(\frac{Ns}{m^2}\right)$

N = Speed (rps)

P = Average bearing pressure $\left(\frac{N}{m^2}\right)$

The calculated minimum film thickness (h) for the rotor on the Stanadyne DB2 pump is plotted in Fig. 4, as a function of kinematic viscosity. The results are plotted for a transfer pump pressure of 130 psi, which is the maximum recommended by Stanadyne.(34) The calculated minimum film thickness for a transfer pump pressure of 300 psi is also given, as this is the maximum pressure achieved in laboratory tests described later in the report. Low-speed operation will decrease the hydrodynamic film strength, however, a concomitant decrease in transfer pump pressure and resulting bearing load will occur under normal operation.
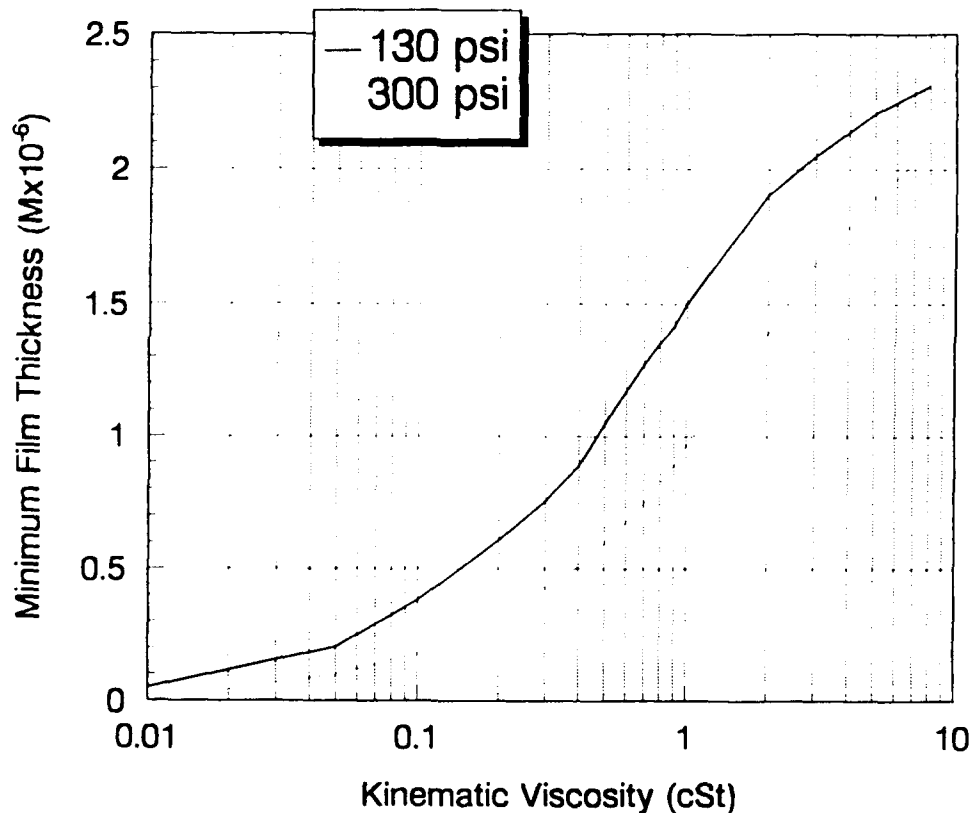
Figure 4. Minimum film thickness (h) predicted to occur around the rotor of the Stanadyne DB2 pump at 1800 rpm

It should be noted that the kinematic viscosity applies to the fuel in the bearing and will be marginally less than that of the incoming fuel, due to energy dissipation and increased temperature due to fluid shear. The temperature rise within the bearing is itself a function of fuel viscosity (and so temperature) and will be approximately 10° and 15°C for Jet A-1 and diesel respectively, at a fuel inlet temperature of 80°C. An appreciably greater temperature rise will occur at low fuel inlet temperatures, particularly with diesel fuel.

Asperity contact will occur before the theoretical film thickness becomes zero, due to the inherent roughness of the opposing surfaces. The degree of separation (λ) may be defined from the ratio of the minimum distance between the mean lines of the opposing surface profiles (h) to the composite surface roughness (σ), as defined in Equation 2.

14

$$\lambda = \frac{h}{\sqrt{\sigma_1 + \sigma_2}} \tag{Eq. 2}$$

The surface roughness of the opposing pump parts was measured using a Talysurf 10 surface profilometer, with a cut-off wavelength of 0.8 mm, over a profile length of 8 mm. The Root Mean Square (RMS) surface roughness of the Stanadyne pump rotor (σ_1) and housing (σ_2) was measured to be 0.12 and 0.15 μm, respectively. In each instance, the measured profile had a skewness and kurtosis close to 0 and 3.5 and so approximate Gaussian random height distributions. For Gaussian surfaces, if λ is greater than 2.5 to 3, then the opposing components may be considered to be completely separated. Values lower than approximately 1.5 will produce severe interasperity contact and probable seizure. As a result, the minimum distance between the rotor and housing on the Stanadyne pump must be greater than approximately 0.48 μm.

The minimum film thickness predicted to exist at a fuel temperature of 90°C is approximately 1.3 and 1.55 μm for the lowest viscosity Jet A-1 commercially available and a typical diesel fuel respectively, as defined in Fig. 3. This worst case example still produced relatively little decrease in hydrodynamic film thickness due to use of Jet A-1 and would indicate that most seizures must be promoted by increased loading transmitted from another section of the pump. Significantly, both the Jet A-1 and diesel fuels produce a Sommerfeld number that is optimized to produce minimum friction and carry maximum load.(33)

The addition of engine oils to the fuel will produce a slight increase in overall viscosity, as shown in Fig. 5. The net increase in hydrodynamic film thickness caused by the addition of reasonable concentrations (<5 vol%) is only a few percent. However, it should be recognized that the addition of such fluids may affect the inherent lubricity of the fuel.
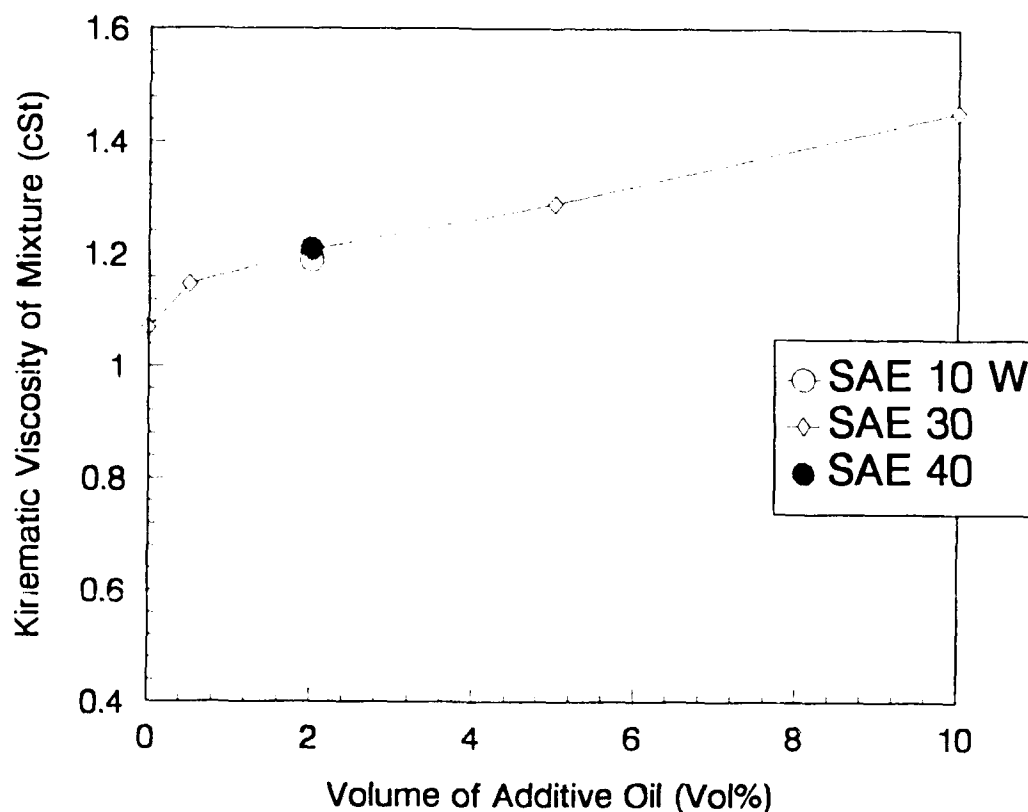
Figure 5. **Kinematic viscosity of Jet A-1/engine oil mixtures**

The previous analysis indicates that seizure of the pump rotor should not occur during normal operation with a very low viscosity Jet A-1. However, effects such as partial misalignment, differential expansion, film whirl, and variation in component geometry may reduce the effective load-carrying capacity of the bearing. For this reason, a number of preliminary wear tests were performed to evaluate the effective strength of the hydrodynamic film formed around the pump rotor, with both neat Jet A-1 and diesel. These tests were performed at 38°C (100°F) and 1800 rpm, which is the maximum specified pump operating speed. Reconditioned Stanadyne DB2 pumps were used due to the relatively short and destructive nature of the test.

The side loading on the pump rotor was affected by increasing the transfer pump pressure. The positive displacement vane-type transfer pump consists of a stationary eccentric liner and spring-loaded blades that are carried in slots at the end of the pump rotor. During normal operation, the required volume of fuel passes to the high-pressure head via the metering valve, while the

NOTE: A more complete description of the transfer pump operation may be found in Reference 20.

remainder is recirculated by means of the transfer pump regulator to the inlet side of the transfer pump. During these preliminary tests, the metering valve was fully closed to minimize fuel flow from the transfer pump. A purpose-made tool was then employed to adjust the transfer pump pressure regulator while the pump was running. The transfer pump pressure was increased in 10-psi increments every 10 minutes until either failure occurred or the pressure regulator was fully closed.

As predicted by the model, pump failure did not occur at an ultimate pressure in excess of 300 psi, with any of three different pump units. The maximum transfer pump pressure specified by the manufacturer is 130 psi.(34) The test series was repeated at 93°C (200°F). The transfer pump pressure achieved decreased at higher temperatures, probably due to increased fuel leakage past the pump vanes and metering valve. Again, none of the pumps failed.

The interfacial film produced by hydrodynamic or elastohydrodynamic lubrication will be lost at low sliding speeds. A short test series was performed using intermittent pump operation at 38°C (100°F). During these tests, the pump was cycled from stationary to full speed over a period of approximately 5 seconds and subsequently decelerated over a similar period. Both the metering valve and the transfer pump regulator were fully closed throughout the test, producing a concomitant rise in transfer pump pressure to 300 psi. This procedure was repeated for one hour without pump seizure. Clearly, extended operation at these artificial conditions will produce severe wear: however, both theory and practical testing indicate that the fluid film around the pump rotor appears sufficient to prevent intermetallic contact and seizure during normal operation.

C.   Effects of Rapid Temperature Changes on Pump Operation

Good sealing of the pumping chambers depends on the close clearances of the elements. After a period of brief shutdown, the temperature of the already-hot fuel injection equipment will be further increased by heat soak-back from the engine, reducing the fuel viscosity so much that leakage may make restarting impossible until the system has cooled down.(35) It has been

17

reported that during Operation De'ert Shield/Storm (36), the fuel injection pumps were occasionally cooled with water to assist with hot restarts.

Close tolerances are required to maintain an effective hydrodynamic film with low-viscosity fluids. Rapid changes in fluid temperature may reduce the clearance between the pump rotor and hydraulic head, due to differential expansion: hot fuel entering a cold pump will increase the temperature of the pump rotor more quickly than the surrounding metal, due to its relatively small thermal mass. In theory, a mean temperature difference of only 20°C between the pump housing and rotor will reduce the 2.5-μm radial clearance between the components to zero, resulting in instant seizure (coefficient of thermal expansion = 10.8 $\mu m/m°C$. It is easily shown that the pump rotor may not be inserted into the housing if such a temperature differential exists.

During practical operation, the temperature of the pump is likely to increase uniformly. For this reason, preliminary tests were performed to determine the importance of this failure mechanism and the effects of fuel lubricity/viscosity. The fuel system schematic shown in Fig. 3 was modified to allow instantaneous changes in fuel in' . ...iperature. Two supply lines provided fuel at either ambient temperature or hot fuel from the regular supply system. A recirculation loop was included to prevent a "dead leg" in the supply line and ensure that hot fuel was available immediately at the pump.

Reconditioned pumps were again used in this test series. Each pump was initially operated at 900 rpm with fuel at ambient temperature (T_a). After stabilizing for 15 minutes, the hot fuel was provided, **without stopping the pump.** The temperature of the hot fuel (T_h) was set at 10°F above ambient for the first run. The complete procedure was repeated with the temperature of the hot fuel raised in 10°F (5.5°C) increments until pump seizure occurred. This procedure was performed with both Cat 1-H diesel fuel and Jet A-1, with the results provided in TABLE 4.

TABLE 4. Fuel Inlet Temperature
Required for Pump Seizure

Test No.	Jet A-1			Diesel		
	1	2	3	4	5	6
T_a	70	70	100	75	80	63
T_h	200	200	175	205	207	210
ΔT	130	130	75	130	127	147

The temperature change (ΔT) required to produce seizure was approximately 130°F (70°C) for both diesel and Jet A-1. Pump No. 3 failed at a lower temperature differential than the remaining pumps, probably due to random variation. After a soak-down period, the fuel temperature in the engine bay of a recently operated vehicle is expected to attain at least 205°F (96°C). Clearly, seizure will occur if the pump is artificially cooled under these conditions.

VI. MAIN TEST PROCEDURE

A. Pump Stand Test Procedure

It was previously demonstrated that the hydrodynamic film around the pump rotor is unlikely to fail during normal operation. As a result, the test series was designed to maximize material removal due to corrosive/oxidative wear and failure of the boundary lubricating film in the remainder of the pump.

Archards wear coefficient indicates that the volume of wear materials is proportional to both sliding distance and load.(37) As a result, fuel-related wear per unit time is likely to be greatest at maximum rated pump speed and wide open throttle (neglecting the effects of hydrodynamic lift). Reduced throttle settings may marginally increase the contact loading in the transfer pump but will greatly decrease the stress on the high-pressure pumping plungers. Where possible, the pumps were operated continuously for 24 hours per day. This continuous operation reduced variation between pumps due to the warm-up cycle. Occasionally, however, regular 8-hour shifts were necessary due to scheduling requirements. The type of operation seen by each pump during

its 200-hour cycle is depicted in Fig. 6. The vertical lines denote a single halt in continuous operation, i.e., at weekends.
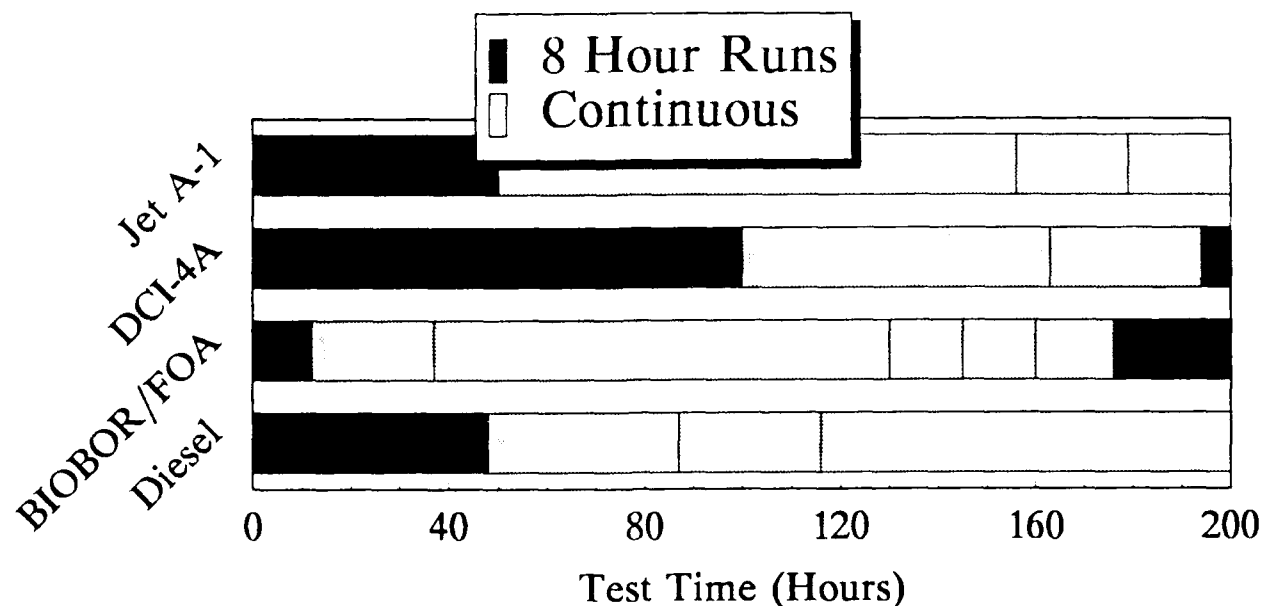
(Note: the vertical lines denote a single halt in continuous operation.)

Figure 6. Operating schedule used during each pump series

Wear with low-lubricity fluids is greatly increased by the presence of moisture.([13]) The ambient temperature and humidity during each of the tests are given in TABLE 5 and should be more than sufficient to promote severe oxidative/corrosive wear. The fuel inlet temperature to each pump was maintained at 170°F (77°C) throughout each test series, which reflects the approximate

TABLE 5. Ambient Conditions During Pump Stand Tests

	Temperature, °C		Relative Humidity, %	
	Mean	Std Dev	Mean	Range
Neat Jet A-1	71.1	7.44	63.1	--
Jet A-1 + DCI-4A	75.0	7.43	67.6	14.6
Jet A-1 + BIOBOR-JF/FOA-15	86.0	7.63	60.4	15.7
Diesel	83.0	6.60	69.9	13.0

temperature expected to exist during practical operation at an ambient temperature of 120°F (49°C).(38) The following parameters were continuously monitored so that the test could be halted prior to catastrophic failure: fuel delivery, transfer pump pressure, fuel inlet pressure, fuel inlet temperature. However, no pump failures occurred, and no adjustments or modifications were made to any of the pumps during the test period.

Low-lubricity fuels are especially susceptible to contamination. Prior to each test, the complete fuel system was disassembled and rinsed with a mixture of 90-percent toluene/10-percent methanol. The system was then rinsed with approximately 10 gallons of the fuel to be used in the subsequent test series. To ensure that the system was completely clean, BOCLE tests were performed on fuel samples removed from the test system. If an increase in lubricity was observed relative to the baseline fuel, the cleaning procedure was repeated. To minimize cross contamination between successive tests, the fuels were used in order of increasing lubricity and level of refinement, i.e., neat Jet A-1, followed by Jet A-1 + DCI-4A, Jet A-1 + BIOBOR-JF/FOA-15, and Cat 1-H diesel.

Wear scar measurements performed with the BOCLE indicated that the lubricity of the new and unused fuel had improved from the as-received value of 0.72 mm to approximately 0.63 mm. Such variation is probably due to a combination of accidental contamination and free radical oxidation mechanisms that occur during storage.(39) As a result, the Jet A-1 fuel was clay treated immediately prior to the inclusion of additives and subsequent use. The clay-treating process used in the current study did not produce an unreal or artificial fuel. The lubricity of the clay-treated fuel as measured in both the BOCLE and in wear maps* was not significantly different from the clean fuel as initially delivered, as shown in Fig. 7. The Cat 1-H diesel fuel was not clay treated, as this would have removed naturally occurring compounds customarily found in such fuels.

Continuous recycling of the fuel during the pump stand tests places an unusual stress on the fuel, which is likely to produce thermal and oxidative degradation. The Jet A-1 fuel with no additive

---

* NOTE: A more complete description of the wear mapping procedure and test methodology may be obtained in Reference 13.
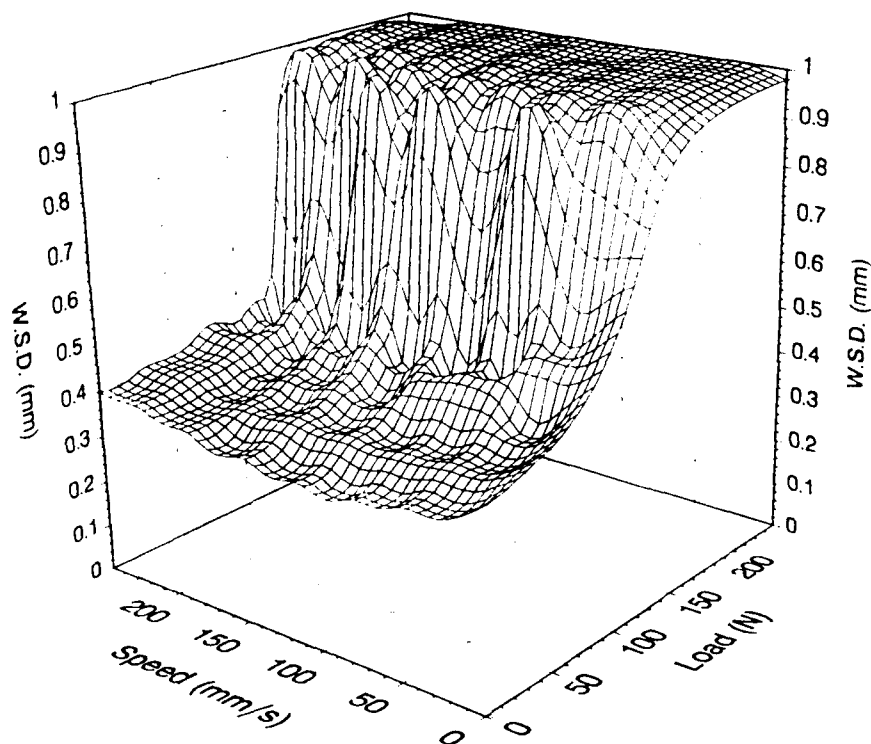
a. As Initially Received (Prior to Aging or Contamination)
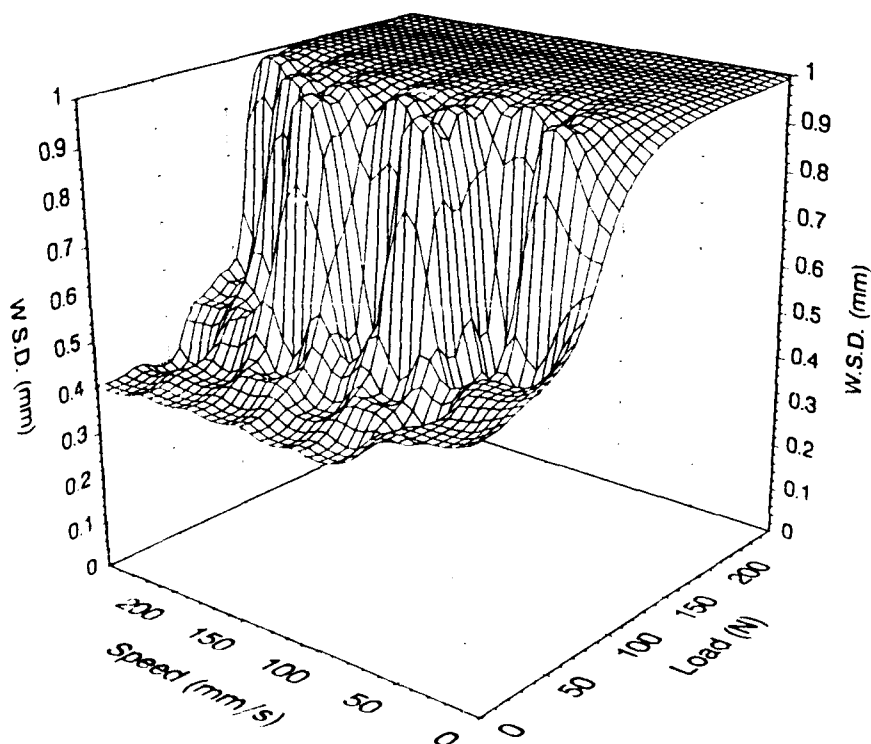
b. After Clay Treatment, Prior to Use

Figure 7. <u>Wear maps for Jet A-1 fuel</u>

was clay treated continuously throughout the pump test to remove possible reactive products.Only the fuel that passed through the injectors was clay treated. The fuel return from the governor housing to the tank was not clay treated, as this is a normal function that exists on the vehicle. The additized Jet A-1 could not be continuously clay treated (**NOTE:** It was clay treated before use); however, reactive degradation products are less likely to have a measurable effect on better lubricity fuels. Nonetheless, samples of fuel were taken from the pump stand every 20 hours of testing and lubricity tests performed using the BOCLE. No variation in lubricity was observed for any test, as shown in Fig. 8. It is recognized that a once-through fuel cycle is the optimum solution, but was not practical for the present study.
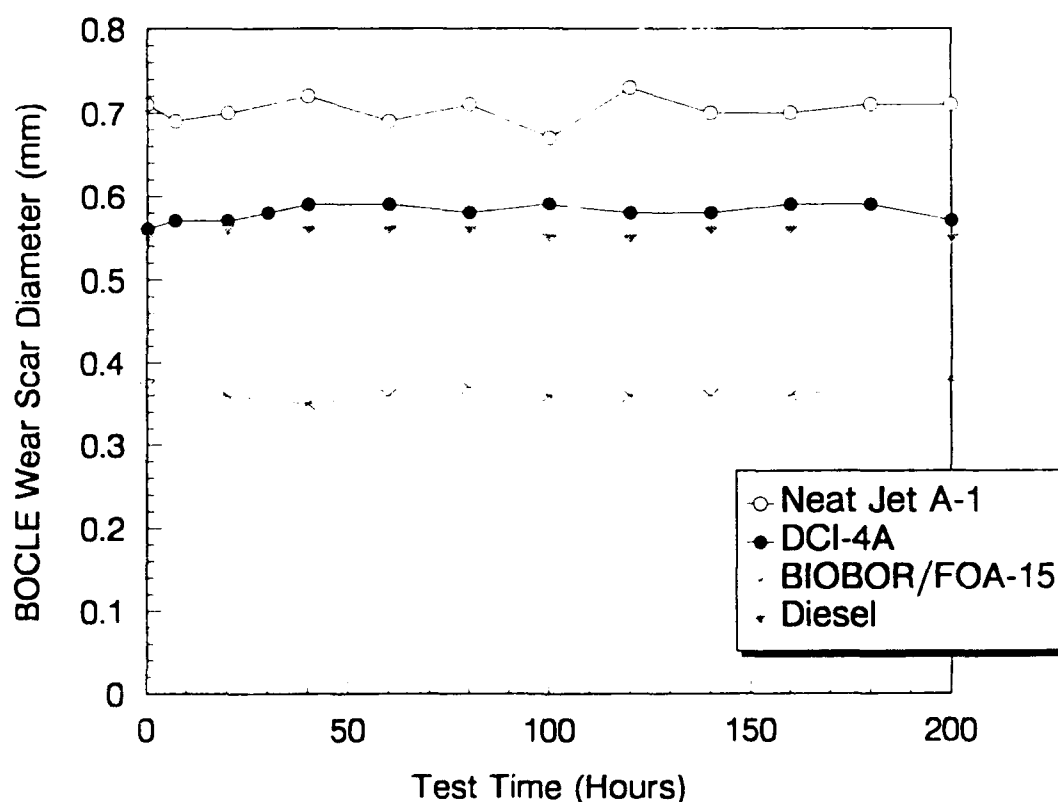
Figure 8. Fuel lubricity as a function of pump stand test duration

A significant amount of debris was observed in the fuel storage tank during the 200-hour test using neat Jet A-1. The particulate matter was not suspended in the fuel but was clearly visible on the bottom of the tank. Similar debris was found around the magnetic field created by the solenoid in the governor housing. X-ray analysis of the powder from the fuel tank indicated that it consisted primarily of iron with some copper and zinc present. Aluminum, silicon, and calcium

were only present at trace levels. The wear debris was probably transferred to the fuel reservoir via the return from the governor housing, as a clay filter was placed on the return line from the fuel injectors. A large volume of debris accumulated at the primary sock filter at the inlet side of the pump, while significantly less was visible in the secondary GM filter. As a result, it is unlikely that much of the debris reentered the pumps to cause cross contamination between the arctic and standard units. However, it is likely that the hard metallic oxide debris contributed to abrasive wear immediately after formation. A similar fuel return system is present on most vehicles to allow an accumulation of work-hardened wear debris in the fuel tank during practical operation.

The transfer pump pressures measured during each 200-hour test are shown in Appendix E and summarized in Fig. 9. This area of the pump has previously been observed to be affected by use of low-lubricity fuels.(20,21) A relatively large decrease in pressure occurred with neat Jet A-1, while the reduction was approximately halved by lubricity additives. Most variation

(Measured with each fuel on pump test stand.)
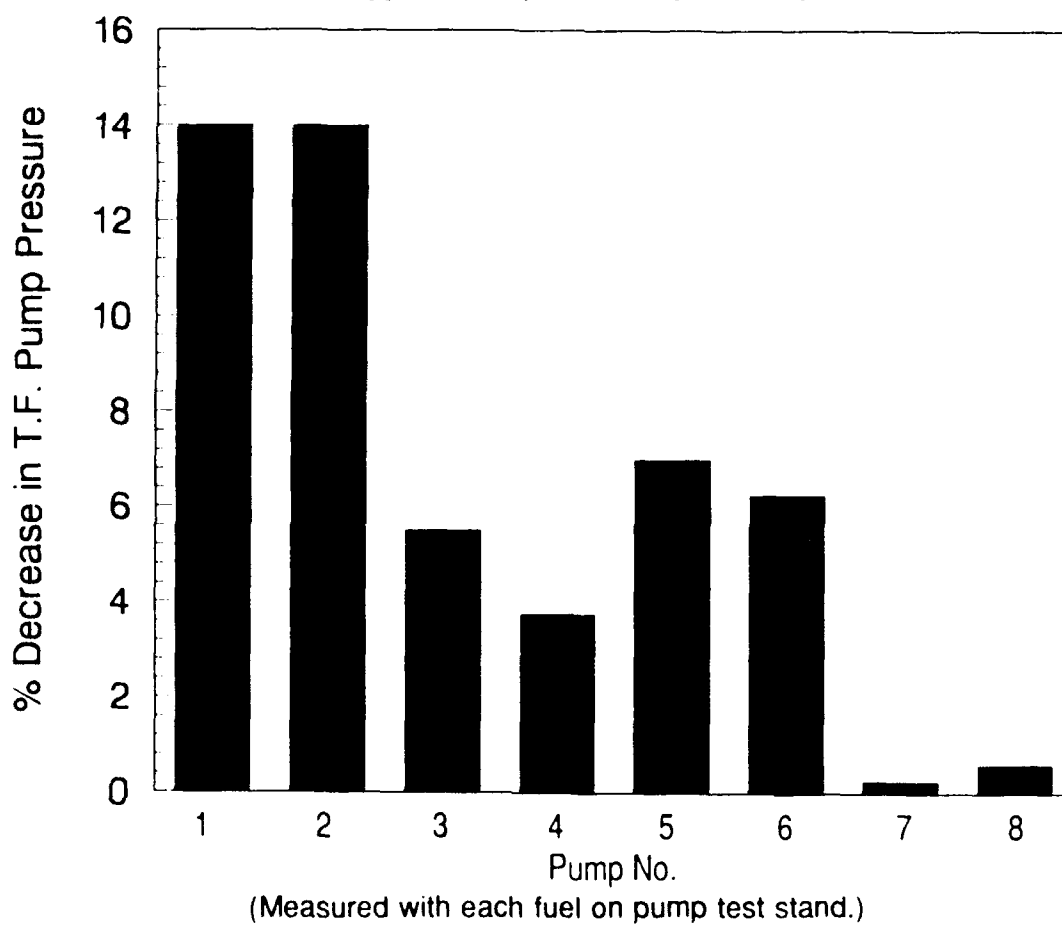
Figure 9. Percentage change in transfer pump pressure

occurred during the first 80 hours of testing, with little change occurring towards the end of the test. The arctic components appear to have had no effect on the observed decrease in transfer pump pressure. Almost no variation in pressure was observed with diesel fuel, even though its lubricity (as measured using the BOCLE) is significantly poorer than that of jet fuel with the BIOBOR-JF/FOA-15 additive package. This result is probably due to the increased viscosity of the diesel fuel, producing both slightly greater hydrodynamic lift and also resisting fuel flow around partially worn components. The pump delivery measured during the 200-hour test was erratic and dependent on fuel temperature. No conclusive results could be drawn from the data, so it is not included in the present report. No evidence of significant wear or degradation of the fuel injectors was observed during any of the 200-hour tests, and the pump pressure required to open the fuel injectors remained constant at the required 1900 psi (nozzle opening pressure). As a result, the same injector components were used throughout the complete test series. Examination of the injector pintles using optical microscopy indicated that relatively mild wear was present after 800 cumulative hours of operation. However, during this study, the injectors were simply mounted in a collection canister; the higher temperatures generated during combustion would probably accelerate the wear process.

B.   Engine Tests

After completion of the 200-hour test cycle, each pump was placed on the same GM 6.2L engine that had been used to derive the pretest power curves. A set of post-test power curves was generated for each pump with **both** Jet A-1 and Cat 1-H diesel, according to the procedure detailed in Appendix C. A reference pump (Pump No. 9) that was not used during the 200-hour tests was also evaluated to ensure that the power output of the engine remained constant. In each instance, the jet fuel was treated with the same additive as had been used during the 200-hour test with that pump. This procedure prevents unintentional surface damage during the 6-hour engine test sequence, while also ensuring that the fuel maintains the same friction characteristics that were present during the 200-hour test. For Pump Nos. 7 and 8, which had operated on diesel during the 200-hour test, the Jet A-1 fuel was treated using BIOBOR-JF/FOA-15. No additive was used with Pump Nos. 1 and 2 or for any of the power curves with diesel fuel.

25

The complete power curve for each pump is provided in Appendix C, while the average change in power output over the entire speed range is summarized in Fig. 10. In each instance, the results are corrected to standard temperature and pressure and are relative to the **same** fuel prior to testing. **The decrease in power for engine tests with low-viscosity jet fuels will be approximately 12 percent greater than the values provided in Fig. 10 when compared with the pretest results on diesel fuel (i.e., see Fig. 1).**
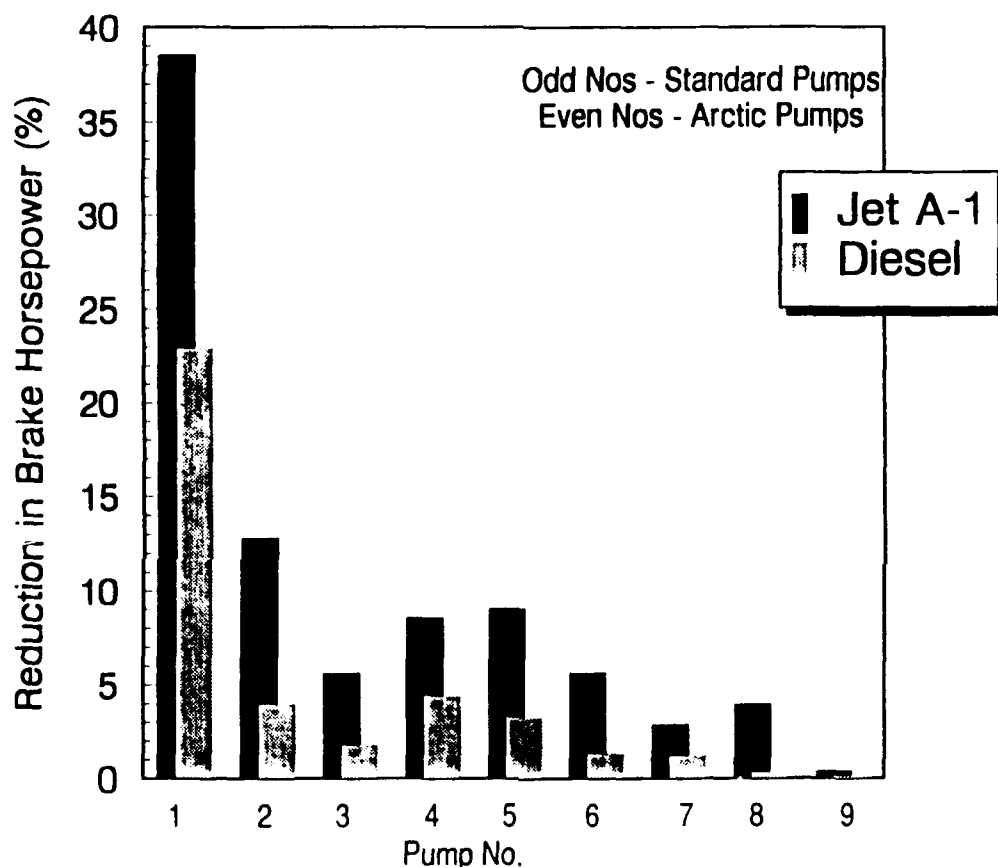
Figure 10. Relative reduction in brake horsepower caused by the 200-hour test

Engine power with Pump No. 1 (operated with Jet A-1 during the 200-hour test) is very significantly reduced when compared with the pretest measurements. Moreover, the relative decrease in power is greater when the pump is operated on Jet A-1 rather than diesel fuel, probably due to internal pump leakage. To confirm these results, the power curve with Pump No. 1 was repeated after the condition of the engine was verified using Pump No. 9 (the reference pump). However, engine power was similarly reduced in the repeat tests. The reduced energy content of Jet A-1 will have no influence on the plotted results, which are relative to the pretest values with the same fuel.

A smaller but measurable decrease in power occurred for each of the remaining pumps (relative to the pretest result with the same fuel), including Pump No. 2, which is an arctic pump tested for 200 hours on Jet A-1. Once again, the relative decrease in power output is greatest (approximately 5 to 10 percent) when the pumps were evaluated with Jet A-1, compared to diesel fuel (<5 percent). The average maximum power output for Pump Nos. 2 to 8 on **Jet A-1** after testing is 132 horsepower, compared to an average of 160 horsepower with **diesel.** This decrease corresponds to an average total decrease in power output of 19 percent on Jet A-1 compared to diesel, irrespective of the fuel used during the 200-hour pump test. Pump Nos. 7 and 8, which operated for 200 hours with diesel fuel, appear marginally better than the remaining units, even when operated with Jet A-1. Use of arctic components did not appear to significantly affect pump performance (as measured by power output) with better lubricity fuels.

The fuel delivery rate measured during the engine test for each pump is given in Appendix C. The decrease in pump delivery relative to the pretest value with the **same** fuel is summarized in Fig. 11. The fuel delivery with each of the tested pumps (Pump Nos. 1 to 8) is reduced by
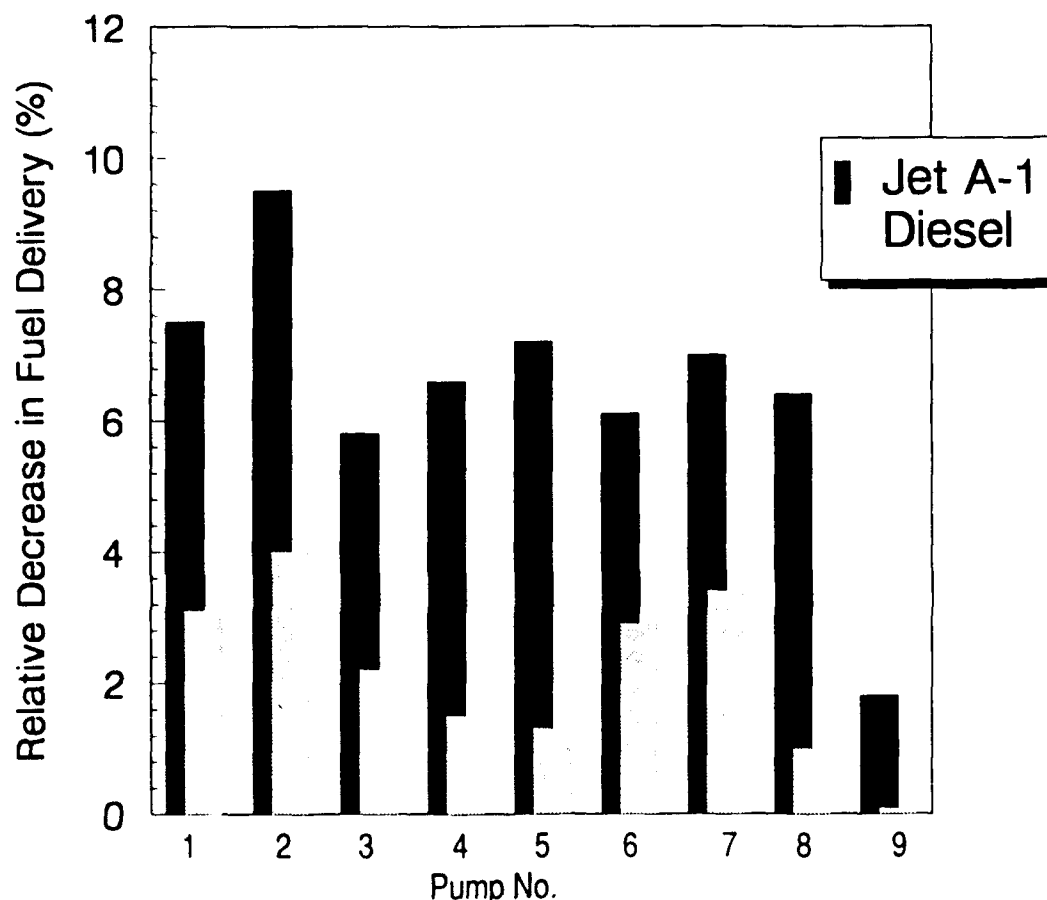

Figure 11. Decrease in pump delivery measured on engine test stand

approximately 7 percent with Jet A-1 and 2 percent with diesel, from the pretest values with the same fuel. These results closely reflect the reduction in horsepower previously noted on most pumps. However, the large decrease in power output of Pump No. 1 is not solely due to a reduction in fuel flow. The overall result is a gross reduction in engine efficiency with Pump No. 1, as reflected in the Brake Specific Fuel Consumption (BSFC) presented in Appendix C.

Fuel flow from each of the pumps with Jet A-1 was originally an additional 6 percent less than diesel prior to testing the pumps for 200 hours. The cumulative reduction in fuel delivery noted for each pump on Jet A-1 is probably due to increased fuel leakage around the pumping plungers and the decrease in transfer pump pressure noted in Fig. 9. These results are contrary to a previous study that noted a net increase in fuel delivery during a 210-hour engine test.(40) The increased delivery in the previous study was probably due to wear or increased flexure of the leaf spring that limits the movement of the pumping plunger. However, it is believed that minor design modifications have since been made to limit this variation.

Increased drive play is ar; arent on Pump No. 1. The angular freedom of the input shaft of each pump was measured using a dial gauge, with the results given in TABLE 6. Clearly, the drive tang and rotor slot on Pump No. 1 are severely worn and will result in delayed injection timing. Significantly less play is present on the remaining pumps. It should be noted that the results provided in TABLE 6 refer to play in the drive train to the pump and are half the effective retardation at the crank shaft.

TABLE 6. Angular Freedom of Pump Drive Due to Tang/Slot Wear

| Pump No.	Drive Play, deg
1	4.50
2	0.46
3	0.38
4	0.37
5	0.70
6	0.22
7	0.29
8	0.27

The luminosity caused by ignition of the fuel during the combustion cycle was measured through the glowplug port using a photo transducer, and the relative position of top dead center located

using a magnetic inductive pickup. These results were recorded at an engine speed of 1400 rpm with Pump No. 1 (standard pump/neat Jet A-1) using a digital oscilloscope. Similar measurements were taken using Pump No. 9 as a baseline for comparison, with the results shown in Fig. 12.

The detonation point for Pump No. 1 is approximately 14 degrees later than the reference pump, which ignited at top dead center. Thus, ignition retardation is marginally greater than predicted by measurements taken from the pump (given in TABLE 6 and later in Fig. 15). Furthermore, final completion of the combustion process is delayed by approximately 70 degrees of crank rotation, and the mixture is still burning after the exhaust valve has opened. The average exhaust gas temperature immediately after discharge is plotted in Appendix C, as a function of engine speed for both the pretest and post-test engine runs. The percentage change in exhaust temperature caused by the 200-hour test is summarized in Fig. 13 for each pump. An increase in temperature was observed for Pump No. 1, when operated on both diesel and Jet A-1. The increase was especially significant at higher speeds, to produce a maximum temperature of 1560°F (848°C) at 3600 rpm with diesel. Extended operation under these conditions would almost certainly promote engine failure. **In general, the exhaust temperature with Jet A-1 is approximately 180°F (100°C) less than that produced with diesel, both before and after the 200-hour test sequence.**

C.   Pump Calibration Stand

After completion of the engine tests, each pump was retested on a calibration stand. The pump characteristics were measured at the conditions recommended by the manufacturer (23), which repeat those made prior to testing. Both the pretest and post-test results are provided in Appendix B. The standard calibration fluid (viscor) has a viscosity of between 2.45 and 2.75 cSt at 40°C and produces a wear scar diameter of 0.6 mm in the standard BOCLE test, which is similar to diesel fuel. However, it should be noted that the fuel inlet temperature specified for the pump calibration procedure (23) is only 110° to 115°F (43° to 46°C) compared to 170°F (77°C) during the pump stand tests. Similarly, high temperatures are expected to exist within the
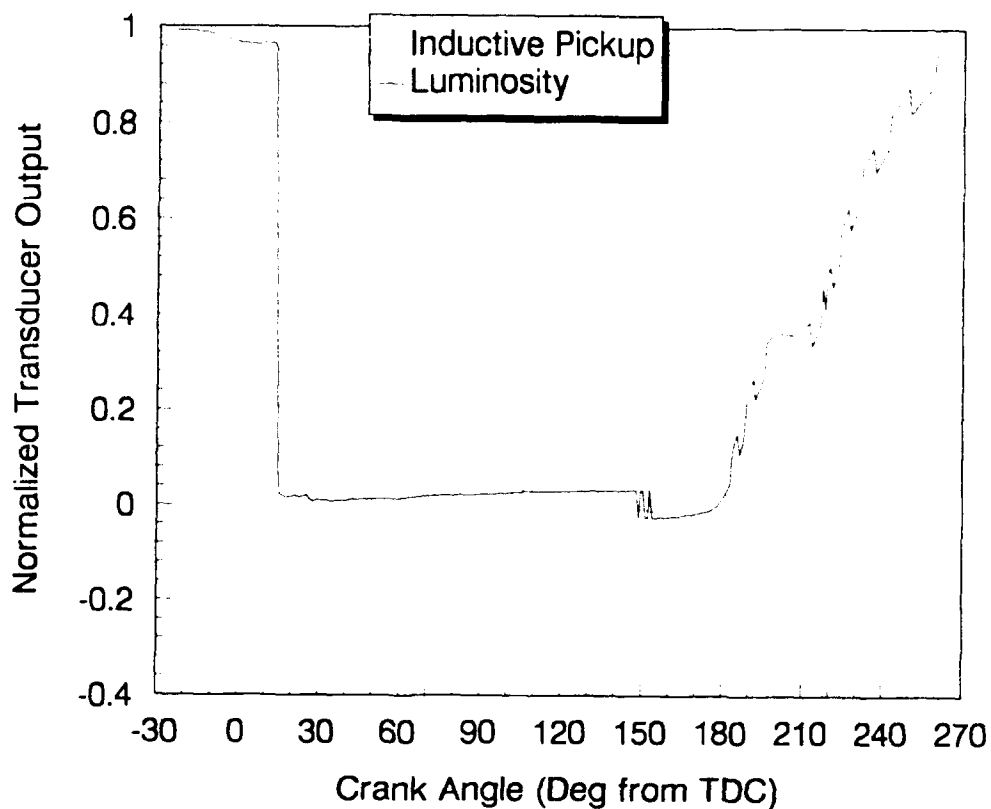
a. Pump No. 1 (Standard Pump/Neat Jet A-1)
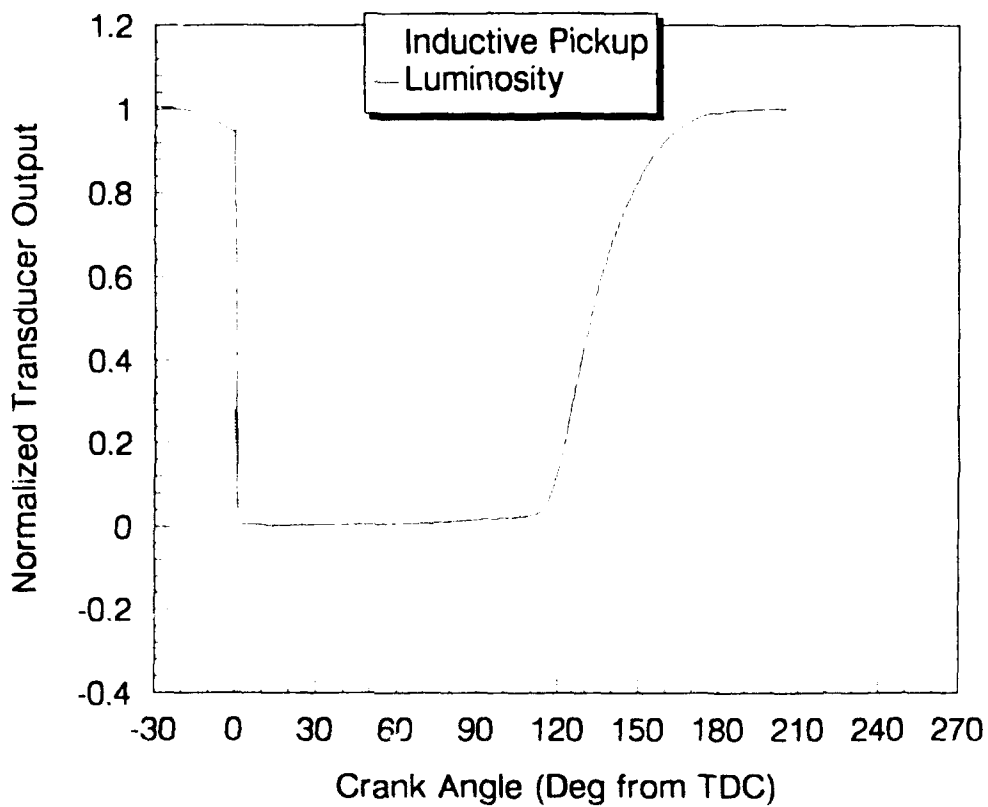
b. Pump No. 9 (Reference Pump)
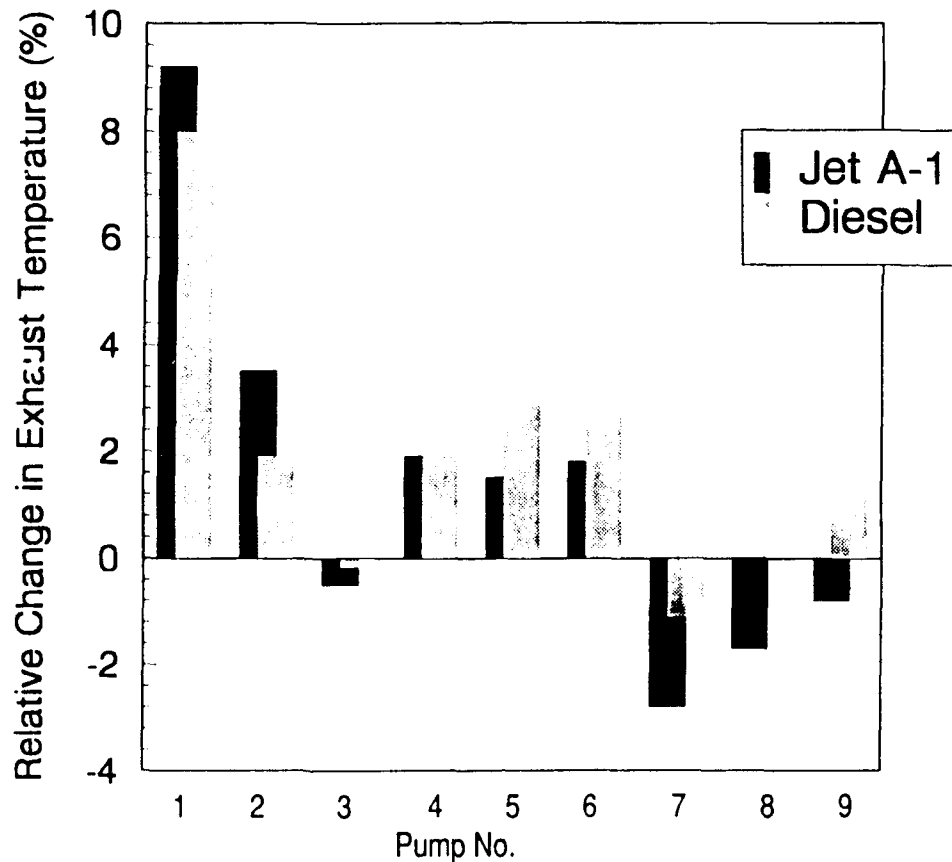
Figure 12. <u>Combustion luminosity</u>

Figure 13. **Relative change in exhaust temperature**

pump during the engine test sequence. The viscosity of the jet fuel used in the present work is reduced to approximately 0.68 cSt at 170°F, and it is unlikely that the calibration stand will completely reflect the pump performance with low-viscosity fuels at high temperature.

The position of the cam ring advance mechanism was measured using a "bat wing gauge." This result defines the motion of the cam ring relative to the pump body and so is not affected by drive tang wear.* Measurements were taken at 1000 and 1600 pump rpm [as specified by the manufacturer (23)] with broadly similar results in each instance, as shown in Fig. 14. Little variation was observed for Pump Nos. 7 and 8 (which operated on diesel fuel), or Pump No. 9, which is the reference pump. Pump Nos. 1, 2, 4, and 5 were each approximately 2 degrees retarded (measured at the crank shaft) at 2000 engine rpm (1000 pump rpm), while Pump No. 1

---

* **NOTE:** In practice. an alternative timing procedure, commonly known as air timing, is available that does account for drive tang wear.
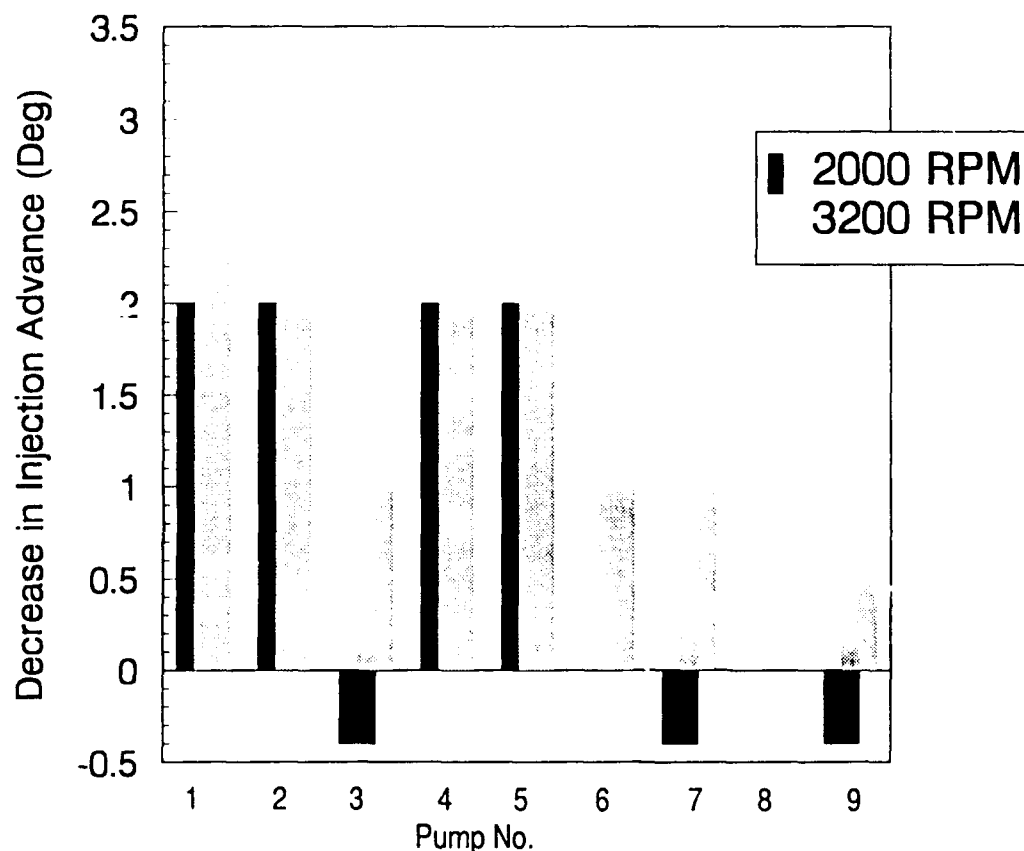
Figure 14. Variation in ignition advance caused by 200-hour pump stand test

was 3 engine degrees retarded at 3200 engine rpm. Particular attention was given to Pump No. 1 (standard pump that operated on neat Jet A-1), which produced retarded injection when tested on the engine. The injection advance curves for both Pump Nos. 1 and 9 (reference pump) were recorded on the pump calibration stand as a function of speed, with the results shown in Fig. 15. Clearly, Pump No. 1 is several degrees retarded over the complete speed range relative to the reference pump. This discrepancy, combined with the severe drive tang wear (TABLE 6), produced retarded fuel ignition and contributed to the overall poor performance of Pump No. 1.

The percentage reduction in transfer pump pressure at 1000 rpm (2000 engine rpm) is depicted in Fig. 16 and closely resembles the measurements taken on the test stand during the 200-hour test. Again, Pump Nos. and 2 show the greatest decrease and are now out of specification by 4 psi and 2 psi, respectively. The remaining pumps are all within specification at 1000 pump
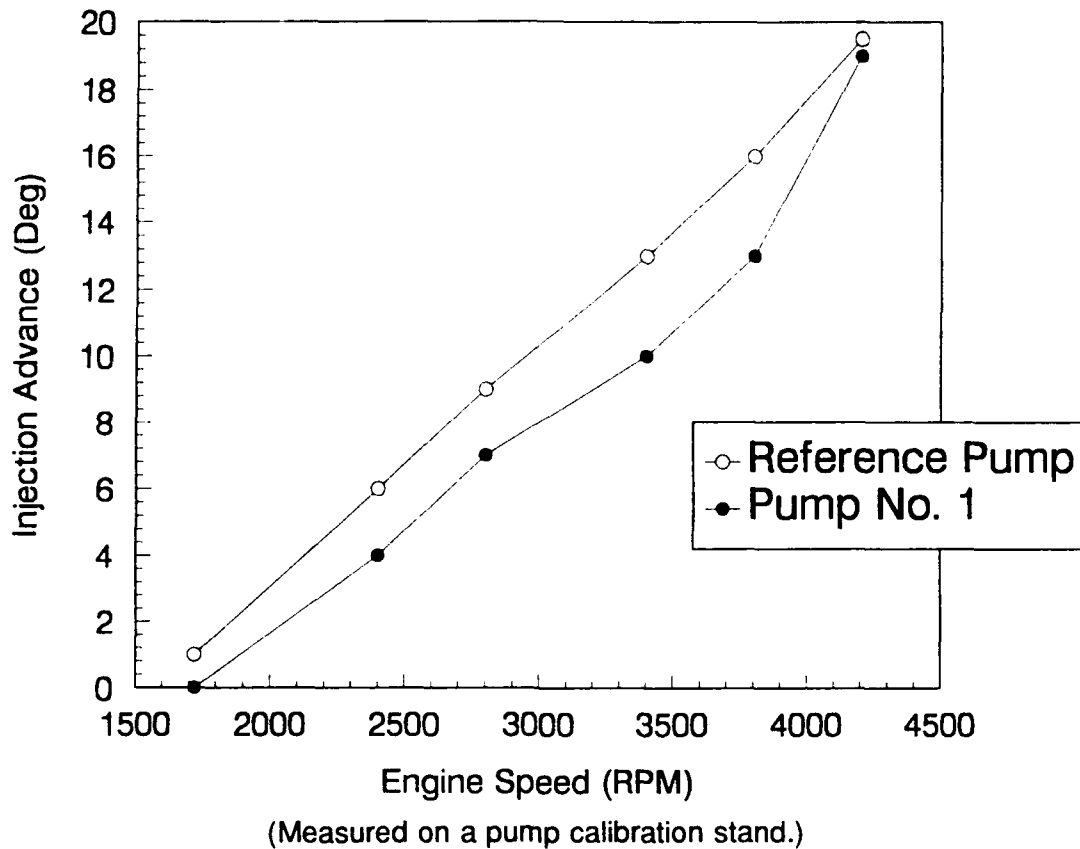
32

Figure 15. **Injection advance characteristics of Pump No. 1 and a reference pump**

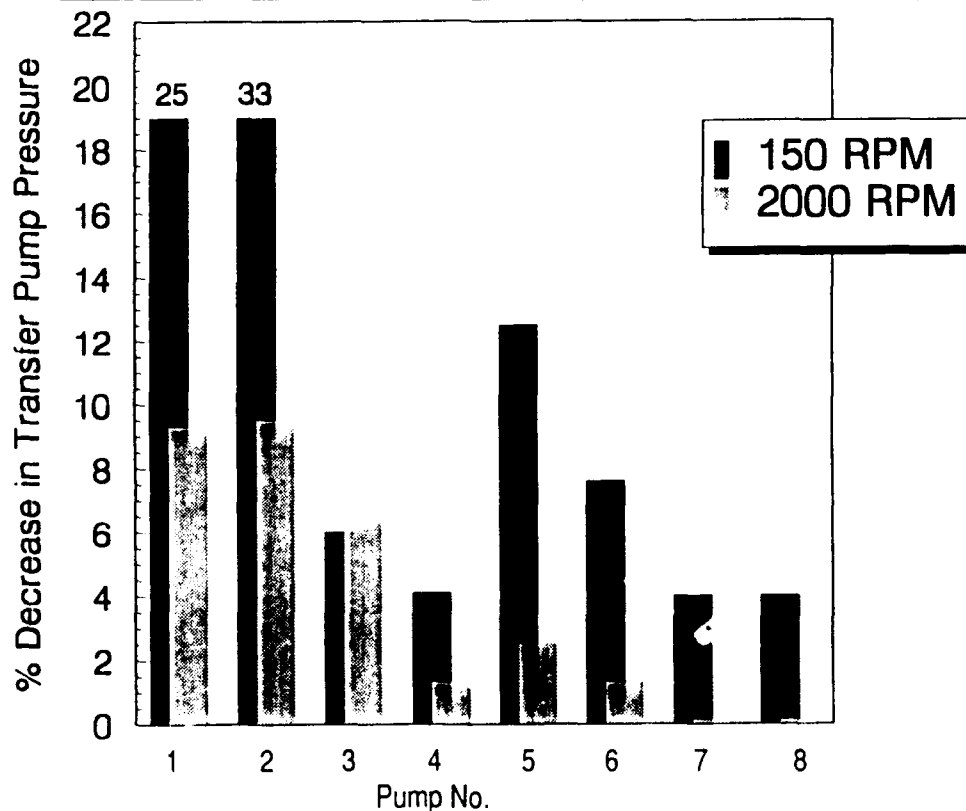**Figure 16.** **Percentage decrease in transfer pump pressure on calibration stand**

33

rpm. A proportionally greater decrease in performance was observed at 75 pump rpm, which corresponds to the cranking speed for the engine, although the same overall trends are present. None of the pumps are outside the manufacturer's specifications with the viscor test fluid at this lower speed. However, use of low viscosity Jet A-1 at higher temperature is likely to produce a further reduction in pressure.

A decrease in overall pump delivery was observed for each pump, as summarized in Fig. 17. A smaller decrease in fuel flow was also reported for the reference pump (Pump No. 9), indicating a slight bias error in the results. As expected, the reduction in delivery at higher speeds (>200 pump rpm) is considerably less than that observed with Jet A-1 measured during the engine tests (Fig. 11). However, at cranking speed (150 pump rpm) pump delivery is down by an average of 5 percent. Such low-speed operation partially compensates for the increased viscosity of the test fluid and allows fuel to leak around the pumping mechanism. However, the
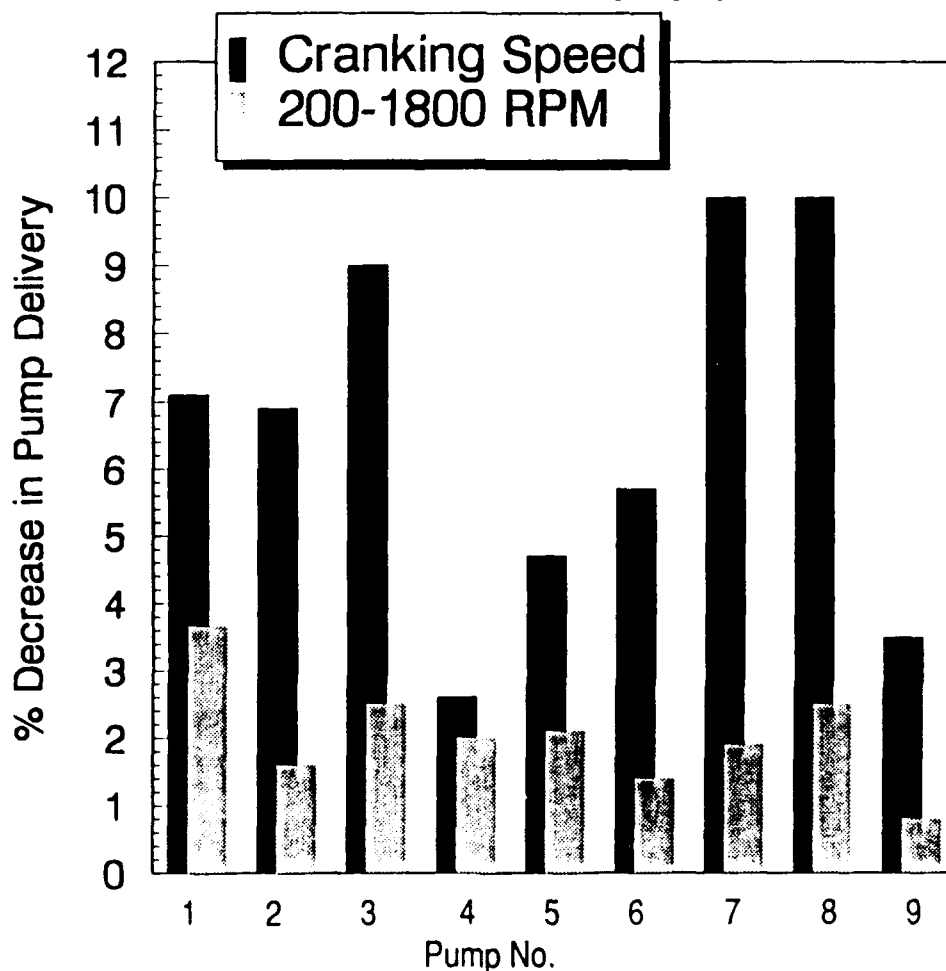

Figure 17. Percentage decrease in overall pump delivery on calibration stand

delivery of each pump remains within the manufacturer's recommended tolerances. Once again, however, use of low-viscosity Jet A-1 at higher temperatures is likely to produce a further reduction in fuel delivery at cranking speeds.

No correlation between the reduced delivery and test fuel lubricity or viscosity is apparent. Indeed, Pump Nos. 7 and 8, which operated on diesel fuel during the 200-hour test sequence, suffered similar degradation to the remaining pumps.

VII. WEAR MEASUREMENT AND PUMP DISASSEMBLY

A. Wear Measurement

The post-test pump operating characteristics described in the previous sections are a complex function of the degradation and wear processes distributed throughout the pump. Some components, such as the drive tang, will have a direct effect on the perceived operation of the pump. Wear of other components, such as the transfer pump vanes, may not be evident until a critical level is reached. In addition, effective correlation of pump durability with the results from bench tests requires accurate measurement of wear throughout the pump. Similarly, consideration of pump performance, although important, would neglect the information contained in the noncritical pump components.

Particular attention was given to areas of the pump previously demonstrated to be susceptible to wear when used with low-lubricity fuels.[20,21] Furthermore, the metallurgy in many of these components is upgraded in the arctic kit, facilitating quantitative comparison between the standard and arctic pumps. The following components were selected and include a wide range of contact conditions:

|	
a. Transfer pump blades	e. Governor weights
b. Drive tang	f. Cam roller shoe
c. Drive slot	g. Rotor retainers
d. Governor sleeve thrust washer	

B. Description of Pump Wear

The wear volume ($mm^3 \times 10^{-3}$) measured in each instance is summarized in TABLE 7. The dimensions of each wear scar were normally defined from surface profiles taken using a Talysurf profilometer, although optical microscopy was also used in some instances. A more complete description of the wear measurement procedures and results obtained is provided in Appendix F.

TABLE 7. Wear Volume on Selected Pump Components ($mm^3 \times 10^{-3}$)
(NOTE: Bold text denotes arctic components with improved metallurgy.)

|	Pump Blades	Drive Tang	Drive Slot	Thrust Washer	Governor Weights	Roller Shoe	Rotor Retainers
Pump No. 1	26	11000	14000	372	408	470	2112
Pump No. 2	**1.7**	**43**	**48**	**274**	264	1160	3300
Pump No. 3	4.9	147	112	145	132	19	1188
Pump No. 4	**2.9**	**28**	**60**	**192**	96	30	1188
Pump No. 5	5.7	3100	496	50	36	9	528
Pump No. 6	**1.8**	**38**	**59**	93	72	77	924
Pump No. 7	7.1	101	31	--	36	38	99
Pump No. 8	**2.4**	**5**	**36**	135	36	24	132

Clearly, a wide variation in the severity of the wear process exists among the components selected for quantitative wear measurement. Most pump components are lightly loaded and produced a corrosive wear mechanism with low-lubricity fuels that formed a polished surface topography, as shown in Fig. 18 for selected thrust washers. The inside of the aluminum housing on both the arctic and standard pumps that operated on neat Jet A-1 contained a brown rust deposit, while the pumps that operated on additized Jet A-1 are relatively clean, as shown in Figs. 19a and 19b, respectively. X-ray analysis confirmed that his deposit was primarily iron with some nickel, zinc, copper, and chrome.
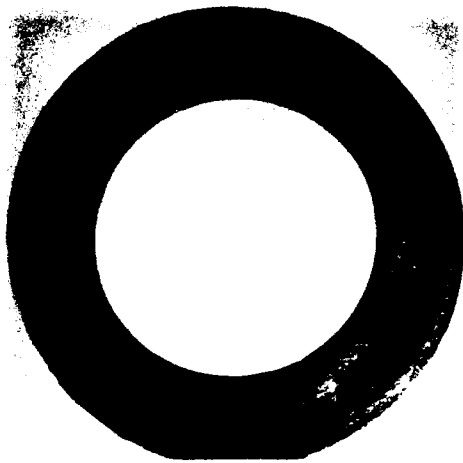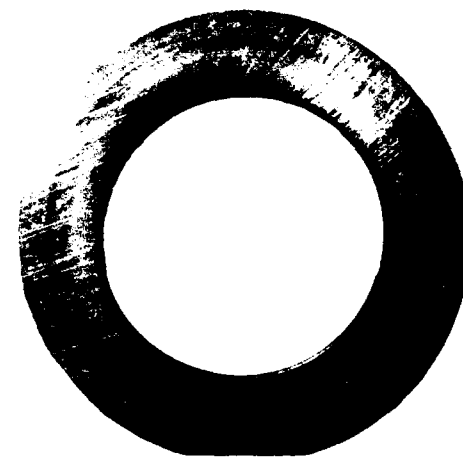
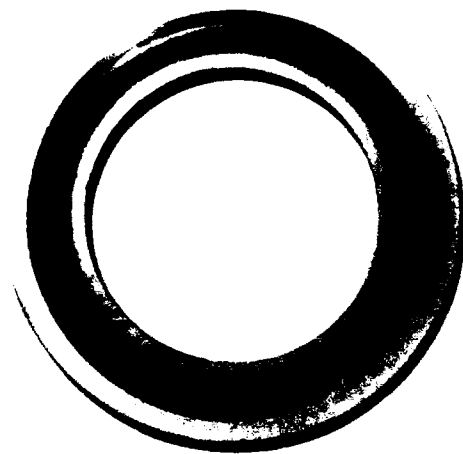*a. Pump No. 1 (Jet A-1/Standard)*
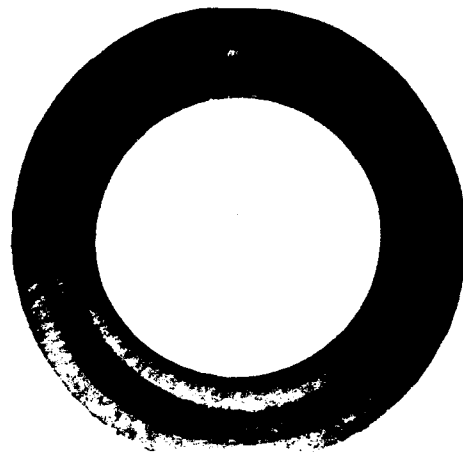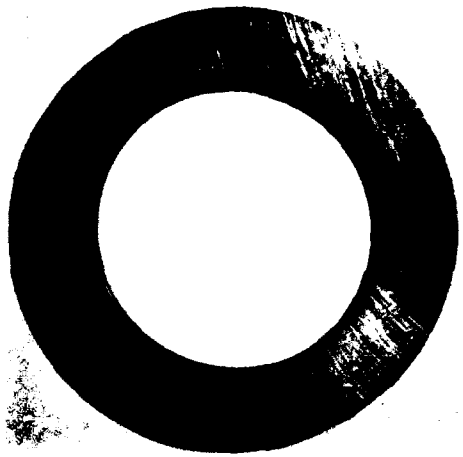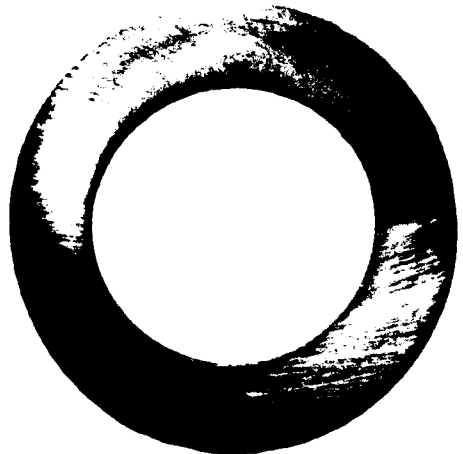
b. Pump No. 3 (DCI-4A/Standard)

c. Pump No. 5 (BIOBOR-JF & FOA-15/Standard)

d. Pump No. 7 (Diesel/Standard)

e. Pump No. 2 (Jet A-1/Arctic)

f. Pump No. 8 (Diesel/Arctic)

Figure 18. Governor thrust washers from selected pumps

37
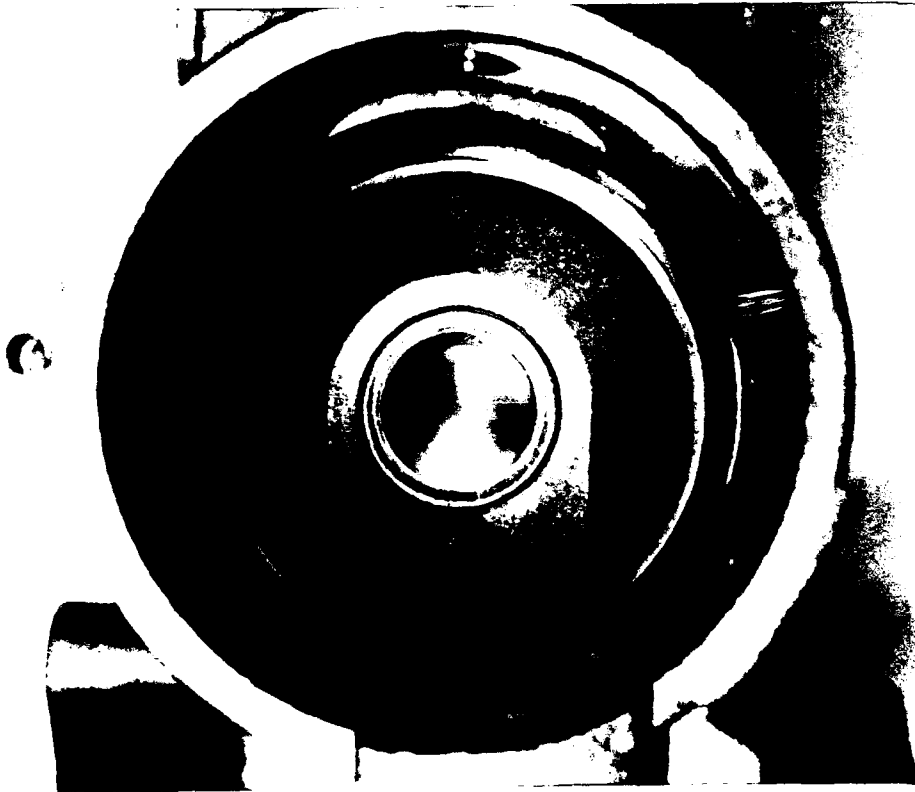
a. Pump No. 1 (Neat Jet A-1)

b. Pump No. 3 (Jet A-1 + DCI-4A)

Figure 19. Interior of selected pumps after conclusion of test

38

Severe wear is present throughout the complete standard pump (Pump No. 1) that operated on neat Jet A-1. Particularly severe wear was present on highly loaded areas such as the drive tang and roller shoe when compared with tests performed with additized fuel. For comparison, Fig. 20 shows surface profiles taken across the sharp step formed at the edge of the wear scar on the drive slot with neat Jet A-1 and Jet A-1 containing the BIOBOR-JF/FOA-15 combination.
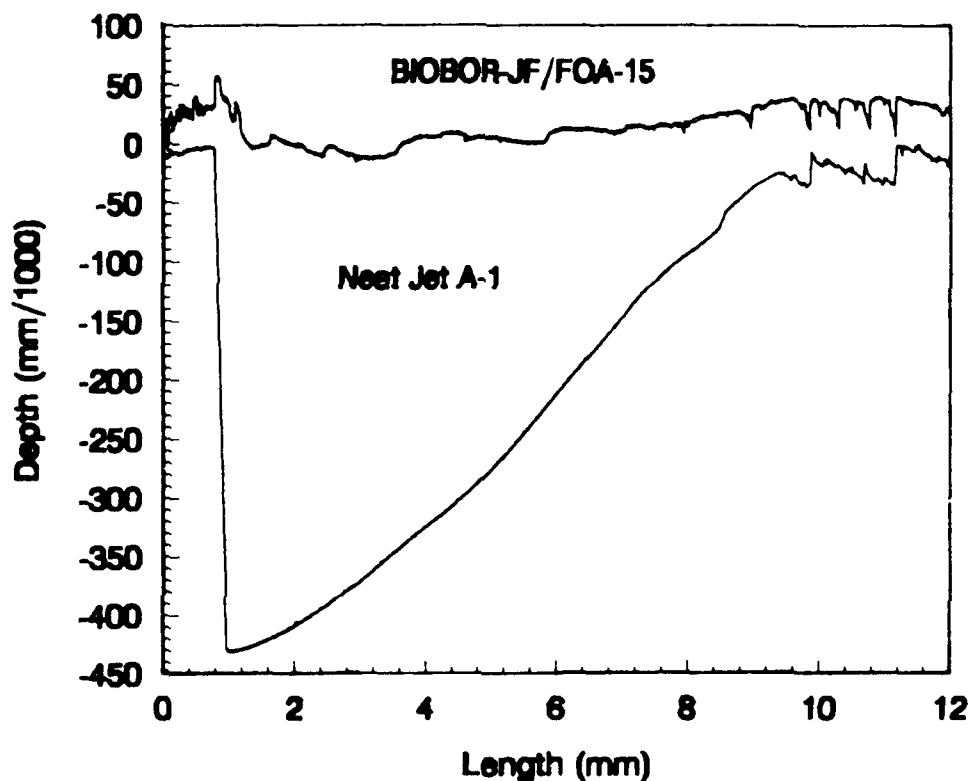
Figure 20. <u>Surface profiles taken from the drive slot on standard pumps</u>

Photographs of the wear scars on selected drive tang and pump roller shoe components are shown in Figs. 21 and 22, respectively.* These severe contacts have an irregular surface topography and were probably produced by failure of the weak boundary film formed by the fuel. Gross plastic deformation of the surface is not evident due to the minute amount of relative motion between the components. However, increased play between the drive tang and the slot in the pump rotor will further contribute to severe wear due to high impact loading. As a result, the contact loads and wear mechanism are likely to change as wear progresses. The indentation

---

* In the figure captions, "Arctic" indicates pumps with the improved metallurgy, and "Standard" indicates the standard pumps.

39

a. Pump No. 1 (Jet A-1/Standard)

b. Pump No. 3 (DCI-4A/Standard)

*c. Pump No. 5 (BIOBOR-JF &
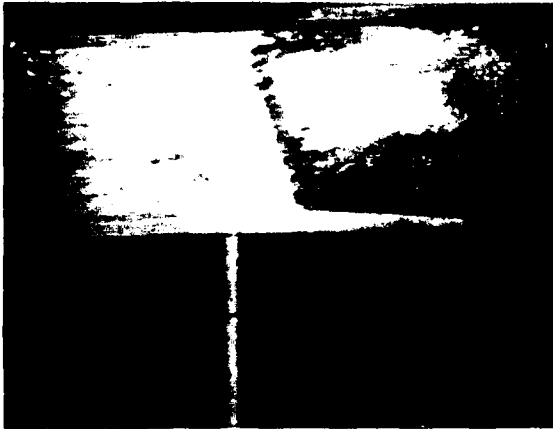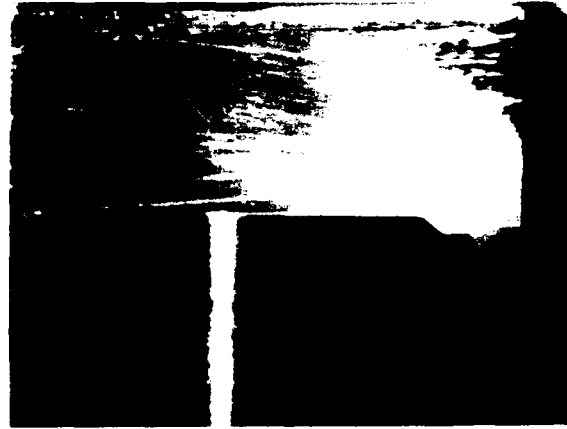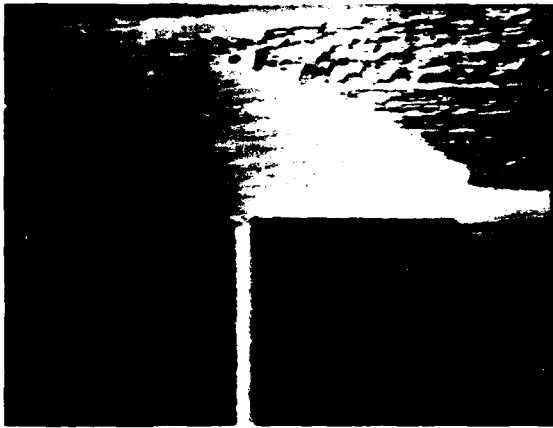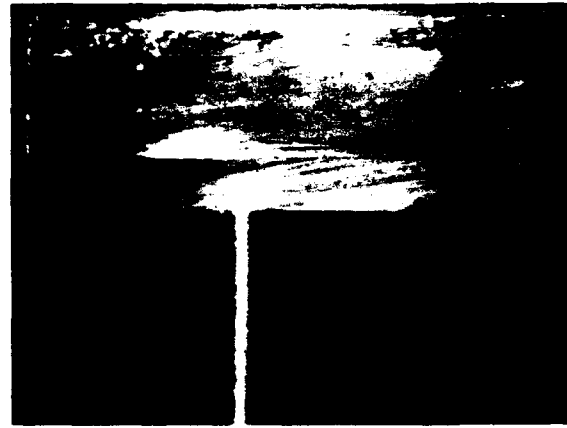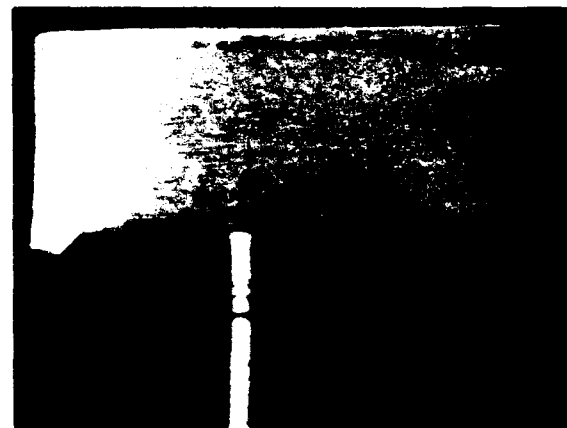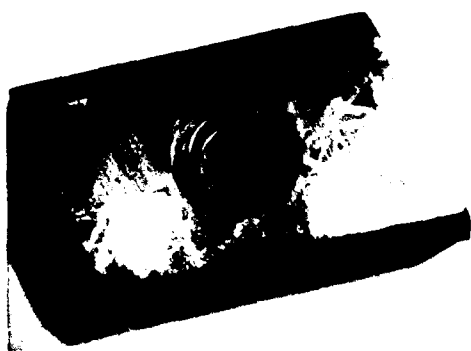FOA-15/Standard)*

d. Pump No. 7 (Diesel/Standard)

e. Pump No. 2 (Jet A-1/Arctic)

f. Pump No. 8 (Diesel/Arctic)

Figure 21. Selected drive tangs
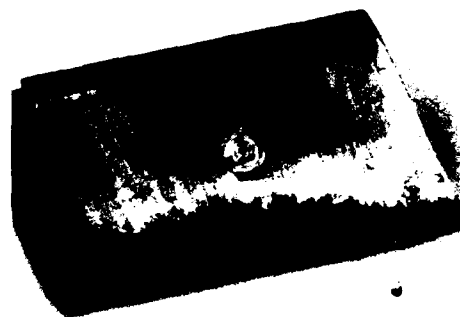
a. Pump No. 2 (Jet A-1)   *b. Pump No. 4 (Jet A-1 + DCI-4A)*
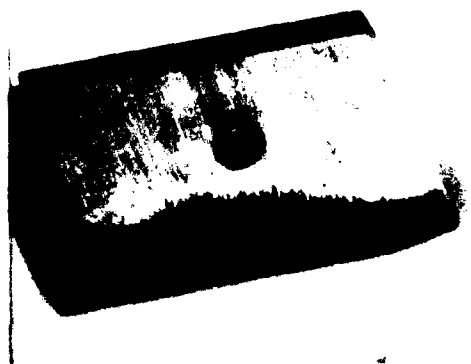
c. Pump No. 6 (Jet A-1 +   *d. Pump No. 8 (Diesel)*
BIOBOR-JF/FOA-15)
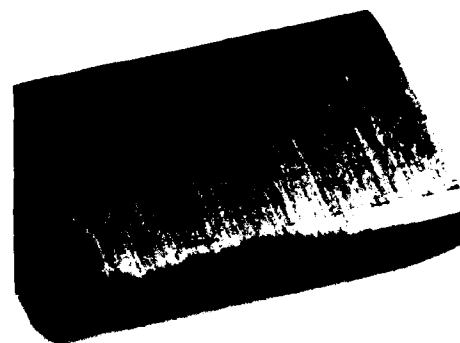
Figure 22. Roller shoes

hardness on these severe wear scars is similar to that of the surrounding area, so the increased wear rate is not due to failure of surface-hardened layers.

The improved metallurgy of the arctic components greatly reduced the amount of wear present on both the drive tang and pump vanes lubricated with neat Jet A-1, as shown in Figs. 21e and 21f. The arctic components also produced a slight reduction in the measured wear rate with the better lubricity fuels when compared with the standard components, as given in TABLE 7. This improvement was especially great for the drive tang lubricated with the BIOBOR-JF/FOA-15

41

additive. Clearly, the arctic kit greatly improves the durability of the components that have the improved metallurgy, particularly with low-lubricity fuels. No disadvantages to the use of the arctic components were apparent. It should be noted, however, that only a limited number of components have the improved metallurgy. The remainder (such as the roller shoes in Fig. 22) are unchanged from the standard pump and still show relatively high wear with neat Jet A-1. Fortunately, most of the remaining components are lightly loaded or do not directly affect pump performance. The governor thrust washer was the only revised component that was not improved by the new metallurgy, as shown in Fig. 18. However, in the present case, the degree of wear of this component was not found to be critical, but was reduced by the use of lubricity additives. It is significant that fuel lubricity did **not** appreciably affect the wear produced on any of the remaining arctic components.

However, the DCI-4A and the BIOBOR-JF/FOA-15 additives successfully reduced both visible and measured wear throughout the standard pump, as shown in Figs. 18, 21, and 22 for selected components. TABLE 7 indicates that the additives commonly reduce the ultimate wear volume by over an order of magnitude. However, the wear mitigation provided by the additives may be load sensitive. The BIOBOR-JF/FOA-15 additive combination was more effective than DCI-4A in reducing wear on lightly loaded components, such as the thrust washer, governor weights, and rotor retainer. However, it was less successful with the more highly loaded drive tang, as shown in Fig. 21. This dependence of the BIOBOR-JF/FOA-15 additive on applied load was previously noted in bench wear tests.(13) The surface topography on the standard drive tang produced by the BIOBOR-JF/FOA-15 combination is relatively rough and is somewhat similar to that seen with neat Jet A-1, as shown in Fig. 21. However, the other highly loaded components lubricated with BIOBOR-JF/FOA-15 (i.e., the roller shoes) did not show unexpectedly high wear. It should be noted that loss of tolerance on the drive tang will greatly increase the contact loads, thereby producing unexpectedly severe wear.

The baseline tests performed with diesel fuel produced little wear. Most components are similar to that seen with additized fuel, and almost no wear is visible on the standard drive tang, as shown in Fig. 21. However, the rotor retainers on the two pumps that operated on diesel fuel are appreciably less worn than those from pumps that operated on either neat or additized Jet

42

A-1, as shown in Fig. 23. This anomalous result is probably due to the increased viscosity of the diesel fuel, which produces greater hydrodynamic lift on this lightly loaded component.
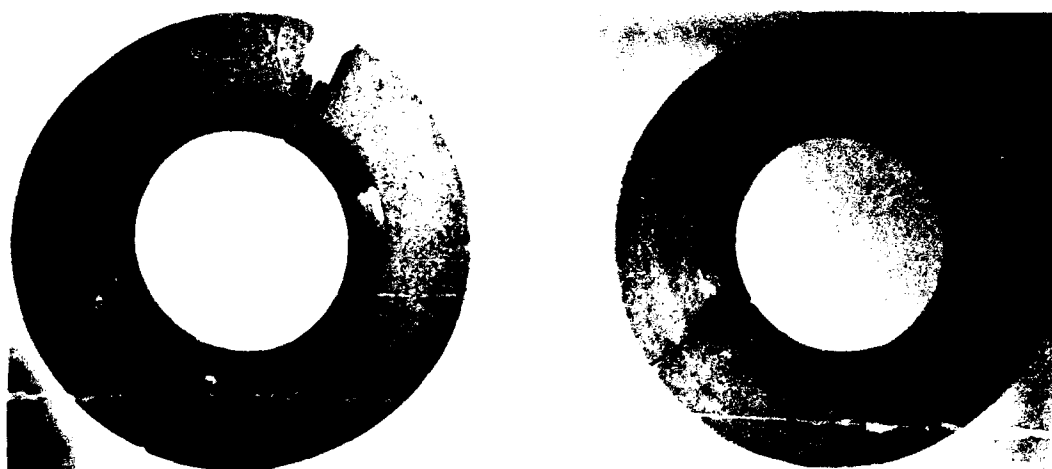
a. Pump No. 5 (BIOBOR-JF & FOA-15)   b. Pump No. 7 (Diesel)

Figure 23. Rotor retainers

Only seven components were selected for quantitative wear measurement. Quantitative wear measurement on the complex geometries of every component in each of the pumps is prohibitively difficult. Instead, the procedure developed in previous reports (20,21) was used; wear-prone components throughout each pump were subjectively graded from 0 to 5 according to the degree of wear present. The results of this process are given in TABLE 8. The overall pattern of wear within the standard pumps is similar to that seen in units returned from the field (20,21); most wear is concentrated in the transfer pump, drive tang, and governor assembly. As would be expected, considerably more wear was present on metering valves returned from the field than from pump stand tests that operated at a constant throttle setting. However, some pitting was present on the metering valves with neat Jet A-1, probably due to a fretting process. An appreciable amount of wear was also visible on each of the advance pistons, even though the injection advance should not have operated during the continuous 200-hour test. However, the degree of wear was not abnormal and is also probably due to small amplitude random vibration and fretting.

TABLE 8. Subjective Wear Level* on Critical Pump Components

Component		Pump 1	2	3	4	5	6	7	8
Hydraulic Head & Rotor	Hydraulic Head	0	0	0	0	0	0	0	0
	Discharge Fittings	0	0	0	0	0	0	0	0
	Distributor Rotor	1	1	1	1	1	0	1	0
	Delivery Valve	2	2	2	2	2	2	1	1
	Plungers	4	3	2	3	1	1	1	1
	Cam Rollers & Shoes	3	4	2	2	1	2	1	1
	Leaf Spring & Screw	1	1	1	1	1	1	1	1
	Cam	1	1	1	1	1	0	1	1
	Governor Weight Retainer	0	0	0	0	0	0	0	0
	Governor Weights	4	3	2	1	1	1	1	1
	Governor Thrust Washer	4	3	2	2	1	1	1	1
	Governor Thrust Sleeve	4	2	1	2	2	1	1	1
	Drive Shaft Tang	5	1	2	1	3	1	2	1
Transfer Pump	Inlet Screen (0 = Clean; 5 = Clogged)	0	0	0	0	0	0	1	0
	Regulating Adj. Plug	0	0	0	0	0	0	0	0
	Regulating Piston	2	2	1	1	1	1	2	2
	Regulator	3	3	2	2	1	2	1	2
	Blades	3	1	2	1	2	1	2	1
	Liner	3	3	2	3	3	2	1	2
	Rotor Retainers	3	3	3	3	2	2	1	1
Governor	Metering Valve	3	2	2	1	1	1	1	1
	Metering Valve Arm	1	0	0	1	0	1	0	0
Advance	Piston	4	3	3	3	3	3	2	2
	Cam Advance Screw	1	2	1	1	1	1	1	1
	Plugs	0	0	0	0	0	0	0	0

* 0 = No Wear; 5 = Failure.

The average results derived from all the components in each complete pump are summarized in Fig. 24. This subjective measure of pump durability qualitatively agrees with the measurements taken from selected components. The improved metallurgy in the arctic components normally reduced wear, with a particularly large decrease for neat Jet A-1. The ranking achieved among the additized jet fuels corresponds with the results predicted by the BOCLE. However, diesel appears to produce marginally less wear than expected. The decreased separation between the

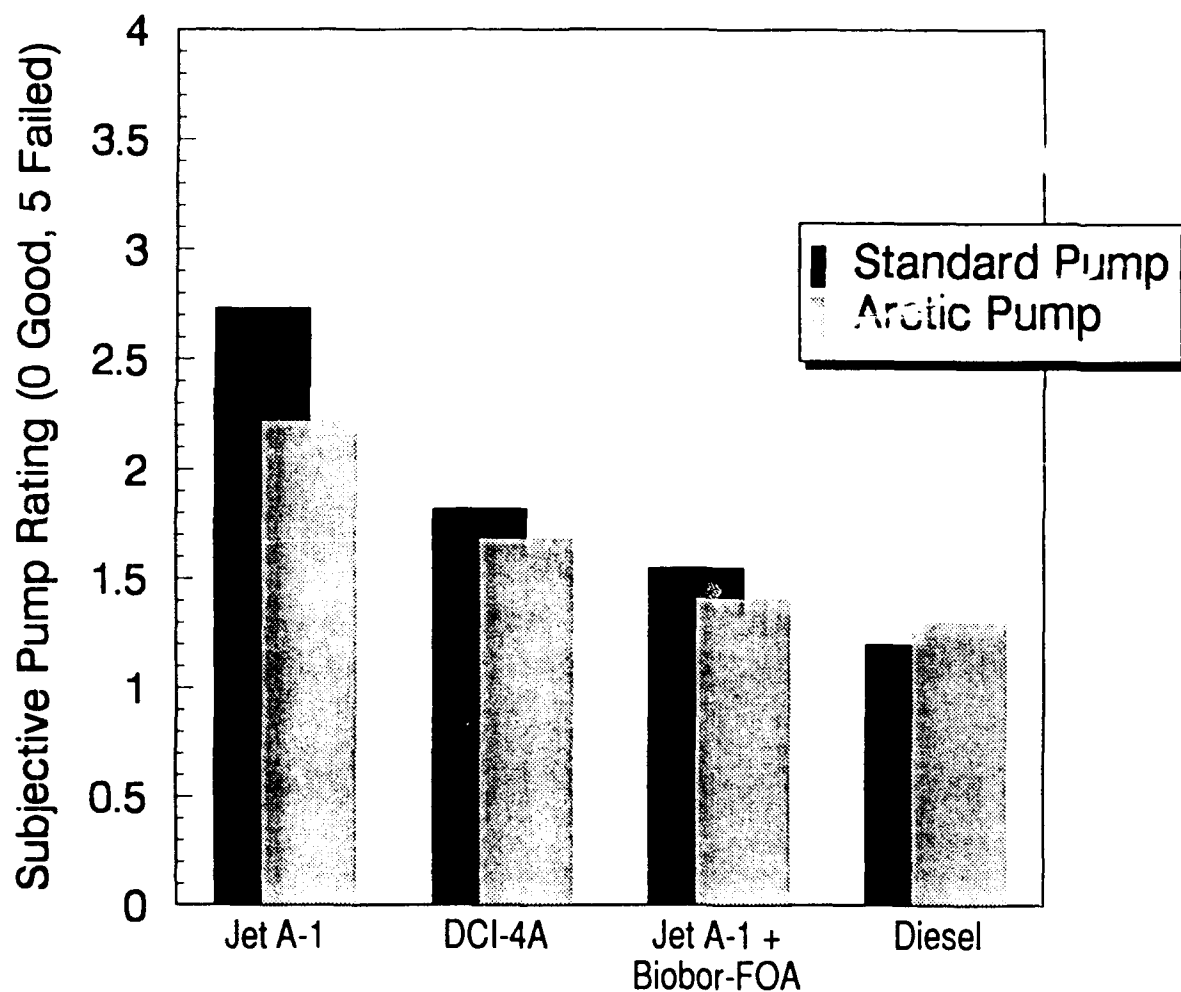**Figure 24. <u>Subjective wear level on pump components—averaged for each pump</u>**

pumps compared with the quantitative measurements is primarily due to the greater range of components considered: not all areas of the pump were effected by fuel lubricity, and no wear was visible on some components.

No evidence of particulate contamination or incipient seizure was visible in any of the pumps.

VIII. CORRELATION WITH BENCH WEAR TESTS

A. Background of Fuel Lubricity Measurement

The relatively poor lubricating characteristics of most fuels demand the use of a test methodology distinct from that commonly used in formulated lubricants.(41,42) In most fluids, air is beneficial to the formation of an effective boundary layer.(43) However, the lack of polar species in highly refined fuels allows formation of an oxide layer on metallic surfaces. According to the Pilling-Bedworth rule, the oxides of iron do not adhere strongly to the base material.(44) The weaker surface material is repeatedly formed and removed during sliding contact to produce a high material removal rate. If the applied load is sufficiently great, failure of the surface layers will occur, allowing adhesive wear between the metallic substrates. This catastrophic form of adhesive wear is commonly known as scuffing and is distinct from the milder oxidative mechanism. Weak oxide layers that promote wear under mild conditions probably also serve to separate the bulk materials and prevent adhesive scuffing. It is generally held that one of the major functions of current MIL-I-25017 lubricity additives is preferential chemisorption of the additive to the metal surface to the exclusion of oxygen and, therefore, mitigation of the corrosive wear process.(26)

The Ball-on-Cylinder Lubricity Evaluator (BOCLE), originally pioneered by Furey (45), has proven to be sensitive to the small amounts of corrosion inhibitor necessary to improve lubricity.(13) The BOCLE test provides a lightly loaded contact in which the oxide layers are removed without introducing alternate wear mechanisms, such as adhesion or severe abrasion between the bulk materials.(43) However, specific components in the pump, such as the drive tang and roller shoe, have a relatively high apparent contact pressure.

Bench wear tests were previously performed using a Cameron-Plint apparatus on specimens machined from both lightly loaded and highly loaded pump components.(13) For lightly loaded components, good correlation was obtained between the BOCLE and the results obtained using the Cameron-Plint apparatus. Under more severe conditions, a different ranking among the fuels emerged. An in-depth parametric study of fuel lubricity was subsequently undertaken using a

wear mapping technique.(13) The results from this study confirm that the onset of scuffing wear and seizure does not appear to be reflected in the wear rate under more lightly loaded conditions. This is in general agreement with some previous work in the same area.(46)

B. Correlation Achieved Between BOCLE and Pump Stand Test Results

The relationship between the expected performance of any single pump component and material removal rate is likely to be a nonlinear function. For example, the change in tolerance between two mating components is a direct linear function of wear depth, while wear volume for many counterformal contacts is proportional to the third or fourth power of the wear scar depth.

In practical bench tests, accurate wear measurement and the need for a reproducible geometry require the use of a counterformal contact. In both the standard BOCLE test and the Cameron-Plint wear mapping procedure, the average wear scar diameter formed between a spherical ball and test flat or cylinder is taken as a measure of fuel lubricity. As a result, the commonly reported BOCLE wear scar diameter does not well reflect the level of wear produced. The true wear volume and maximum wear scar depth for both the BOCLE and Cameron-Plint are given in Fig. 25, as a function of scar diameter. More accurate calculations may be performed for the Cameron-Plint and BOCLE using Equations 3 and 4, respectively.

$$V_c = \frac{\left(\pi \times D^4 \right)}{\left(64 \times R_c \right)} \qquad \text{(Eq. 3)}$$

where: V_c = Cameron-Plint wear volume

D = Mean wear scar diameter.

R_c = Ball diameter (6.35 mm).

$$V_b = \left(\frac{\pi}{3} \right) \left\{ 2R^3 - \left[\left(\frac{D}{2} \right)^2 + 2R^2 \right] \left[R^2 - \left(\frac{D}{2} \right)^2 \right]^{0.5} \right\} \qquad \text{(Eq. 4)}$$
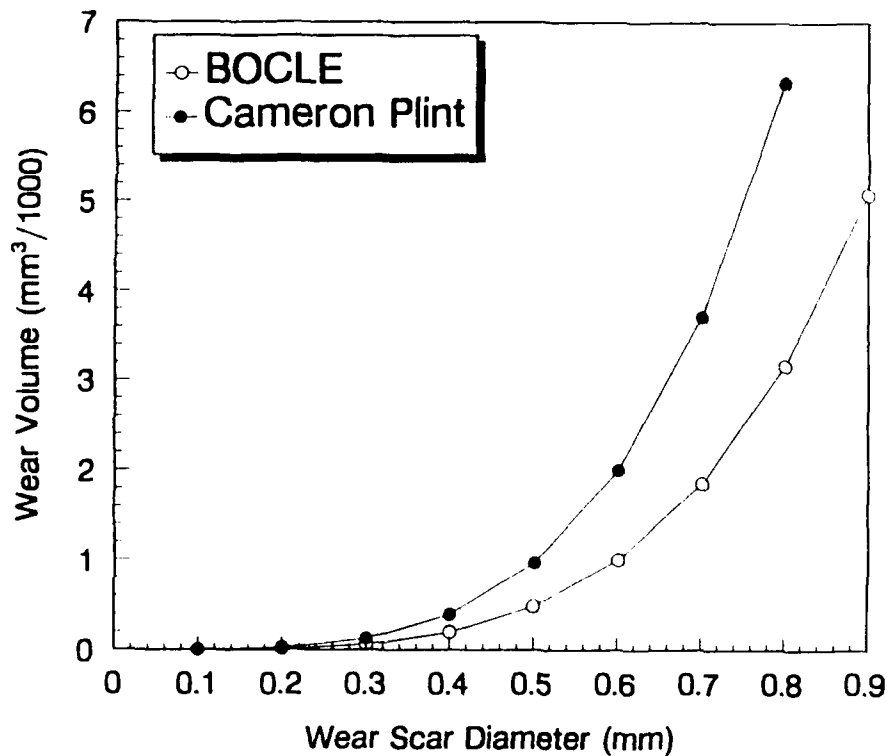
47

Figure 25. Relationship between wear volume and wear scar diameter in the BOCLE and Cameron-Plint wear tests

where: V_b = BOCLE wear volume

D = Mean wear scar diameter

R = Ball diameter (12.7 mm).

As the interrelationship between wear scar diameter/volume and pump performance is undefined, the wear volume of selected pump components is the most reliable measure of bench test performance. The seven components discussed in the previous section are representative of wear throughout the pump, but the overall wear volume varies by over three orders of magnitude. A more uniform format is required to facilitate directional comparison with the BOCLE results.

Archards equation produces a dimensionless wear coefficient (K) that is commonly used to normalize test results. Although this technique is most suited to adhesive wear, if the test conditions and wear mechanisms are well defined, it also provides a good description of wear rates for many rubbing systems.

$$V = \frac{KFS}{\sigma} \qquad \text{(Eq. 5)}$$

48

where: K = An empirical constant

F = Normal force on the contact

S = Sliding distance

σ = Material yield strength.

A detailed description of the calculation of Archards wear coefficient may be found in Appendix F. The results obtained are plotted in Figs. 26 and 27, for mild and severe contacts, respectively, as a function of the BOCLE results. Application of Archards equation reduces the relative difference between the wear of the components by approximately an order of magnitude, although a wide variation in wear still exists. Moreover, the wear coefficient observed for the lightly loaded components is several times less than that observed in the BOCLE. However, Archard himself noted that the constant K can vary widely with seemingly minor changes in test conditions.(37) The effects of metallurgy on corrosion resistance and the effects of surface
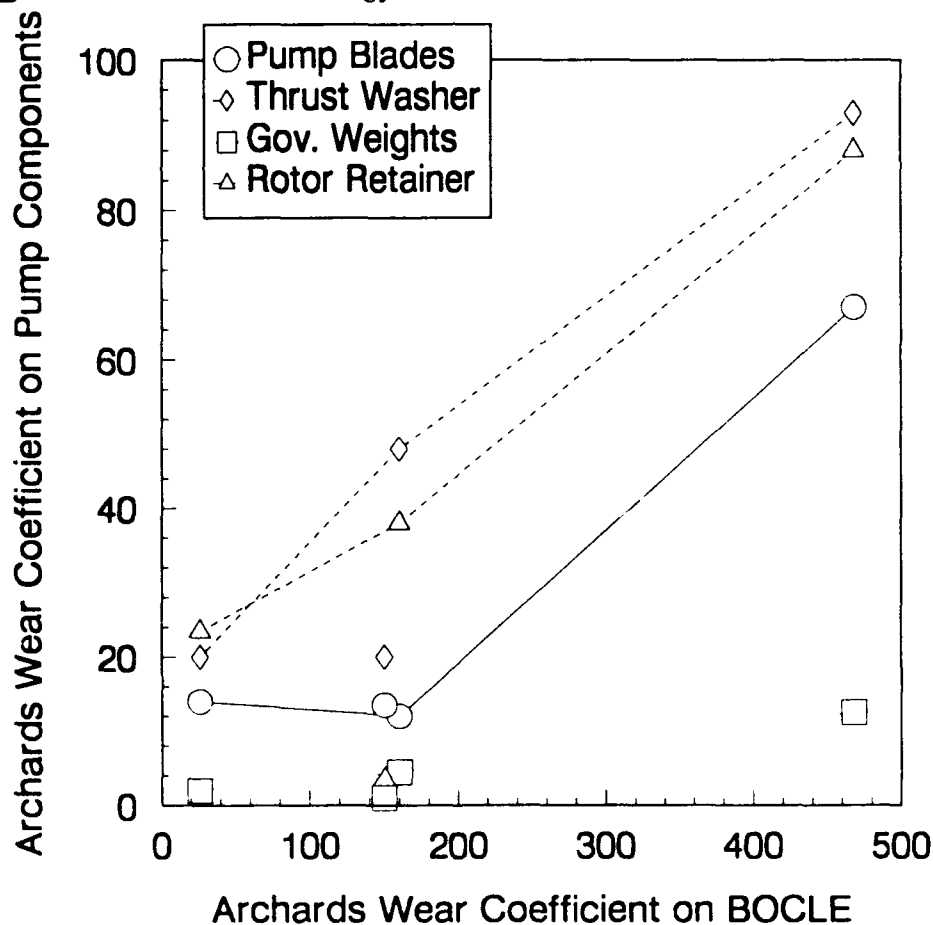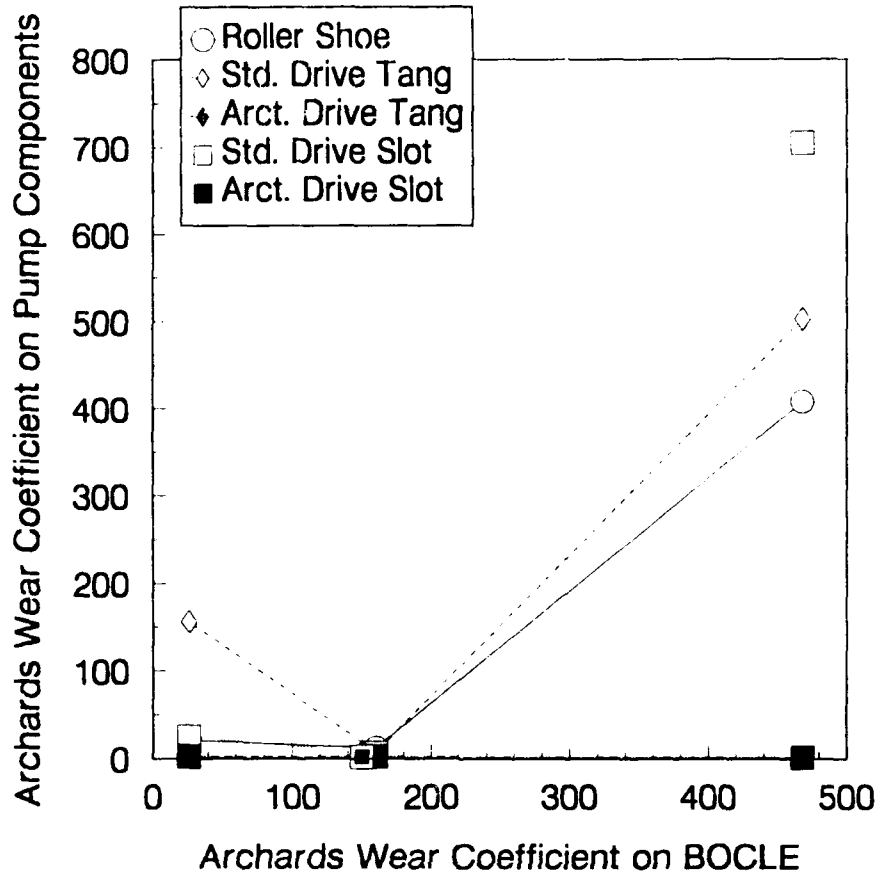

Figure 26. Correlation between BOCLE and wear measurements on lightly loaded components from pump stand tests

49

Figure 27. <u>Correlation between BOCLE and wear measurements on highly loaded components from pump stand tests</u>

roughness and hydrodynamic/elastohydrodynamic lift are all ignored. BOCLE tests performed using a polished test ring in place of the standard textured component produce appreciably less wear.

Relatively good directional correlation was achieved between the BOCLE and the more lightly loaded pump components, as shown in Fig. 26. It should be noted that the results plotted in Fig. 26 are all standard metallurgy parts. The results for the arctic transfer pump blades are not included, as fuel lubricity did not measurably affect the wear seen with these components. At higher loads, the results were still directionally correct, although disproportionately severe wear was observed on standard metallurgy components lubricated with neat Jet A-1. In addition, unexpectedly severe wear was observed on the standard drive tang/drive slot lubricated with the

50

BIOBOR-JF/FOA-15 combination. Once again, the improved or arctic metallurgy was not appreciably affected by fuel lubricity, although the results are included for comparison.

C.   Wear Map Results

The primary wear mechanism in the pumps that operated on neat clay treated Jet A-1 was due to oxidation of the metallic surface, and a brown oxide coating was present on the inside of the pump at the conclusion of the test. Figs. 28a and 28b are wear maps for AISI 52100 steel lubricated with neat clay-treated Jet A-1 in a controlled test environment of air and nitrogen, respectively. The lightly loaded region of both wear maps are highly dependent on the presence of both moisture and oxygen, indicating a similar oxidative/corrosive material removal process. However, higher loads caused failure of the weak boundary layer formed by the fuel. Subsequent metal-to-metal contact between the opposing surfaces caused severe adhesive wear and high friction, halting the test. **When seizure forced premature termination of the test, the wear scar diameter was arbitrarily set to 1.** It should be noted that the wear scar diameter in the wear maps and the commonly reported BOCLE scar diameter are not directly comparable due to the differences in test specimen geometry. However, quantitative comparison is possible using Equations 2 and 3.

Wear maps were produced as a simultaneous function of speed and load for each of the fuel additive combinations used in the full-scale pump tests. Each of these tests was performed with AISI E-52100 steel, similar to that used in the standard BOCLE wear test. As shown in Fig. 29, two distinct regions are visible in each map. As previously indicated, the lower region represents a mild corrosive mechanism and is relatively independent of both test speed and load. Lubricity additives effectively reduce wear under these lightly loaded conditions, and the results correlate with those obtained using the BOCLE, as shown in Fig. 30 The wear map data plotted represents test results at a 10 N applied load and 250 mm/s sliding speed. Wear rate with the BIOBOR-JF/FOA-15 additive combination at low loads is very low and is comparable to that of neat clay-treated Jet A-1 in the absence of both moisture and oxygen, as previously shown in Fig. 28b. However, this additive combination becomes less effective at higher loads and
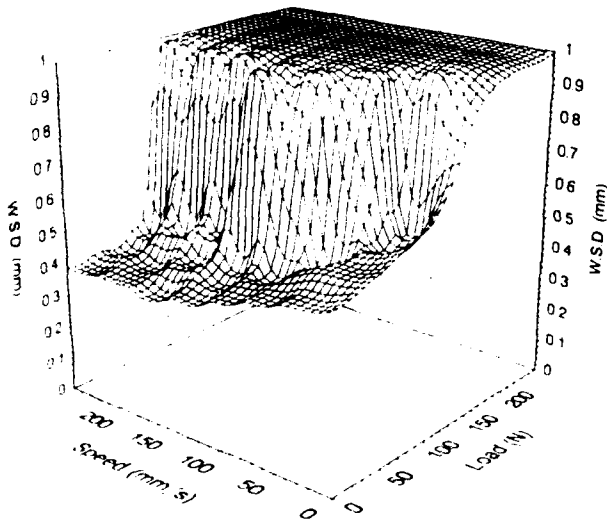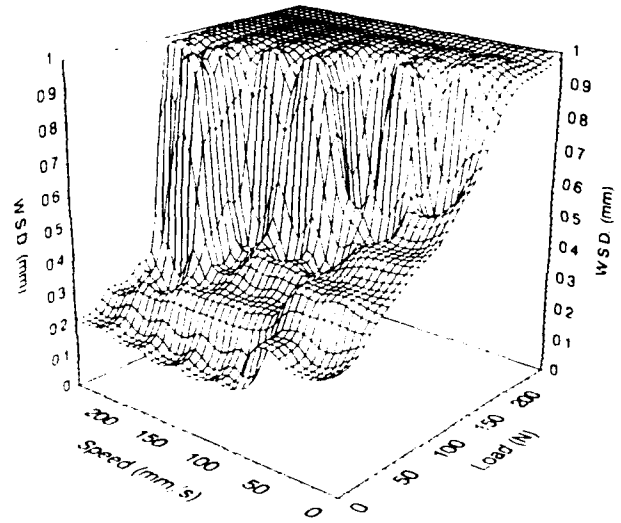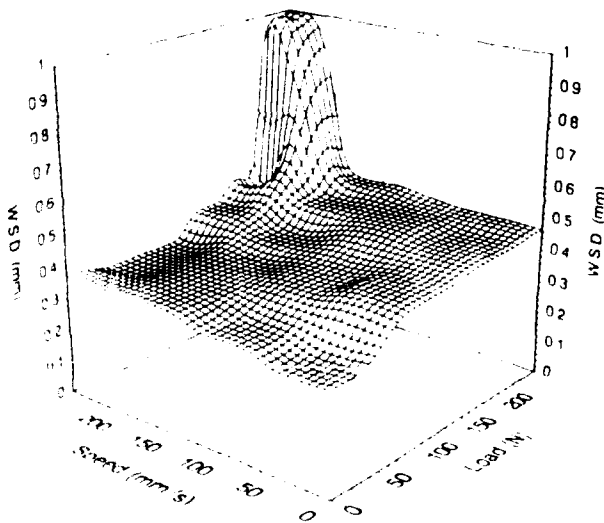
51
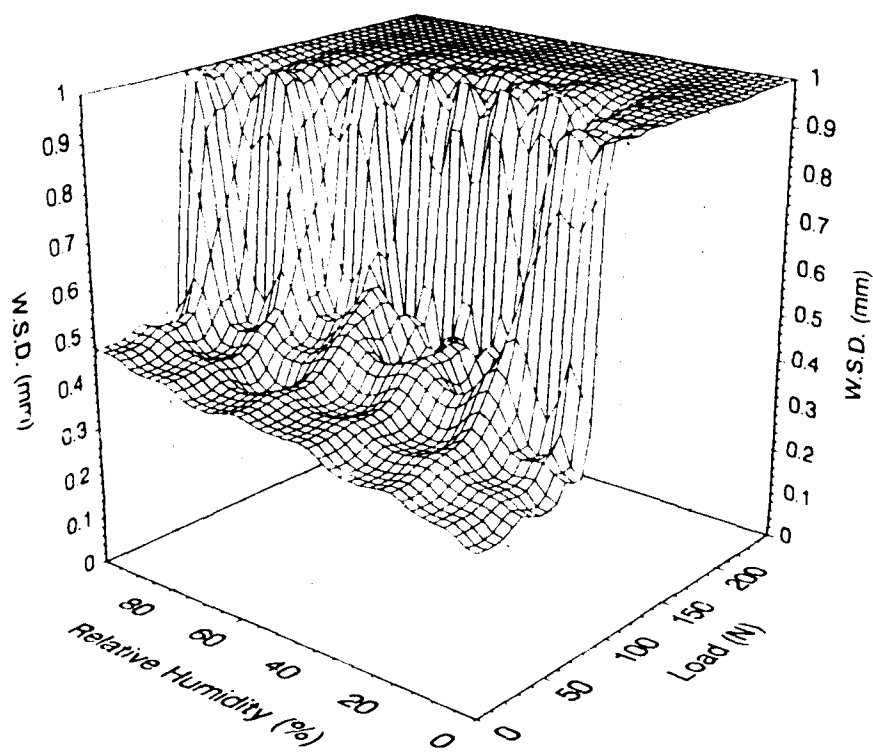
a. Air
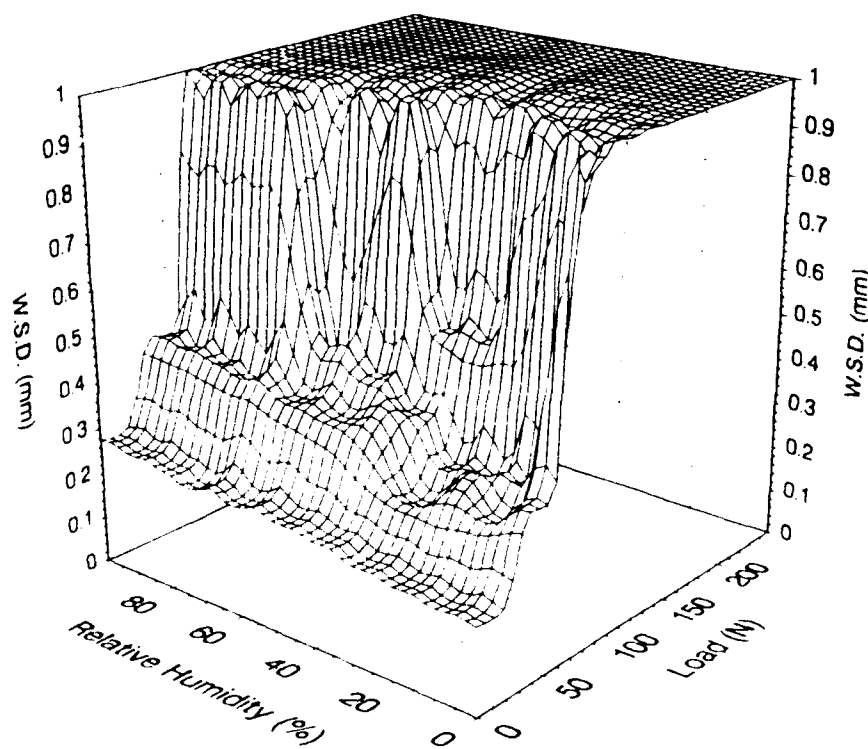
b. Nitrogen

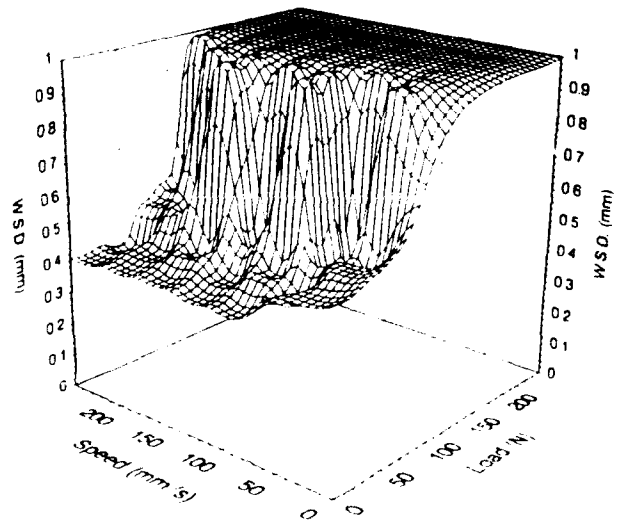**Figure 28. <u>Wear maps for 52100 steel lubricated with neat clay-treated Jet A-1 in controlled test atmospheres</u>**

a. 52100 Lubricated With
MIL-I-25017

b. 52100 Lubricated With
MIL-S-53021
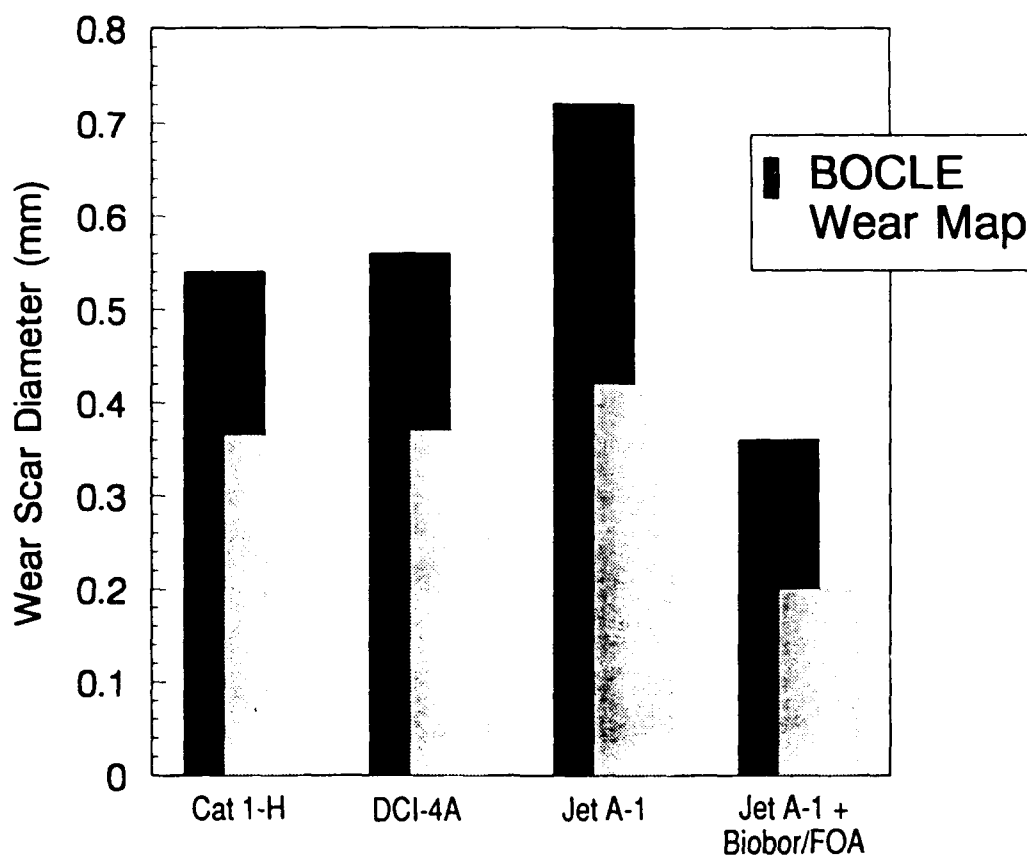
c. 52100 Lubricated With
Cat 1-H Diesel

d. 52100 Lubricated With
Clay-Treated Jet A-1

Figure 29. Wear maps for fuel/additive combinations used in test series

Figure 30. Qualitative comparison between BOCLE test data and data from a lightly loaded region of the wear maps

produces only a marginal increase in the applied load required for the onset of scuffing. The dependence of the wear rate seen with the BIOBOR-JF/FOA-15 additive on applied load reflects the results observed for the complete pump in the previous section. Furthermore, diesel is appreciably more effective at high loads than clay-treated Jet A-1 either with or without additives. The interrelationship between contact load and wear for both BIOBOR-JF/FOA-15 and diesel seen in the wear maps was **not** predicted by the standard BOCLE wear test. Previous workers have observed similar effects with different fuels.(46)

Fig. 31 shows a wear map constructed for M-50 steel analogous to that used in the upgraded "arctic" pump vanes, lubricated with clay-treated Jet A-1. Clearly, fuel-related wear is highly dependent on metallurgy: wear is reduced at low loads compared with 52100 steel, while scuffing failure did not take place up to the maximum applied load available on the
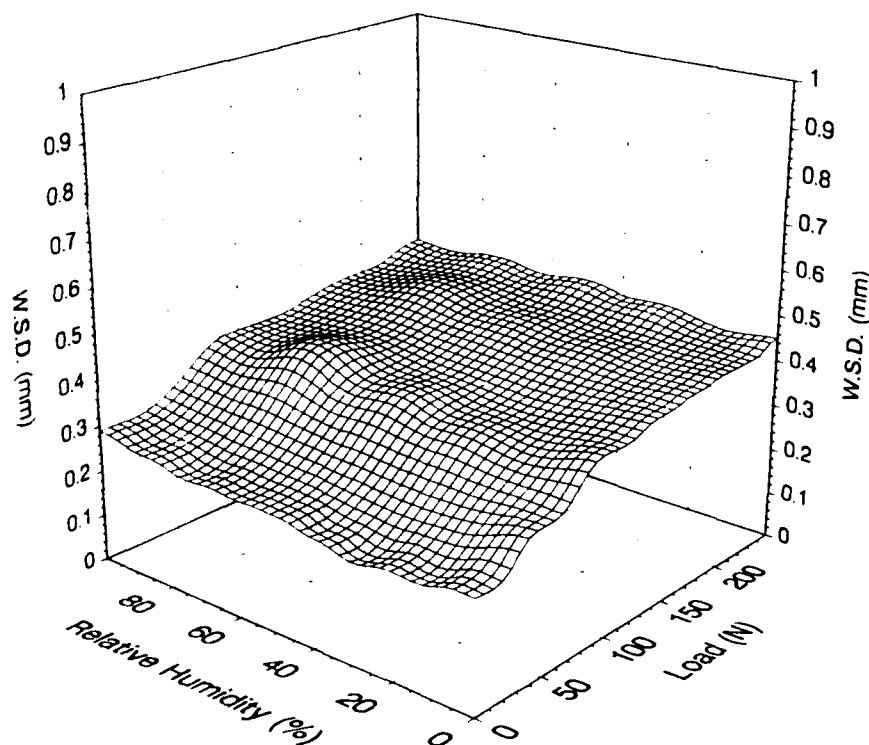
Figure 31. Wear map for M-50 steel lubricated with neat Jet A-1

Cameron-Plint apparatus. It should be noted that the indentation hardness readings of both the AISI E-52100 and M-50 materials are approximately equal. Thus, the improved metallurgy has a significant effect on both oxidative/corrosive wear and scuffing resistance distinct from the physical hardness of the metal. Moreover, previous nonstandard bench wear tests performed using the Cameron-Plint apparatus indicate that such materials are appreciably less influenced by fuel lubricity and additives than is the AISI E-52100 steel used in the standard tests.(13,47) As noted in Section VI, the improved metallurgy in the arctic pump is similarly independent of fuel lubricity. Although the results are not contradictory, the apparent resistance of the improved metallurgy to fuel lubricity is not reflected in the standard BOCLE test results.

The primary factor affecting the intrinsic lubricity of aviation turbine fuels is the type and amount of nonhydrocarbon impurities present, with most chemical impurities serving to decrease oxidative/corrosive wear. However, Wei and Spikes (42) observed that most sulfur compounds commonly found in diesel fuels increase wear. Sulfur compounds are likely to produce a corrosive wear mechanism on the metallic surfaces, distinct from the oxidative/corrosive material

55

removal process present with the highly refined Jet A-1 used in the present study. The maximum allowable sulfur content for Jet A-1 fuel is 0.3 wt% sulfur, while the present study was based on a single, highly refined, low-sulfur (0.002 percent) fuel.

A wear map obtained for 0.3 wt% sulfur [di-*tert*-butyl disulfide (TBDS)] added to the clay-treated Jet A-1 is shown in Fig. 32a (see Fig. 29a for a wear map of the neat clay-treated fuel). As expected, the 0.3 wt% TBDS greatly increased wear at low loads, but increased the scuffing load capacity of the fuel at low speeds. A second wear map for a commercially available nonclay-treated Jet A-1 fuel, with the physical characteristics given in Appendix D, is shown in Fig. 32b.

This less severely refined fuel has a higher sulfur, aromatic, and olefin content than the fuel used as the basis for the present study. Again, this higher sulfur fuel produced similar or slightly more wear at low loads, but was more resistant to scuffing and seizure than the standard test fuel. Most jet fuels have a relatively low-sulfur content; however, the effects of this contradictory behavior on the correlation achieved between bench wear tests and operating equipment is currently unknown. Clearly, considerable variation in both wear and scuffing resistance may exist among Jet A-1 fuels that conform to ASTM D 1655.(1) Moreover, the effect is likely to be particularly great for high-sulfur diesel fuels.

IX. DISCUSSION

Each of the lubricity additives tested was successful in reducing wear at a single concentration in a single low-sulfur Jet A-1. Previous work indicates that the DCI-4A and BIOBOR-JF/FOA-15 additives remain effective in a number of other Jet A-1 fuels procured in Saudi Arabia, although the effectiveness of the BIOBOR-JF/FOA-15 additive was shown to decrease at high relative humidity.(13) DCI-4A consistently appears less effective than BIOBOR-JF/FOA-15 at low loads, but remains effective in more highly loaded contacts, which are most prone to severe wear. In addition, DCI-4A is qualified under MIL-I-25017 and so appears to be the obvious choice for practical application. The effect of additive depletion in the supply system
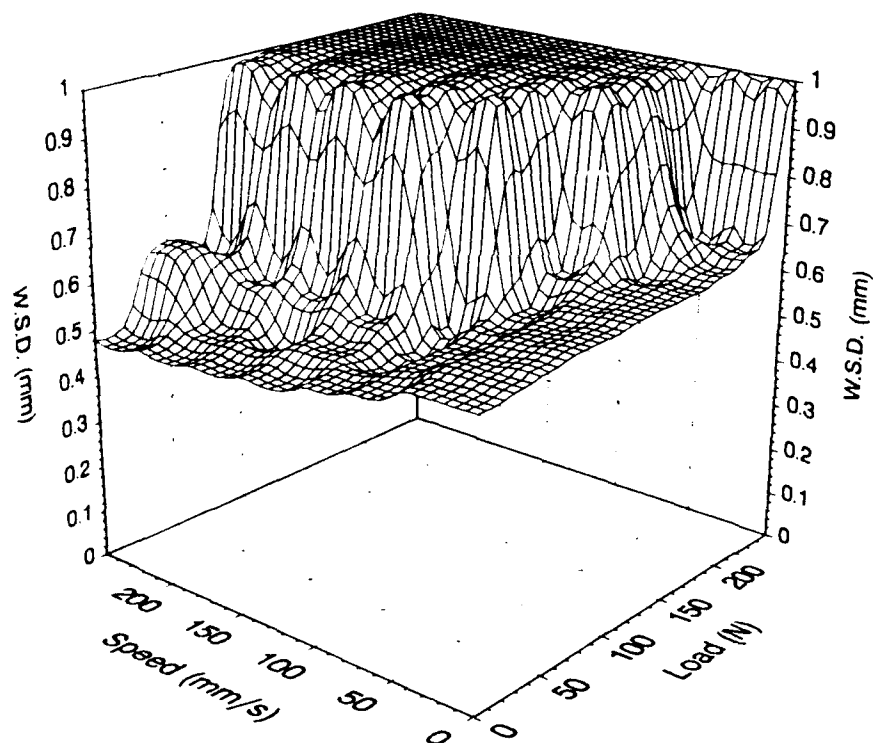
a. Clay-Treated Jet A-1 (TABLE D-1) With 0.3 wt% TBDS Added
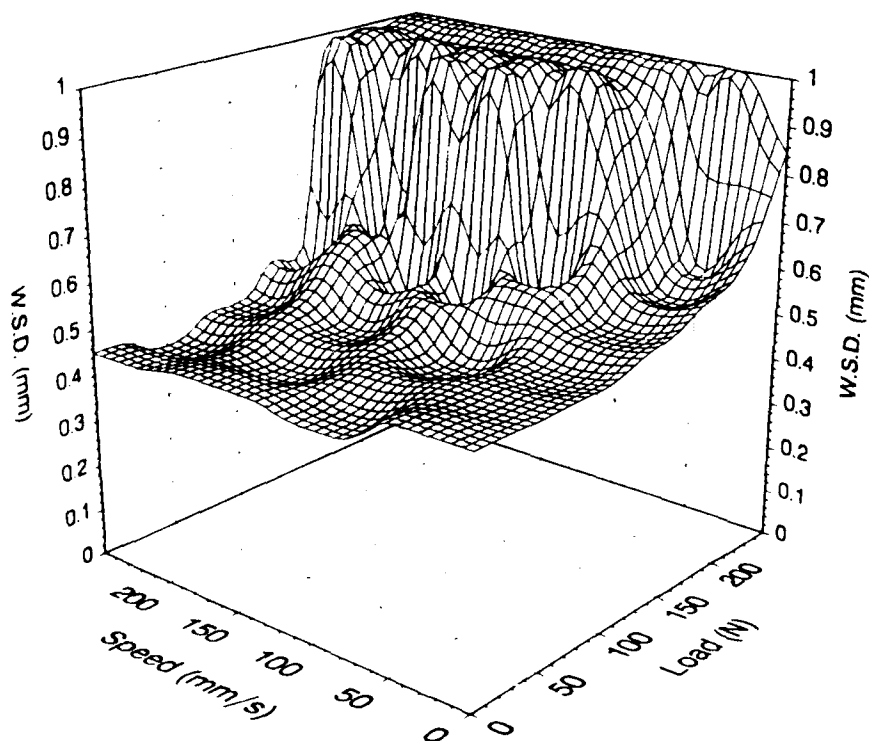
b. Commercially Available Jet A-1 With Characteristics Given in TABLE D-2

Figure 32. Wear maps for high-sulfur Jet A-1 fuels

(i.e., due to the additives plating out) has not been conclusively determined. However, it is likely that a steady state will quickly be attained, after which the additive content is likely to remain constant and unaffected. In addition, bench tests have indicated that both additives remain effective over a range of concentrations.(48) If required, the effective concentration of a known additive may be determined using Reverse Phase High Performance Liquid Chromatography (RPHPLC).(48,49)

The primary objective of the current study is to derive a bench wear test that reflects the lubricity requirements of the fuel injection system. Good correlation was achieved between the BOCLE and wear measurements on lightly loaded standard components with each of the fuel additive combinations. The correlation achieved was less accurate for some highly loaded components, possibly due to a scuffing wear process. However, only a single component in one of the pumps was directly contradictory to the BOCLE results. The statistical significance of this error is relatively low. If required, an alternative BOCLE procedure is available to predict the scuffing limited performance of low-lubricity fuels (46), although some further development is probably necessary before this procedure could be accepted as a standardized test.(13) Fuel lubricity had little effect on the wear of components that contain an improved metallurgy, both in the pump and also in nonstandard bench wear tests. As a result, no correlation with the BOCLE could be expected for these components.

In general, the standard BOCLE test was at least directionally correct and clearly distinguished between the additized fuel and neat Jet A-1, which produced severe pump wear. Most importantly, the pump wear was reflected in degraded engine performance that was qualitatively similar to the BOCLE results.

Both the bench wear tests and pump stand tests indicate that the wear mechanism in fuel-lubricated contacts is highly dependent on the contact parameters, especially applied load. Additive effectiveness is similarly dependent. As a result, extreme caution must be exercised when designing accelerated test methodologies that use overspeed or overload conditions. If the revised contact conditions produce a significant change in wear mechanism from that normally found, the results are not meaningful.

From the results of the present study, a wear scar diameter of less than 0.6 mm in the standard BOCLE test would be expected to indicate relatively mild wear, while a wear scar of 0.7 or more should indicate severe wear. These results are in good agreement with informal reports of previous work at Stanadyne Automotive.(50) It is believed that the Stanadyne test series indicated that a BOCLE result of between 0.6 and 0.75 mm corresponds to the transition between mild and severe wear. These results obtained with automotive equipment are in good agreement with previous experience in aircraft turbine engine applications. The minimum BOCLE wear scar diameter is 0.65 mm for assuring adequate treatment of corrosion inhibitor (28); that is, JP-4/JP-8/JP-5 fuels must have BOCLE ratings lower than 0.65 mm. Lucas Aerospace and Rolls Royce produced the criterion in TABLE 9 for aviation turbine engine fuel lubricity requirements.(51)

TABLE 9. Summary of Results From Lucas Aerospace/Rolls Royce Study (3)

Wear Scar Diameter, mm	Qualitative Rating
>0.86	Very Poor
0.77 to 0.85	Poor
0.68 to 0.76	Medium
0.60 to 0.67	Good
<0.6	Very Good

The BOCLE wear scar diameters suggested in the joint study by Lucas Aerospace and Rolls Royce for acceptable lubricity are marginally greater than proposed in the present work. This discrepancy is probably not due to random test error. The derived experimental repeatability of the BOCLE is a function of the wear level, i.e.,

$$\text{Repeatability} = 0.167(WSD)^{1.8} \qquad \text{(Eq. 6)}$$

At the MIL-I-25017 specification limit of 0.65 mm, the repeatability value of 0.07 applies as the maximum difference between two test results, using different apparatus each with a controlled test atmosphere, in 95 percent of cases. However, the Lucas test series was performed without a controlled atmosphere and so had an effective humidity of approximately 50 percent.(3) The standard BOCLE procedure (4) used in the present work provides a regulated test atmosphere with a relative humidity of 10 percent. Wear with low-lubricity fluids is strongly influenced by the presence of moisture, as shown in Fig. 26a, and the greater wear observed in the Lucas Aerospace study is probably due to the relatively high test humidity.

A single jet fuel is used as the basis for the present study, the lubricity of which is adjusted using selected additives. The baseline results obtained using the more viscous diesel fuel were marginally better than would be expected from simple consideration of the BOCLE results. The effects of hydrodynamic and elastohydrodynamic lift are not predicted by the BOCLE and are primarily defined by the contact geometry, fluid viscosity and the relative motion between the opposing surfaces. Viscosity and the variation in viscosity with increasing contact pressure in elastohydrodynamic contacts are intrinsic properties of the fuel and are predictably affected by test temperature. The effects of temperature on the surface-active films required for boundary lubrication are more complex. DF-A, which is similar to Jet A-1, is widely used in arctic climates, with few durability problems reported. However, the fuel inlet temperatures in the present study were selected to represent those likely to exist in subtropical conditions. Both the formation of surface oxide layers (which promote wear) and formation of oxygenated species from the fuel (which prevent wear) are controlled by Arrhenious rate reactions. Moreover, Kanakia (52) demonstrated that dilinoleic acid (thought to be the main active ingredient in DCI-4A) did not adsorb appreciably below 30°C and then started desorbing at temperatures from 90° to 100°C. Further study is required to define the net effect of these interrelated parameters promoted by fuel inlet temperature and viscosity on pump wear.

It is unlikely that a direct correlation will ever be achieved between a single bench wear test and the decrease in pump performance as measured on the pump calibration stand or engine. The effects that have been shown to cause deviation from the trends indicated by the standard BOCLE test (or probably any other single test) include temperature, metallurgy, contact load, and fuel composition, especially sulfur. Each fuel injection system is comprised of many contact configurations and metallurgical pairs. As a result, any single bench test must be a compromise derived from among the comparing variables. The most that can be expected of a practical bench lubricity test is good qualitative correlation with the majority of pump components and the resulting degradation in pump performance in a "normal" test environment. Moreover, the dividing line between acceptable and unacceptable lubricity can never be absolutely precise. In broad terms, however, the standard BOCLE test as defined in ASTM D 5001-89 (4) appears to reflect the lubricity requirements of the Stanadyne fuel injection system.

The current study was largely confined to the Stanadyne rotary fuel injection pump, as this unit is believed to be more lubricity sensitive than most other fuel system components in military ground equipment. The decreased wear rate in less sensitive injection systems may be due to improved me.allurgy, less severe contact configurations, or, ideally, by having formulated crankcase lubricants at severely loaded contacts. However, the results of the present study indicate that the wear rate of most metallurgical contacts is likely to be increased by low-lubricity fuels. Further work is required to better define the relationship between lubricity and the durability of less fuel-sensitive equipment.

The results of the present study indicate that fuel system component wear may be reduced by either improved lubricity via additives and fuel formulation or by a metallurgical fix. Ideally, improved metallurgy would allow good pump durability with an almost unlimited range of fuels. However, the majority of pumps currently in service were designed for use with diesel. The optimum solution may be a minimum fuel lubricity requirement to protect existing equipment, while incorporating improved metallurgy into future pump specifications.

X. CONCLUSIONS

The following conclusions were derived from this study:

1. The durability of the Stanadyne fuel injection pump is highly dependent on fuel lubricity, and severe wear was observed with neat Jet A-1 at 170°F (77°C).

2. The DCI-4A additive (MIL-I-25017) (equivalent to JP-8 without the antistatic and antiicing additives) measurably reduced fuel-related wear to a level similar to that seen with diesel. A significant difference in lubricity generally exists between JP-8 and Jet A-1. The two should not be considered to have identical or similar lubricity properties.

3. The BIOBOR-JF/FOA-15 additive combination (MIL-S-53021) significantly reduced wear on most pump components. However, its effectiveness may be load dependent.

61

4. Little wear was observed in the Stanadyne pump operated on diesel fuel.

5. The improved metallurgy in the "arctic" pump conversion significantly reduced wear in critical areas of the pump with neat Jet A-1.

6. The improved metallurgy in the "arctic" pump conversion produces a marginal reduction in wear with better lubricity fuels compared to the standard pump.

7. No disadvantages were apparent with the arctic conversion.

8. Engine power with new, unused pumps using low-viscosity aviation turbine fuel is reduced by approximately 12 percent compared to diesel. The reduced engine power is due to a combination of decreased fuel delivery and the lower energy content of Jet A-1.

9. Engine power when operated on Jet A-1 was further reduced after conclusion of the 200-hour pump stand test, relative to the pretest results on the same fuel:

   a) Standard pump, 200 hours on neat Jet A-1: 40 percent reduction

   b) Arctic pump, 200 hours on neat Jet A-1: 13 percent reduction

   c) Arctic and standard, 200 hours on additized Jet A-1: 5 to 10 percent reduction

   d) Arctic and standard, 200 hours on diesel: 4 percent reduction.

10. The reduction in engine power when operated on diesel after conclusion of the 200-hour pump stand tests with each of the pumps was approximately half that observed with Jet A-1.

11. The reduction in engine power after conclusion of the 200-hour tests was due to:

    a) Severe drive tang wear on the standard pump with neat Jet A-1
    b) Decreased fuel delivery.

12. The standard BOCLE wear test accurately reflects wear of lightly loaded pump components with a standard metallurgy.

13. The BOCLE was normally directionally correct for more highly loaded components with a standard metallurgy; however, use of different fuel compositions may reduce the correlation observed. The BOCLE failed to predict severe wear of a single highly loaded component with a "good lubricity" fuel.

14. Bench wear tests indicate that use of improved metallurgy such as M-50 steel (which reflects the metallurgy of the arctic component) reduces both corrosive wear under lightly loaded conditions and greatly delays the onset of scuffing and seizure.

15. The improved metallurgy in the arctic components is largely independent of fuel lubricity and so cannot be expected to correlate with the BOCLE results. However, the BOCLE results are not contradictory.

16. A wear scar diameter of greater than approximately 0.65 mm in the standard BOCLE test as specified in ASTM D 5001-89 appears to correspond to the onset of severe wear in the fuel injection system.

17. Qualitatively correct agreement was achieved between nonstandard wear tests performed using the Cameron-Plint apparatus and highly loaded components and also components that contain an improved metallurgy.

18. A direct correlation does not appear to exist between mild corrosive wear, as predicted by the BOCLE, and scuffing load capacity.

63

19. Oxidative wear was the primary material removal process with neat Jet A-1, and produced a brown oxide coating on the inside of the pump and in the fuel reservoir. This deposit was not visible on the remaining pumps tested with better lubricity fuels.

20. The effects of alternate wear mechanisms introduced by high-sulfur fuels on the correlation achieved between the BOCLE and the pump is unclear.

21. Pump seizure may be promoted by rapid cooling of the pump, or by passing hot fuel through a relatively cool pump. This seizure mode is not affected by either the viscosity or the lubricity of the fuel.

22. Most commercially available jet fuels have higher viscosity than those used in the present work, and so should provide greater hydrodynamic/elastohydrodynamic protection.

23. Both bench tests and theoretical calculations indicate that the reduced viscosity of either Jet A-1 or JP-8 should not alone promote pump failure.

24. The addition of higher viscosity lubricating oils (<5 percent conc.) should not significantly increase hydrodynamic film strength.

25. Use of low-viscosity fuels at high temperatures may contribute to hot-restart problems.

XI. RECOMMENDATIONS

The following recommendations are made as a result of this study:

1. In areas **outside arctic** applications (i.e., Alaska), continuous use of neat Jet A-1 should be discontinued in Stanadyne pumps.

2. JP-8 or equivalent appears to provide acceptable pump durability.

3. The metallurgy in the arctic components represents a significant improvement and should be used if possible.

4. The results from the present limited study indicate that a BOCLE wear scar diameter of approximately 0.65 mm corresponds to the minimum acceptable fuel lubricity.

5. The following areas require further study:

    a) The effects of temperature on fuel system wear. For example, until data to the contrary are obtained, continuous use of Jet A-1/DF-A fuel on year-round basis in arctic areas such as Alaska is judged to be acceptable.

    b) The effects of sulfur content and fuel composition in general on fuel system wear and its relation to the standard bench wear tests.

    c) Scuffing wear and its measurement.

    d) The effects of fuel lubricity on the durability of other fuel injection systems besides Stanadyne, especially unit injector systems.

XII. REFERENCES

1. American Society for Testing and Materials Standard D 1655, "Aviation Turbine Fuel, Grades Jet A-1/Jet A," 1989.

2. Military Specification MIL-T-83133C, "Turbine Fuels, Aviation Turbine Kerosene Types," NATO F-34 (JP-8) and NATO F-35, 22 March 1990.

3. Datschefski, G., "History, Development and Status of the Ball-on-Cylinder Lubricity Evaluator for Aero Gas Turbine Fuels," A report prepared under MOD contract AE12a/193, by the Esso Research Center, Abingdon, Oxfordshire, OX136AE, UK.

4. American Society for Testing and Materials Method D 5001-89, "Test Method for Measurement of Lubricity of Aviation Turbine Fuels by the Ball on Cylinder Lubricity Evaluator (BOCLE)," ASTM, 1916 Race Street, Philadelphia, PA, 1989.

5. Department of Defense Directive 4140.43, subject: "Fuel Standardization," March 1988.

6. "Development of Military Fuel/Lubricant/Engine Compatibility Test," Coordinating Research Council, Inc., New York, NY, Final Report, January 1967.

7. Engine Compatibility Test, 240-Hour Tracked Vehicle Cycle Using 6V-53T Engine, prepared by U.S. Army Fuels and Lubricants Research Laboratory, Southwest Research Institute, San Antonio, TX, 6V-53T Test No. 39, 14 March 1984.

8. "Accelerated Fuel-Engines Qualification Procedures Methodology Engine Test 210-Hour Wheeled Vehicle Cycle Using the Cummins NHC-250 Diesel Engine Operating on JP-8 Fuel," prepared by U.S. Army Fuels and Lubricants Research Laboratory, Southwest Research Institute, San Antonio, TX, October 1985.

9. "Accelerated Fuel-Engines Qualification Procedures Methodology Engine Test 210-Hour Wheeled Vehicle Cycle Using the GM 6.2L Diesel Engine Operating on JP-8 Fuel," prepared by U.S. Army Fuels and Lubricants Research Laboratory, Southwest Research Institute, San Antonio, TX, October 1985.

10. "Accelerated Fuel-Engines Qualification Procedures Methodology Engine Test 400-Hour NATO Qualification Cycle Using the GM 6.2L Diesel Engine Operating on JP-8 Fuel," prepared by U.S. Army Fuels and Lubricants Research Laboratory, Southwest Research Institute, San Antonio, TX, January 1986.

11. "10,000 Mile JP-8 Fuel Test of 6.2L Diesel Engines in M1028 CUCV Vehicles", prepared by General Motors Corporation Military Vehicles Operations, STS CUCV % PROJECT REQUEST 87-027, Warren, MI, July 1987.

12. Montemayor, A.F. and Owens, E.C., "Comparison of 6.2L Arctic and Standard Fuel Injection Pumps Using JP-8 Fuel," Interim Report BFLRF No. 232 (AD A175597), prepared by Belvoir Fuels and Lubricants Research Facility (SwRI), Southwest Research Institute, San Antonio, TX, October 1986.

13. Lacey, P.I. and Lestz, S.J., "Fuel Lubricity Requirements for Diesel Injection Systems," Interim Report BFLRF No. 270 (AD A235972), prepared by Belvoir Fuels and Lubricants Research Facility (SwRI), Southwest Research Institute, San Antonio, TX, February 1991.

14. LePera, M.E., Trip Report to Belvoir Fuels and Lubricants Research Facility (SwRI), Southwest Research Institute, San Antonio, TX, 13-14 January 1987.

15. Appeldoorn, J.K. and Dukek, W.G., "Lubricity of Jet Fuels," SAE Paper No. 660712, Society of Automotive Engineers, Warrendale, PA, 1966.

16. Butler, W.E., Jr., Alvarez, R.A., Yost, D.M., Westbrook, S.R., Buckingham, J.P., and Lestz, S.J., "Field Demonstration of Aviation Turbine Fuel MIL-T-83133C, Grade JP-8 (NATO Code F-34) at Fort Bliss, TX, Interim Report BFLRF No. 264 (AD A233441), prepared by Belvoir Fuels and Lubricants Research Facility (SwRI), Southwest Research Institute, San Antonio, TX, December 1990.

17. Bowden, J.N. and Westbrook, S.R., "A Survey of JP-8 and JP-5 Properties," Interim Report BFLRF No. 253 (AD A207721), prepared by Belvoir Fuels and Lubricants Research Facility (SwRI), Southwest Research Institute, San Antonio, TX, September 1988.

18. LePera, M.E., "Investigation of the Use of Jet A-1 Fuel During Operation Desert Shield," Trip Report, Travel Order Number 11534, 2-13 December 1990.

19. Tonnemaker, F.M., Logistics Assistance Special Report: Use of Jet A-1 Fuel in Generators, TROSCOM LAR, 101st Airborne Div-SWA, Saudi Arabia, 15 January 1991.

20. Lacey, P.I. and Lestz, S.J., "Failure Analysis of Fuel Injection Pumps From Generator Sets Fueled With Jet A-1," Interim Report BFLRF No. 268 (AD A234930), prepared by Belvoir Fuels and Lubricants Research Facility (SwRI), Southwest Research Institute, San Antonio, TX, January 1991.

21. Lacey, P.I. and Lestz, S.J., "Wear Analysis of Diesel Engine Fuel Injection Pumps From Military Ground Equipment Fueled With Jet A-1," Interim Report BFLRF No. 272 (AD A239022), prepared by Belvoir Fuels and Lubricants Research Facility (SwRI), Southwest Research Institute, San Antonio, TX, May 1991.

22. NATO Pipeline Committee Working Group NO4 Ground Fuels Working Party (AC/112 (WG4) (GFWP), "Report of Tests Performed in France," September 1989.

23. "Stanadyne Injection Pump Specification for Customer Part No. 23500415," Stanadyne Diesel Systems, P.O. Box 1440, Hartford, CT 06143.

24. Federal Specification VV-F-800D, "Fuel Oil, Diesel," Grade DF-2, 27 October 1987.

25. Stanadyne Service Bulletin No. 125R1, "Field Conversions for Low Viscosity Fuel Operation," December 1990.

26. Grabel, L., "Lubricity Properties of High Temperature Jet Fuel," Naval Air Propulsion Test Center, NAPTC-PE-112, August 1977.

27. Henderson, P., Information Exchange at U.S. Army Tank-Automotive Command, Warren, MI, August 1991.

28. Military Specification MIL-I-25017E, "Inhibitor, Corrosion/Lubricity Improver, Fuel Soluble (Metric)," 15 June 1989.

29. Military Specification MIL-I-53021A, "Stabilizer Additive, Diesel Fuel," 15 August 1988.

30. "Fuels, Mobility Users Handbook," MIL-HDBK-114A, July 1990.

31. Roosa Master Service Bulletin, No. 203 R1, January 1965.

32. Raimondi, A.A. and Boyd, J., "A Solution of the Finite Journal Bearing and its Application to Analysis and Design", Parts I, II, and III," *Trans* ASLE, 1, No. 1, pp. 159-209.

33. *Wear Control Handbook*, Ed. M.B. Peterson and W.O. Winer, pp. 82-86, ASME 1980

34. "Operation and Instruction Manual Model DB2 Pump," Stanadyne Diesel Systems, P.O. Box 1440, Hartford, CT 06143.

35. Owen, K. and Coley, T., "Automotive Fuels Handbook," published by Society of Automotive Engineers, Inc., 400 Commonwealth Drive, Warrendale, PA, 1990.

36. Meeting With Representatives of H & S Co., 1st. Tank Battalion, 1st Marine Division, Camp Pendleton, CA, 12-16 August 1991.

37. Archard, J.F., "Contact and Rubbing of Flat Surfaces." *J. Appl. Phys.*, 24, pp. 981-988, 1953.

38. Northon, P.E., "Final Report Development Test II (PQT-G) (Desert) of High Mobility Multipurpose Wheeled Vehicle (HMMWV)," U.S. Army Tank-Automotive Command, Warren, MI 48090, November 1982.

39. Black, B.H. and Wechter, M.A., "The Lubricity Properties of Jet Fuel as Measured by the Ball-on-Cylinder Lubricity Evaluator," American Chemical Society, Division of Fuel Chemistry, Vol. 35, No. 2, 1990.

40. Likos, W.E., Owens, E.C., and Lestz, S.J., "Laboratory Evaluation of MIL-T-83133 JP-8 Fuel in Army Diesel Engines," Interim Report BFLRF No. 232 (AD A205281), prepared by Belvoir Fuels and Lubricants Research Facility (SwPI), Southwest Research Institute, San Antonio, TX, January 1988.

41. Tao, F.F. and Appeldoorn, J.K., "The Ball on Cylinder Test for Evaluating Jet Fuel Lubricity," *Trans.*, ASLE, 11, pp. 345-352, 1968.

42. Wei, D. and Spikes H.A., "The Lubricity of Diesel Fuels," *Wear*, 111, 2, 1986.

43. Appeldoorn, J.K., Goldman, I.B., and Tao, F.F., "Corrosive Wear by Atmospheric Oxygen and Moisture," *Trans.*, ASLE, 12, pp. 140-150, 1969.

44. Pilling, N.B. and Bedworth, R.E., *J. Inst. Metals*, 529, 1923.

45. Furey, M.J., "Metallic Contact and Friction Between Sliding Surfaces," *Trans.*, ASLE, 4, pp. 1-11, 1961.

46. Hadley, J.W. and Blackhurst, P., "An Appraisal of the Ball-on-Cylinder Technique for Measuring Aviation Turbine Fuel Lubricity," STLE, Vol. 47, 5, pp. 404-411, 1991.

47. Cuellar, J.P., Jr., "Advanced Thermally Stable Jet Fuels Development Program Annual Report, Volume III Fuel Lubricity," Aero Propulsion and Power Laboratory, Wright Research and Development Center, Air Force Systems Command, Wright-Patterson Air Force Base, OH, January 1991.

48. Biddle, T.B. and Edwards, W.H., "Evaluation of Corrosion Inhibitors as Lubricity Improvers," AF Wright Aeronautical Laboratories, AD A198743, July 1988.

49. Edwards, W.H., Biddle, T.B., "Determination of Corrosion Inhibitor Content in Aviation Fuels," Topical Report No. 7, F33615-85-C-2508, March 1987.

50. Henderson, P. (Stanadyne Automotive), Telephone Conversation With M.E. LePera, U.S. Army Belvoir Research, Development and Engineering Center, Fort Belvoir, VA, 8 February 1991.

51. Lowe, G.R. and Hughes, F. Report Rolls Royce/Lucas No. 3, February 1987.

52. Kanakia, M.D. and Moses, C.A., "Study of Mechanisms of Fuel Lubricity," Letter Report BFLRF No. 250, prepared by Belvoir Fuels and Lubricants Research Facility (SwRI), Southwest Research Institute, San Antonio, TX, August 1989.

APPENDIX A

Stanadyne Fuel Injection Pump

Stanadyne Fuel Injection Pump

The manufacturer describes this pump as a single-cylinder, opposed plunger, inlet metering, distributor type. Power is transmitted to the pump by a removable drive shaft, connected to the pump rotor through a drive tang. A weak point is provided in the drive shaft to protect the engine in case of pump seizure. Fuel is drawn into the unit by a positive displacement, vane-type transfer pump. During normal operation, a precisely metered volume of fuel passes from the transfer pump to the hydraulic head at relatively low pressure (<130 psi). The volume of fuel transferred is defined by a metering valve, the position of which is determined by the throttle setting and a centrifugal governor. Fuel is forced from the hydraulic head at high pressure by two plungers and is sent to the appropriate injector connection through a distributor rotor. The final component in the pump mechanism is a delivery valve that ensures a sharp fuel cut off at the end of the delivery cycle.

A schematic diagram of the Stanadyne DB2 series pump is shown in Fig. A-1. The mechanical configuration of the DB, DB2 and DC pumps are very similar, although subtle differences exist in both metallurgy and configuration.

The DB and DC series pumps are designed to operate on low-viscosity/lubricity fuels. Critical components within the pumps have an improved metallurgy, corresponding to the "arctic" conversion for the standard DB2 pump. The Rockwell hardness of a number of standard and arctic components is given in TABLE A-1. The increased hardness of the arctic parts would be expected to decrease adhesive and abrasive wear, although its effect on corrosive wear is less well defined.

EXPLODED VIEW

1. NUT, drive shaft	36. SHAFT ASSY., shut-off	71. WEIGHT, governor
2. WASHER, drive shaft	37. SEAL, torque screw	72. RETAINER ASSY., gov weight
3. SHAFT, drive	38. SCREW, torque	73. CAM RING
4. SEAL, drive shaft	39. NUT, torque screw	74. SEAL, hydraulic head
5. HOUSING ASSY., pump	40. NUT, pivot shaft	75. HEAD AND ROTOR ASSY
6. SEAL, pump flange	41. SEAL, pivot shaft	76. SCREW, leaf spring
7. SCREW, head locking	42. SHAFT, gov. arm pivot	77. SPRING, leaf
8. SCREW ASSY., vent	43. SCREWS, nameplate	78. ROLLER, cam
9. SPRING, metering valve	44. PLATE, name	79. SHOE, cam roller
10. VALVE, metering	45. SCREW, timing line cover	80. PLUNGERS
11. SHIM, metering valve	46. COVER, timing line	81. FITTING, discharge
12. ARM ASSY., metering valve	47. GASKET, timing line cover	82. SEAL, locking plate
13. ARM, governor	48. WASHER, guide stud	83. PLATE, locking
14. SPRING, linkage hook	49. STUD, guide	84. SCREW, locking plate
15. SPRING, governor	50. NUT, adv. adj. screw	85. VALVE, delivery
16. LINKAGE ASSY., gov. hook adj	51. SEAL, adv. adj. screw	86. SPRING, delivery valve
17. RETAINER, spring	52. SCREW, advance adjusting	87. STOP, delivery valve
18. SPRING, idling	53. PLUG, piston hole (trimmer side)	88. SCREW, delivery valve
19. GUIDE, idling spring	54. SEAL, piston hole plug	89. SEAL, transfer pump
20. LEVER, throttle shaft	55. GUIDE, adv adj. spring	90. RETAINERS, rotor
21. CAM, shut-off	56. SPRING, advance adjusting	91. LINER, transfer pump
22. GASKET, governor cover	57. PISTON, spring	92. BLADES, transfer pump
23. COVER, governor control	58. WASHER, slide	93. SPRINGS, transfer pump blade
24. WASHER, cover screw	59. PISTON, power	94. RING, liner locating
25. LOCK WASHER, cover screw	60. SEAL, piston ring	95. ROLLPIN, regulator
26. SCREW, cover hold-down	61. RING, piston	96. SEAL, inlet filter screen
27. CONNECTOR ASSY., return line	62. PLUG, piston hole (power side)	97. REGULATOR ASSY., transfer pump
28. SCREW, low idle adjusting	63. SCREW, cam advance	98. SEAL, inlet filter screen
29. NUT, low idle screw	64. SEAL, advance hole plug	99. PISTON, regulating
30. SCREW, high idle adjusting	65. PLUG, advance screw hole	100. SPRING, regulating
31. NUT, high idle screw	66. SEAL, head locating screw	101. PLUG ASSY., end plate adjusting
32. SHAFT ASSY., throttle	67. SCREW ASSY., head locating	102. RING, filter screen retaining
33. WASHER, throttle shaft seal	68. SLEEVE, governor thrust	103. SCREEN, inlet filter
34. SEAL, throttle shaft	69. WASHER, gov. thrust sleeve	104. PLATE, transfer pump pressure
35. SEAL, shut-off shaft	70. RING, gov. cage retaining	105. CAP, transfer pump end

(Figure A-1 presented in "Operation and Instruction Manual DB2 Pump," Stanadyne Diesel Systems, Inc., P.O. Box 1440, Hartford, CT.)

Figure A-1. Exploded diagram of the Stanadyne DB2 series pump

74

TABLE A-1. Rockwell Hardness of Standard and Arctic Components

Item	Standard Component, HRC	Arctic Component, HRC
TRANSFER PUMP		
Liner	43	63
Vanes	44	67
Rotor Retainer	51	--
HYDRAULIC HEAD		
Cam Ring	64	--
Roller	64	--
Shoe	67	--
Governor Weight	34	--
ROTOR		
Drive Tang (DB2)	55	55
Drive Splines (DC)	55	--

APPENDIX B

Pump Calibration Stand Results

Pump Calibration Stand Measurements

Both the pretest and post-test pump calibration series were performed at a local San Antonio Stanadyne-appointed dealer, with a BFLRF member staff present. Initially, the pumps were set to within the limits specified in "Stanadyne Injection Pump Specification for Customer Part No. 23500414." In addition, the exact values were recorded in each instance for comparison with the post-test measurements.

The test stand conformed to ISO 4008 with SAE 0968/ISO 7440 calibrating injectors. The calibration fluid was Viscor conforming to SAE 0967/ISO 4113. The fluid supply temperature to the pump was maintained between 110° to 115°F (43° to 46°C) at a pressure of 5 ± 0.5 psi (34.5 ± 3 kPa).

The pump was operated for 10 minutes prior to calibration to allow the system to stabilize. The computerized stand provided a digital readout of pump delivery per stroke at the required test speeds, eliminating errors. Injection advance is measured by a mechanical attachment that follows the movement of the cam ring (commonly known as a bat wing gauge).

Results From Pretest Calibration of Fuel Pumps

TABLE B-1. Pretest Pump Delivery

Pump No.	Delivery, mm³/St at rpm				
	75	200	1000	1800	1950
Spec.	>29	>47	51 to 55	>46	>44
1	38.1	50.7	53.4	53.6	51.1
2	42.8	51.0	53.3	52.0	49.1
3	42.2	51.3	54.0	54.0	51.6
4	41.4	50.2	53.0	52.6	50.1
5	38.2	51.1	54.6	52.9	51.1
6	41.6	50.8	53.5	53.0	50.7
7	39.9	50.2	54.1	54.1	51.1
8	42.1	51.5	53.1	51.7	49.8
9	40.1	51.6	54.4	52.8	51.0
10	44.9	51.8	53.1	52.1	51.0

NOTE: Readings at wide open throttle (St = Stroke).

TABLE B-2. Pretest Transfer Pump Pressure

Pump No.	Pressure, psi at rpm			
	75	1000	1800	2100
Spec.	>12	70 to 76	70 to 76	<135
1	--	75	--	130
2	27	73	--	130
3	20	75	--	120
4	24	73	--	133
5	24	75	--	135
6	26	73	--	130
7	25	75	--	135
8	25	73	--	130
9	20	75	--	130
10	25	73	--	130

NOTE: Readings at wide open throttle.

TABLE B-3. Pretest Injection Advance Measurement

Pump No.	Advance, degrees on pump			
Speed	325	1000	1600	1600
Throttle	LI	WOT	WOT	LI
Spec.	>1.5	0.5 to 2.5	4.2 to 6.7	<10
1	3.0	1.5	6.0	10
2	3.5	1.5	5.5	10
3	3.0	1.5	5.5	10
4	2.5	1.5	6.0	10
,	3.0	1.5	6.0	10
6	3.0	1.5	5.5	10
7	3.0	1.5	6.0	10
8	2.5	1.5	5.5	10
9	3.0	1.5	6.0	10
10	2.5	1.5	4.7	10

NOTE: LI = Low Idle: WOT = Wide Open Throttle.

TABLE B-4. Pretest Sundry Measurements

Pump No.	RF	SO	BA
Units	cc/min	mm³/St	mm³/St
Spec.	225 to 375	<4	<8
1	350	0	0
2	200	0	0
3	375	0	1
4	200	0	0
5	350	0	0
6	200	0	0
7	350	0	0.7
8	200	0	2.8
9	375	0	0
10	225	0	0

NOTE: RF = Return Fuel From Housing to Tank.
SO = Shut Off Fuel Flow.
BA = Fuel Flow at Break-Away Speed (2100 pump rpm).
St = Stroke.

Results From Post-Test Calibration of Fuel Pumps

TABLE B-5. Post-Test Pump Delivery

Pump No.	Delivery, mm³/St at rpm				
	75	200	1000	1800	1950
Spec.	>29	>47	51 to 55	>46	>44
1	35.4	49.5	51.6	51.1	51.3
2	39.9	50.5	51.9	51.5	50.0
3	38.4	50.1	52.5	52.5	50.5
4	40.3	50.0	51.6	51.0	49.7
5	36.4	50.1	53.1	52.1	50.2
6	39.3	50.0	53.0	52.2	50.8
7	35.7	50.0	52.8	52.5	50.2
8	37.9	49.1	52.4	51.0	48.7
9	38.7	50.8	54.0	52.9	50.8

NOTE: Readings at wide open throttle (St = Stroke).

TABLE B-6. Post-Test Transfer Pump Pressure

Pump No.	Pressure, psi at rpm			
	75	1000	1800	2100
Spec.	>12	70 to 76	70 to 76	<135
1	18	68	96	115
2	18	66	95	123
3	17	70	98	120
4	23	72	104	134
5	21	73	105	120
6	24	72	99	126
7	24	76	107	129
8	24	73	103	129
9	20	75	106	128

NOTE: Readings at wide open throttle.

TABLE B-7. Post-Test Injection Advance Measurement

Pump No.	Advance, degrees on pump			
Speed	325	1000	1600	1600
Throttle	LI	WOT	WOT	LI
Spec.	>1.5	0.5 to 2.5	4.2 to 6.7	<10
1	2.5	0.5	4.5	10
2	2.2	0.5	4.5	10
3	3.0	1.7	5.0	10
4	2.2	0.5	5.0	9.5
5	2.5	0.5	5.0	10
6	3.2	1.5	5.0	10
7	2.7	2.0	5.5	9.7
8	2.5	1.5	5.5	10
9	3.0	1.7	5.7	9.7

NOTE: LI = Low Idle; WOT = Wide Open Throttle.

TABLE B-8. Post-Test Sundry Measurements

Pump No.	RF	SO	BA
Units	cc/min	mm³/St	mm³/St
Spec.	225 to 375	<4	<8
1	325	0	1.6
2	200	0	47
3	450	0	48
4	200	0	47
5	375	0	0
6	200	0	0.4
7	375	0	0
8	220	0	47
9	375	0	0

NOTE: RF = Return Fuel From Housing to Tank.
SO = Shut Off Fuel Flow.
BA = Fuel Flow at Break-Away Speed (2100 pump rpm).
St = Stroke.

APPENDIX C

Engine Test Procedure and Results

Engine Test Procedure and Results

The engine tests were performed using a General Motors (GM) 6.2L engine with the specifications given in TABLE C-1. The engine was completely overhauled prior to testing, with new injectors (Bosch NA52X with DNOSD 248 Nozzle) and piston rings fitted. The normal opening pressure on each injector was established to be 1900 psi. The run-in procedure defined in the GM 210-hour wheeled vehicle cycle endurance test* was used.

The power curve was defined from 1400 to 3600 rpm in 200 rpm increments. The engine was warmed up prior to testing for 30 minutes at 1200 rpm and allowed to stabilize for 10 minutes between each test speed. The fuel return from the governor housing was collected in a day tank at the inlet side of the pump. A fuel flow meter was connected prior to the day tank to measure the net volume of fuel burned.

Test results are illustrated in Figs. C-1 through C-36.

TABLE C-1. Specifications of the General Motors 6.2L Diesel Engine†

Engine Type	Naturally aspirated, Ricardo Swirl Precombustion Chamber, Four-Stroke, Compression Ignition.
No. of Cylinders, arrangement	8, V
Displacement, liters (in^3)	6.2 (380)
Bore × stroke, mm (in)	101 × 97 (3.98 × 3.82)
Rated Power, kW (Bhp)	107.7 (145) (With HMMWV Pump)
Rated Torque, N•m (ft-lb)	325 (240)
Engine Structure	Cast Iron Head and Block (no cylinder liners), Aluminum Pistons
Injection System	Stanadyne DB-2 F/I Pump With Bosch Pintle Injectors

---

* "Accelerated Fuel-Engines Qualification Procedures Methodology Engine Test 210-Hour Wheeled Vehicle Cycle Using the GM 6.2L Diesel Engine Operating on JP-8 Fuel," prepared by U.S. Army Fuels and Lubricants Research Laboratory, Southwest Research Institute, San Antonio, TX, October 1985.

† Likos, W.E., Owens, E.C., and Lestz, SJ., "Laboratory Evaluation of MIL-T-83133 JP-8 Fuel in Army Diesel Engines," Interim Report BFLRF No. 233 (AD A205281), prepared by Belvoir Fuels and Lubricants Research Facility (SwRI), Southwest Research Institute, San Antonio, TX, January 1988.
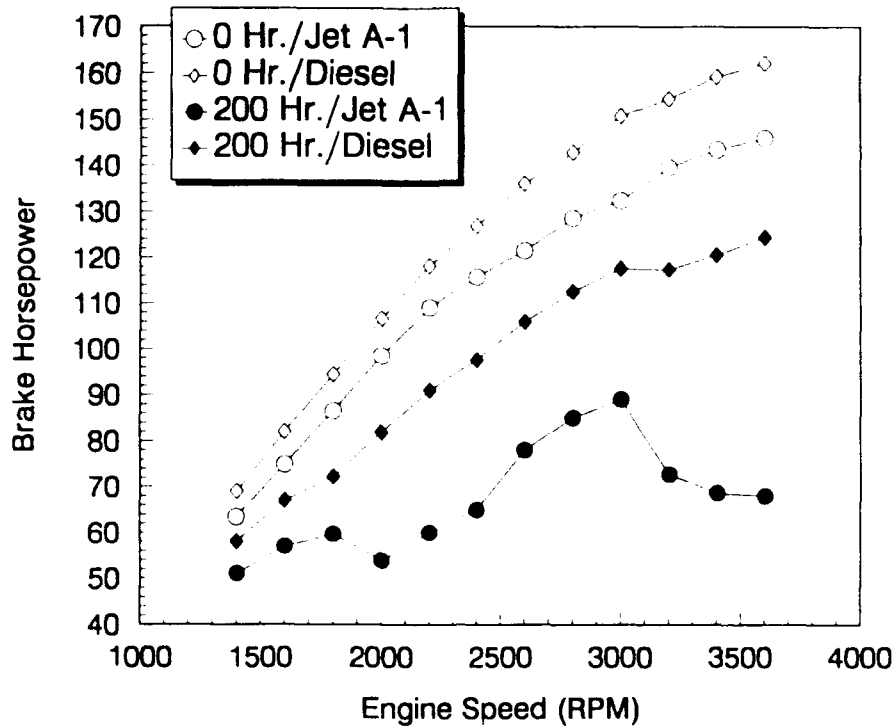
(Standard pump - tested for 200 hours on neat Jet A-1)

Figure C-1. Engine power curves for Pump No. 1
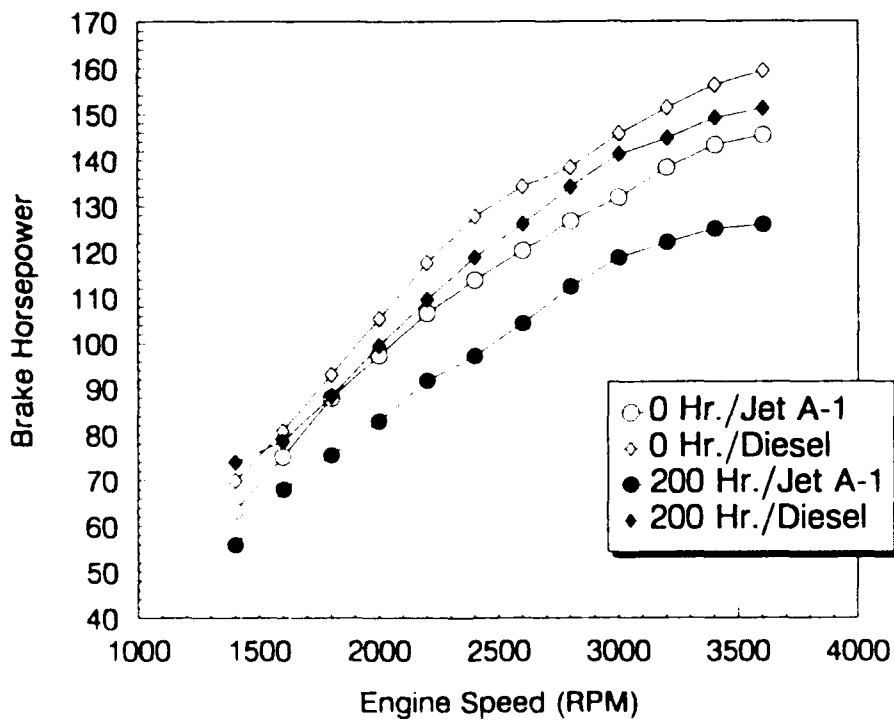
(Arctic pump - tested for 200 hours on neat Jet A-1)

Figure C-2. Engine power curves for Pump No. 2
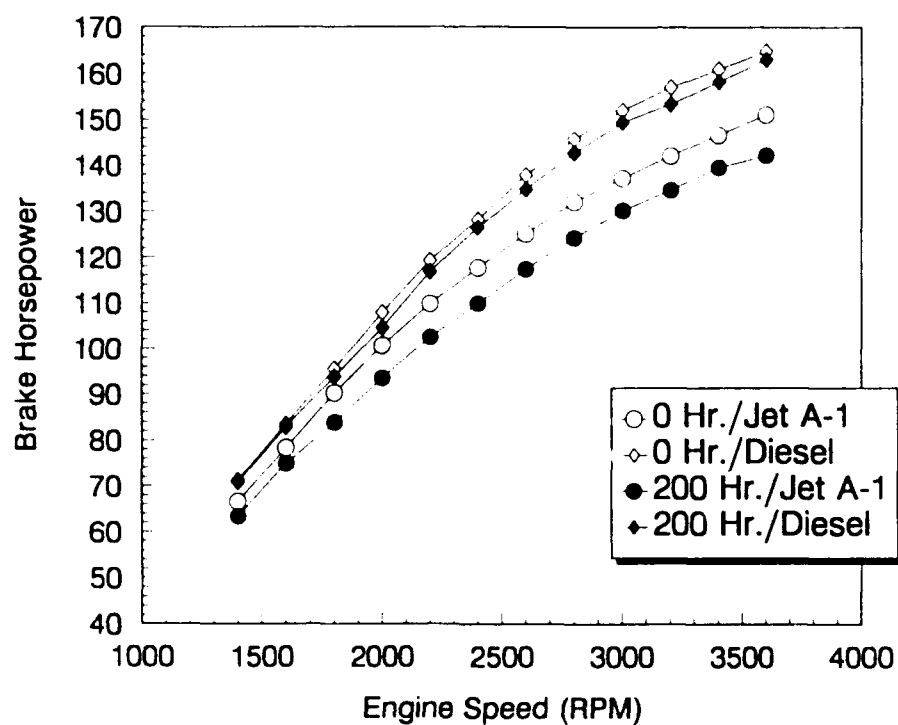
(Standard pump - tested for 200 hours on neat Jet A-1 + DCI-4A)

Figure C-3. Engine power curves for Pump No. 3
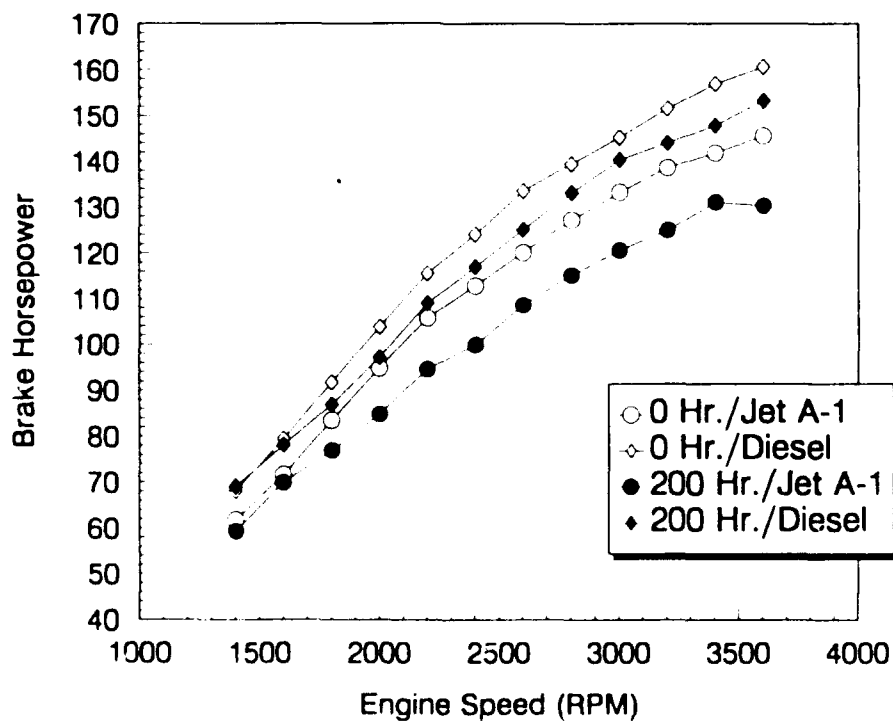
(Arctic pump - tested for 200 hours on neat Jet A-1 + DCI-4A)

Figure C-4. Engine power curves for Pump No. 4

87
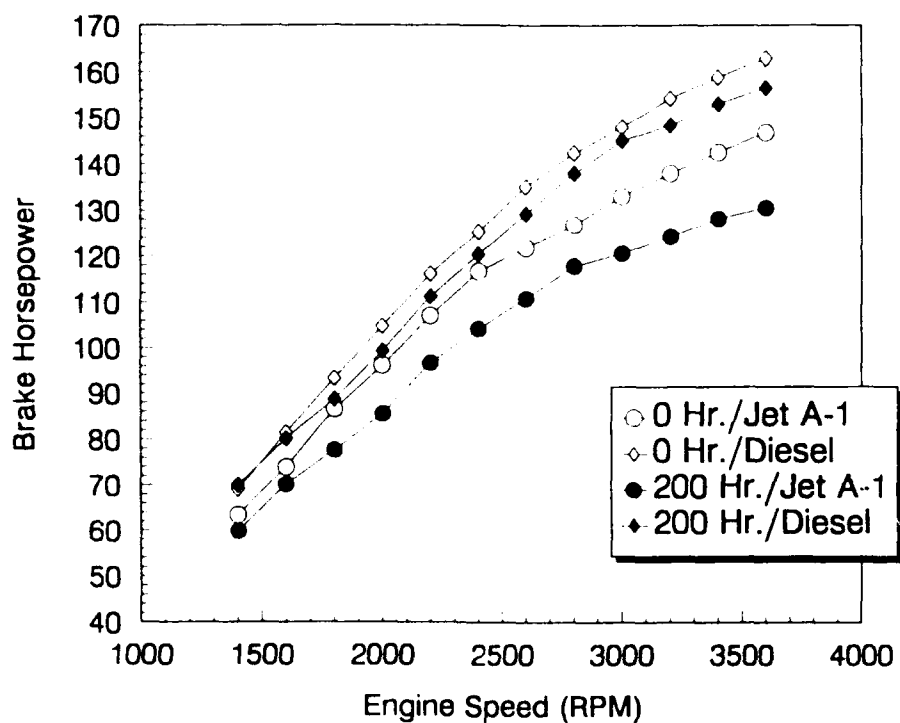
(Standard pump - tested for 200 hours on Jet A-1 + BIOBOR-JF/FOA-15)

Figure C-5. Engine power curves for Pump No. 5
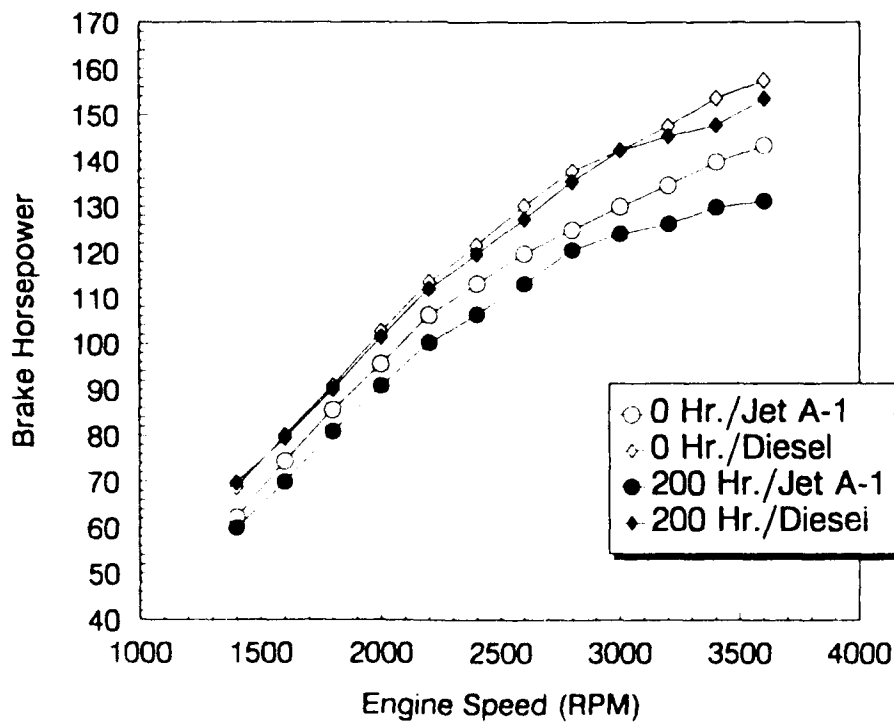
(Arctic pump - tested for 200 hours on Jet A-1 + BIOBOR-JF/FOA-15)

Figure C-6. Engine power curves for Pump No. 6
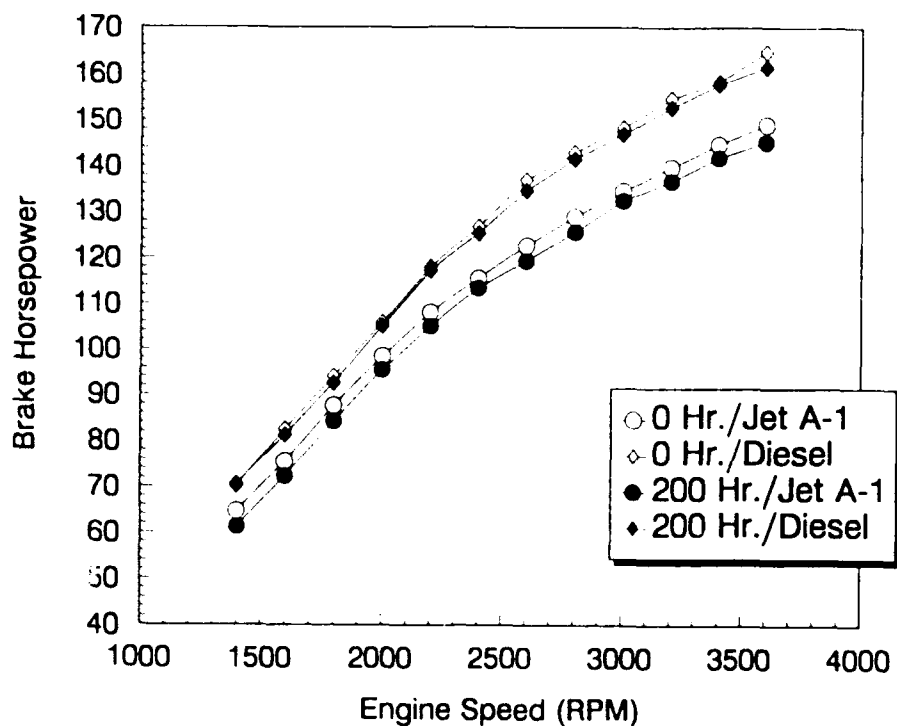
(Standard pump - tested for 200 hours on diesel)

Figure C-7. Engine power curves for Pump No. 7
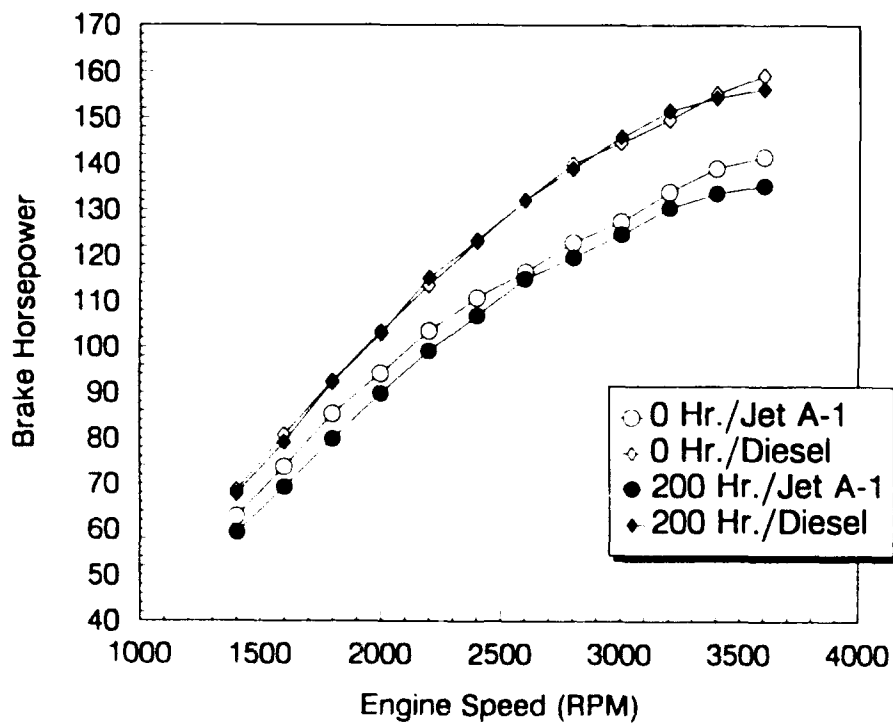
(Arctic pump - tested for 200 hours on diesel)

Figure C-8. Engine power curves for Pump No. 8
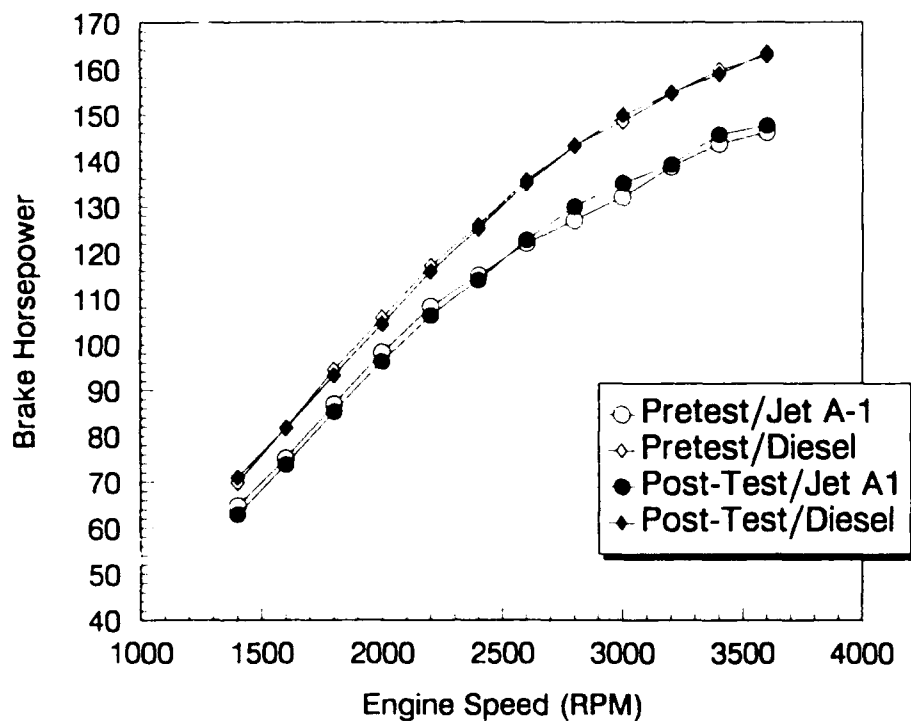
(Reference pump - standard unit, never tested on stand)

Figure C-9. Engine power curves for Pump No. 9
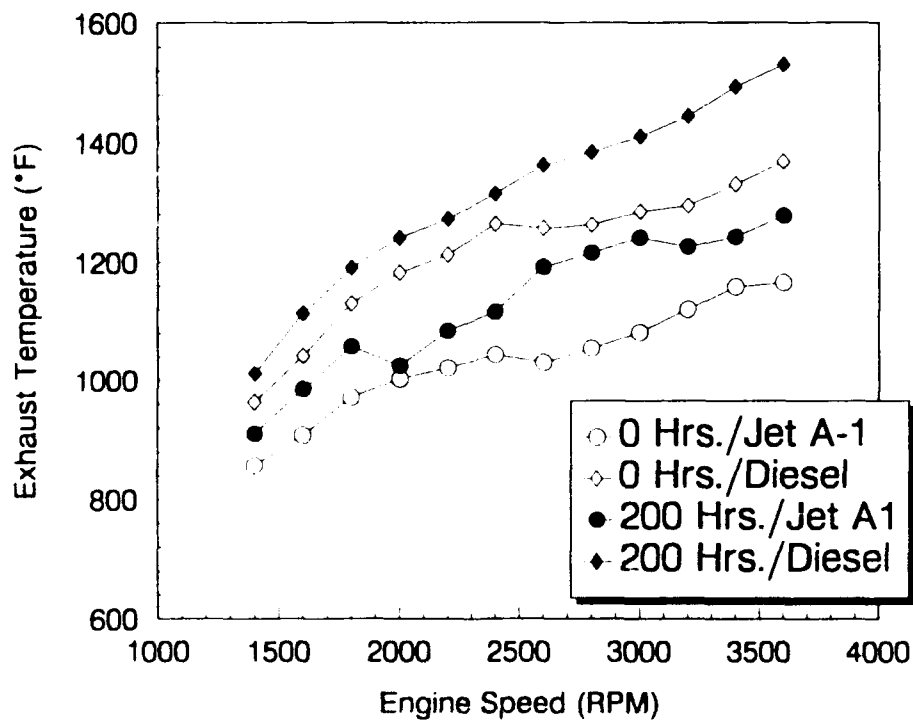
(Standard pump - tested for 200 hours on neat Jet A-1)

Figure C-10. Average exhaust temperature during engine tests with Pump No. 1

90
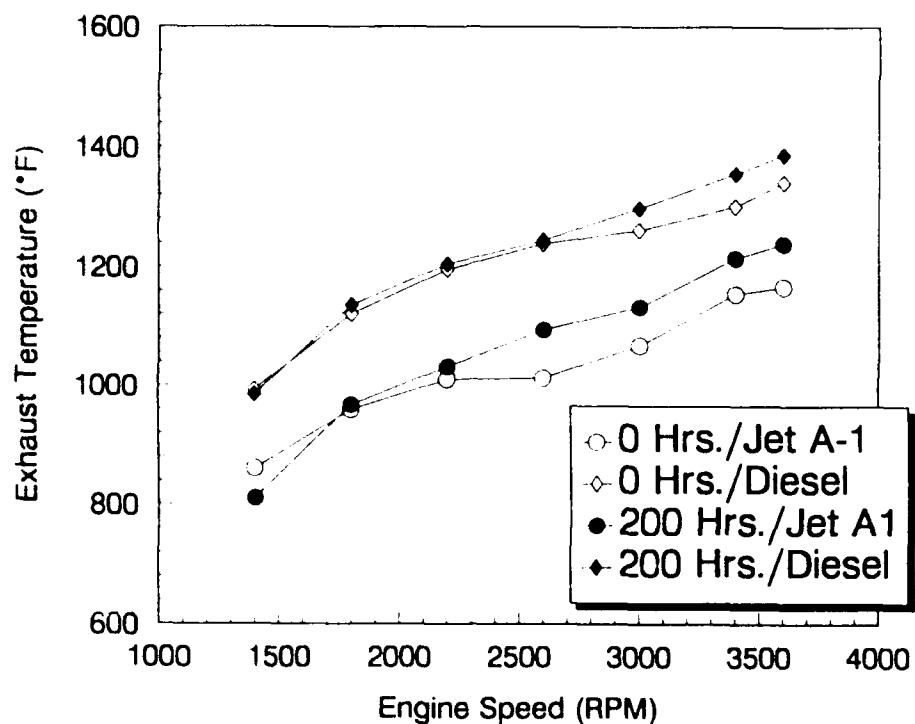
(Arctic pump - tested for 200 hours on neat Jet A-1)

Figure C-11. <u>Average exhaust temperature during engine tests with Pump No. 2</u>
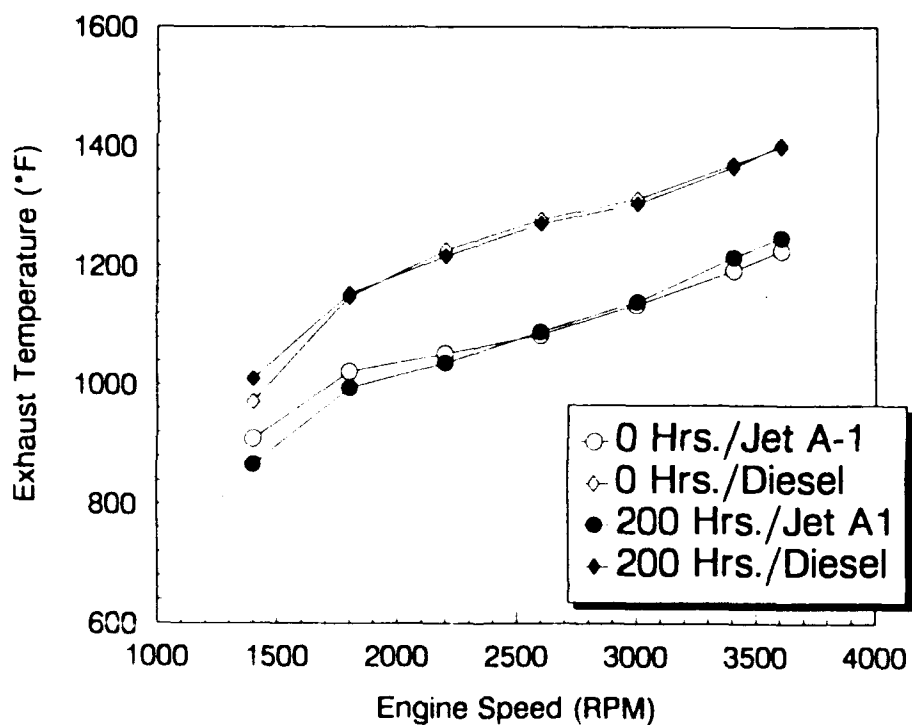
(Standard pump - tested for 200 hours on Jet A-1 + DCI-4A)

Figure C-12. <u>Average exhaust temperature during engine tests with Pump No. 3</u>
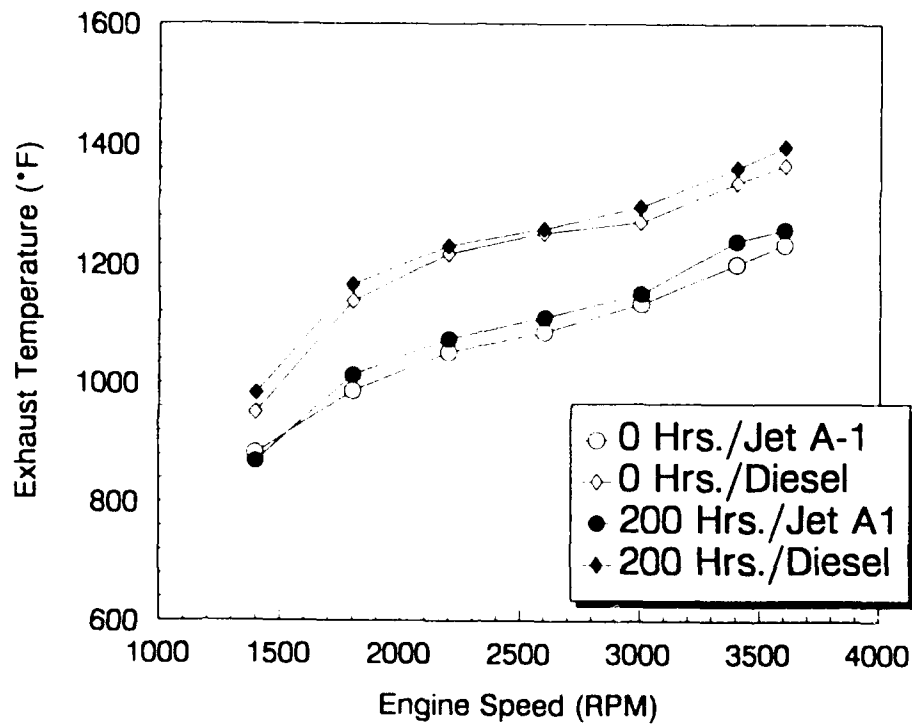
(Arctic pump - tested for 200 hours on Jet A-1 + DCI-4A)

Figure C-13. **Average exhaust temperature during engine tests with Pump No. 4**
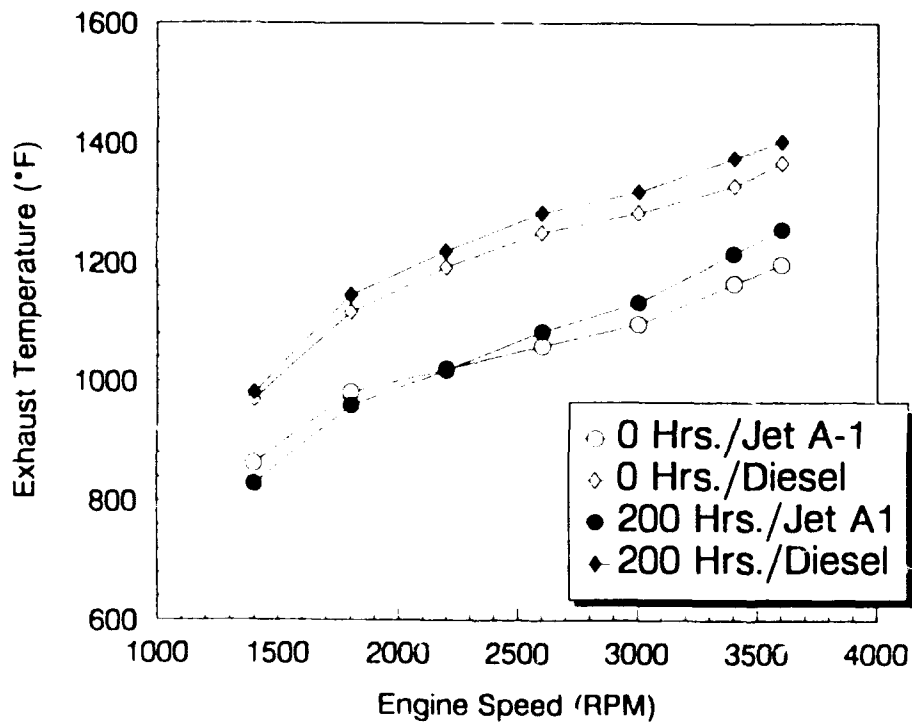
(Standard pump - tested for 200 hours on Jet A-1 + BIOBOR-JF/FOA-15)

Figure C-14. **Average exhaust temperature during engine tests with Pump No. 5**
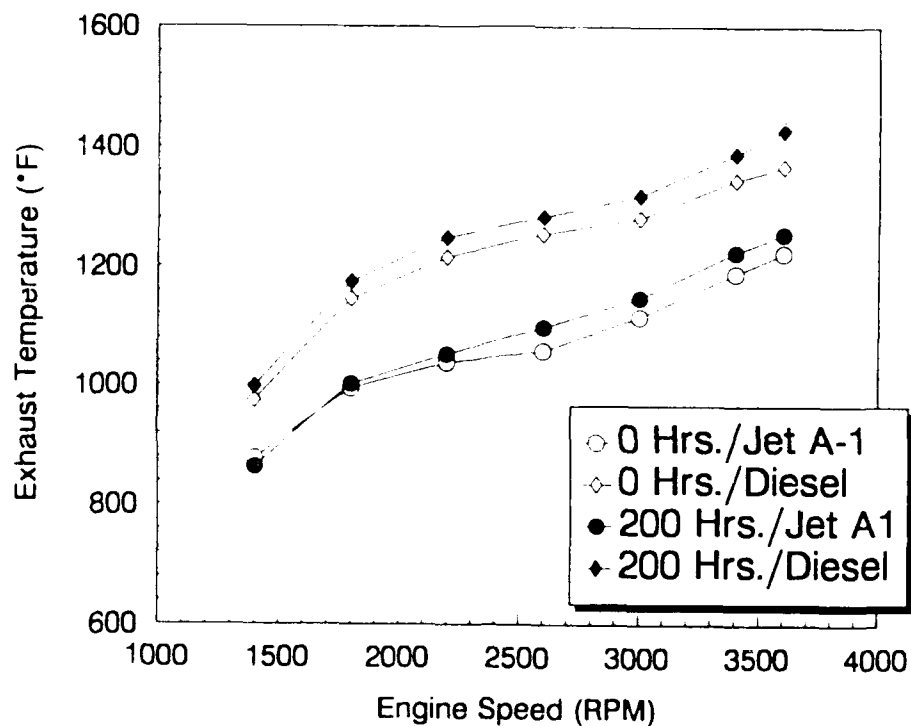
(Arctic pump - tested for 200 hours on Jet A-1 + BIOBOR-JF/FOA-15)

Figure C-15. Average exhaust temperature during engine tests with Pump No. 6
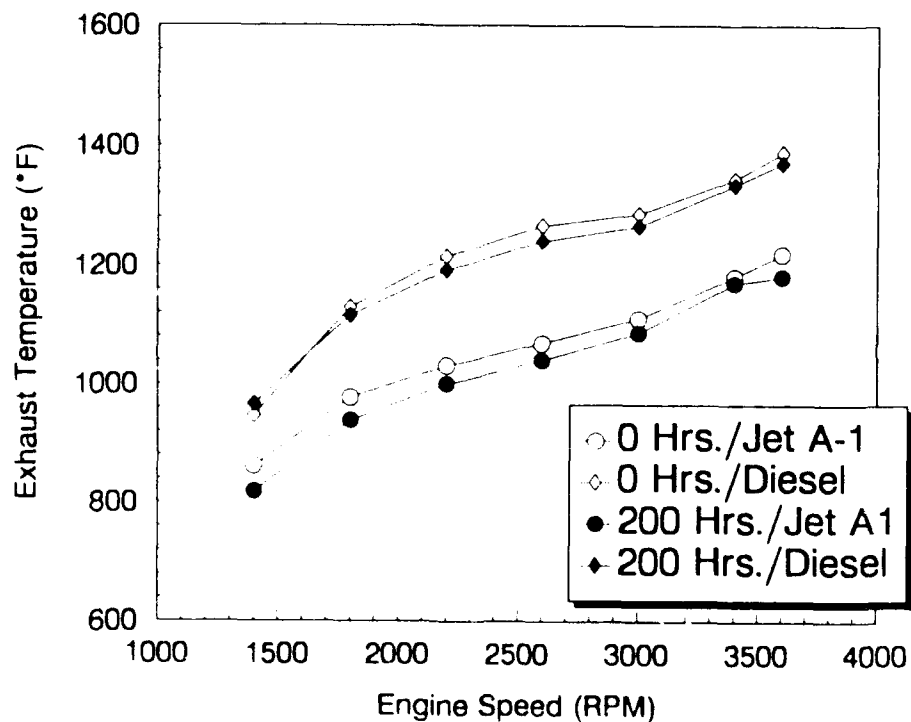
(Standard pump - tested for 200 hours on diesel fuel)

Figure C-16. Average exhaust temperature during engine tests with Pump No. 7

93
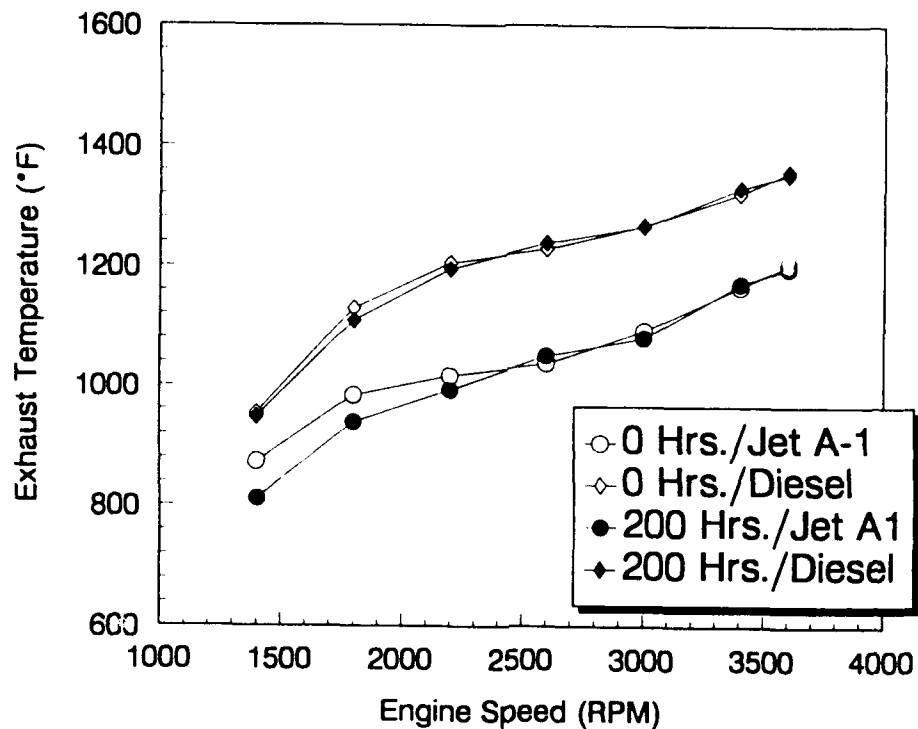
(Arctic pump - tested for 200 hours on diesel fuel)

Figure C-17. **Average exhaust temperature during engine tests with Pump No. 8**
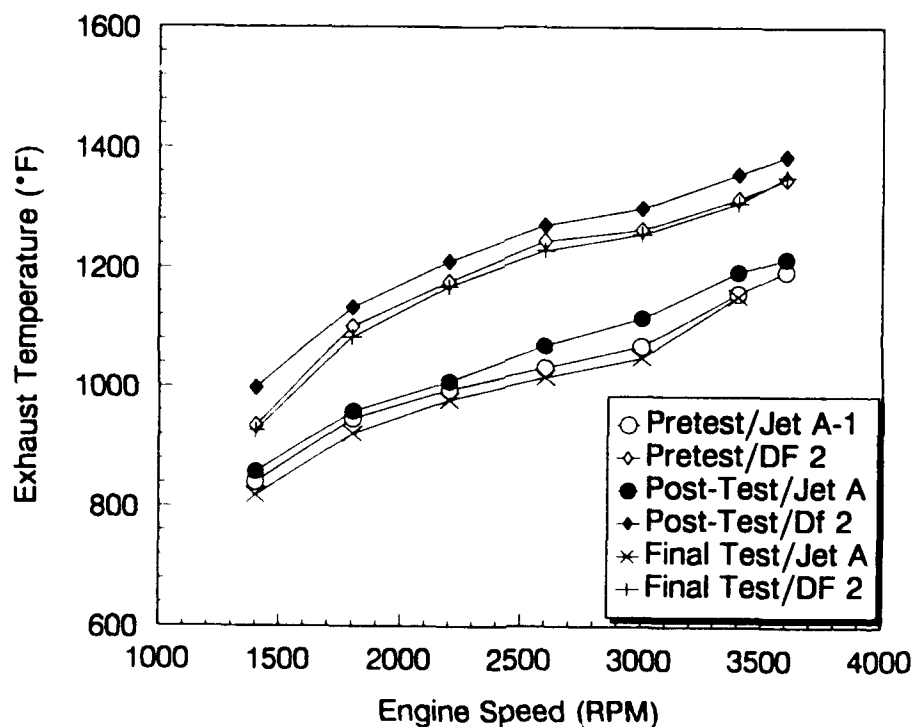
(Reference pump - arctic unit, never tested on pump stand)

Figure C-18. **Average exhaust temperature during engine tests with Pump No. 9**

94
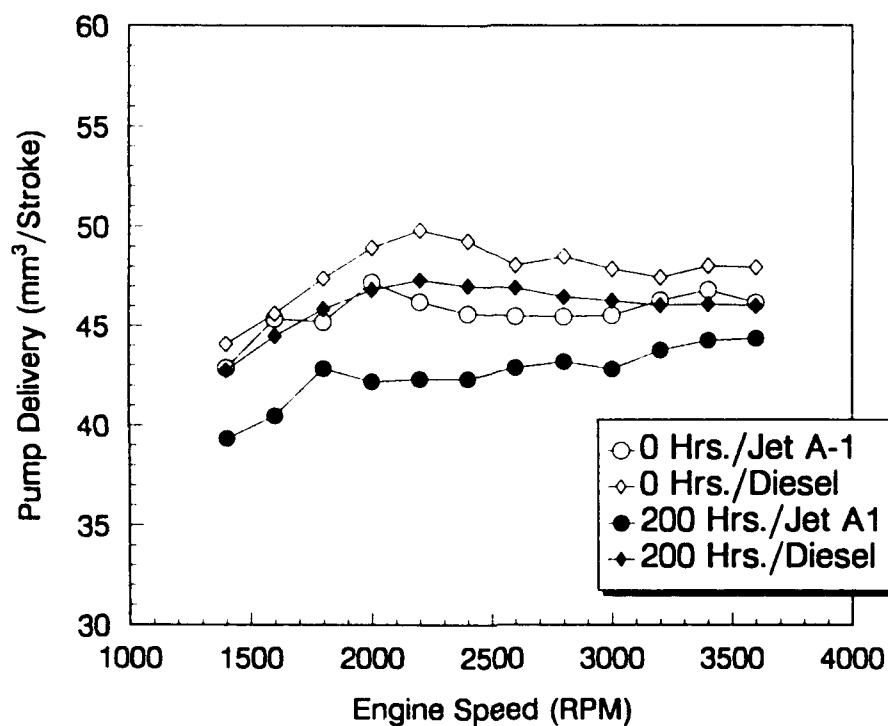
(Standard pump - tested for 200 hours on neat Jet A-1)

Figure C-19. **Fuel delivery during engine tests with Pump No. 1**
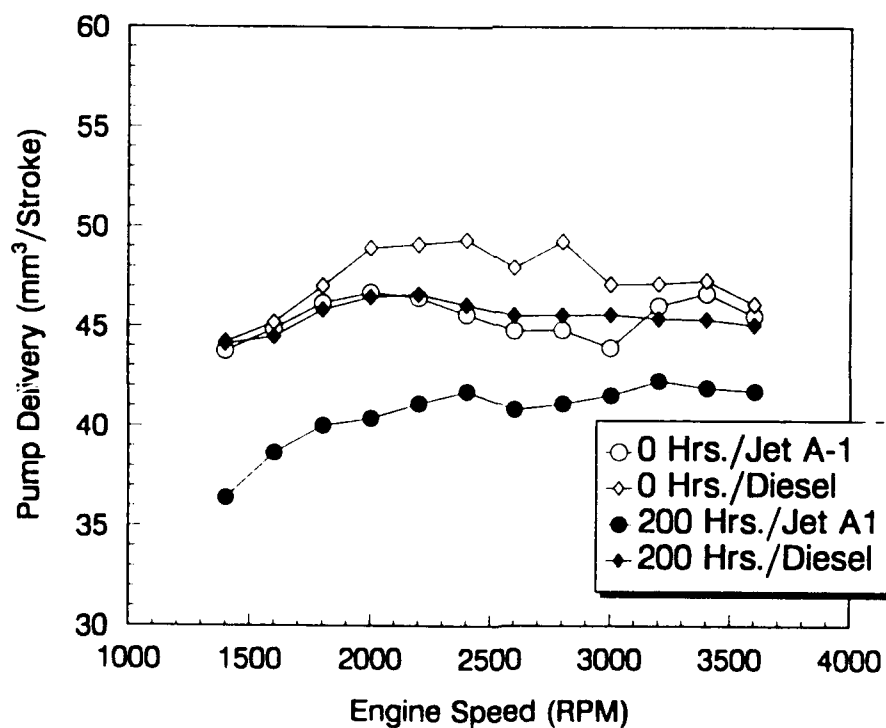
(Arctic pump - tested for 200 hours on neat Jet A-1)

Figure C-20. **Fuel delivery during engine tests with Pump No. 2**
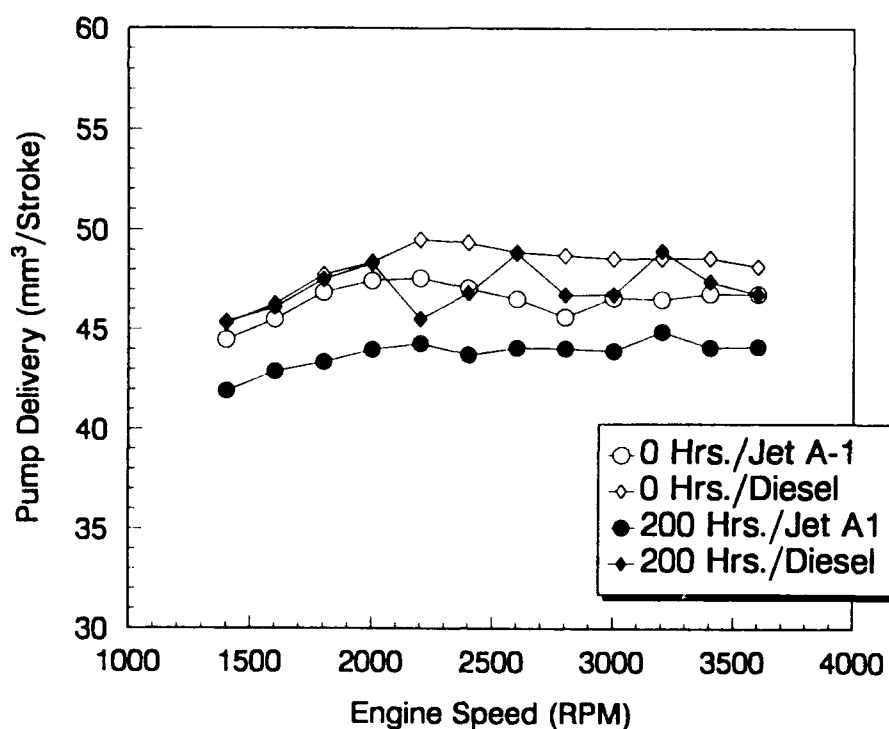
(Standard pump - tested for 200 hours on Jet A-1 + DCI-4A)

Figure C-21. <u>Fuel delivery during engine tests with Pump No. 3</u>
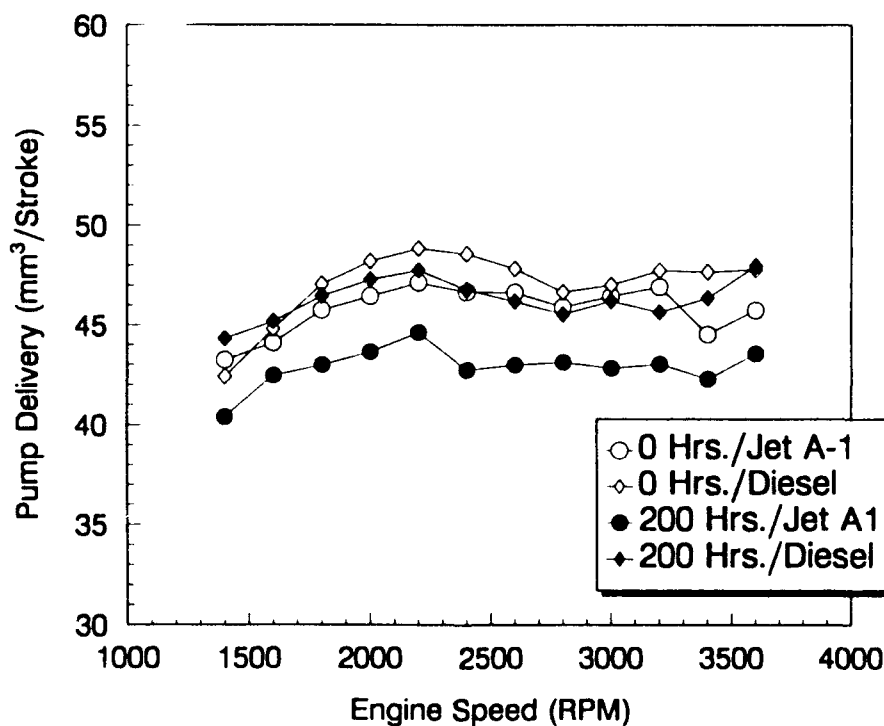
(Arctic pump - tested for 200 hours on Jet A-1 + DCI-4A)

Figure C-22. <u>Fuel delivery during engine tests with Pump No. 4</u>
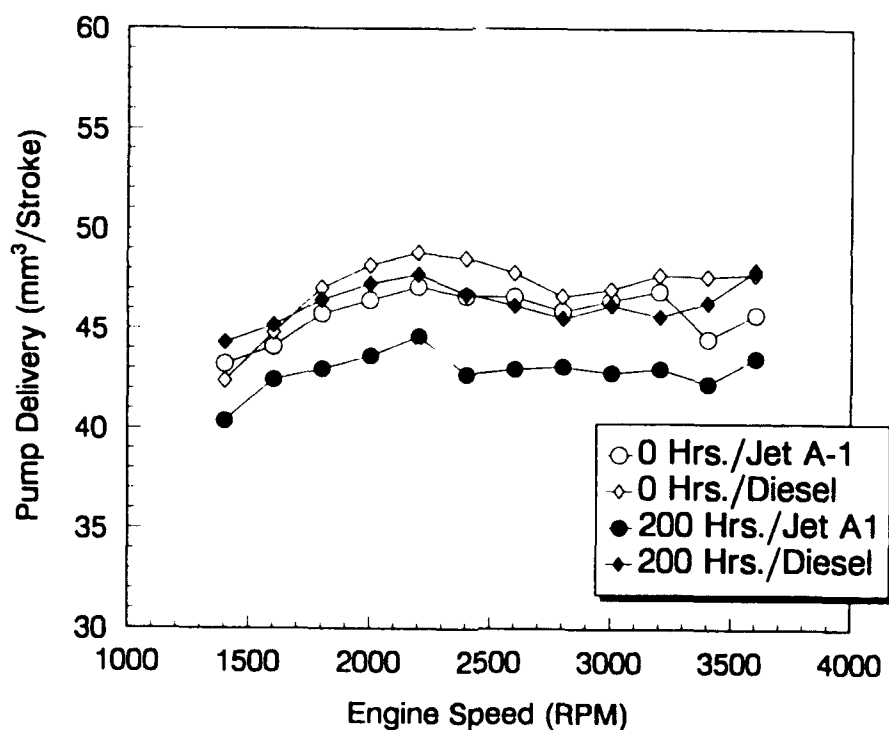
(Standard pump - tested for 200 hours on Jet A-1 + BIOBOR-JF/FOA-15)

Figure C-23. __Fuel delivery during engine tests with Pump No. 5__
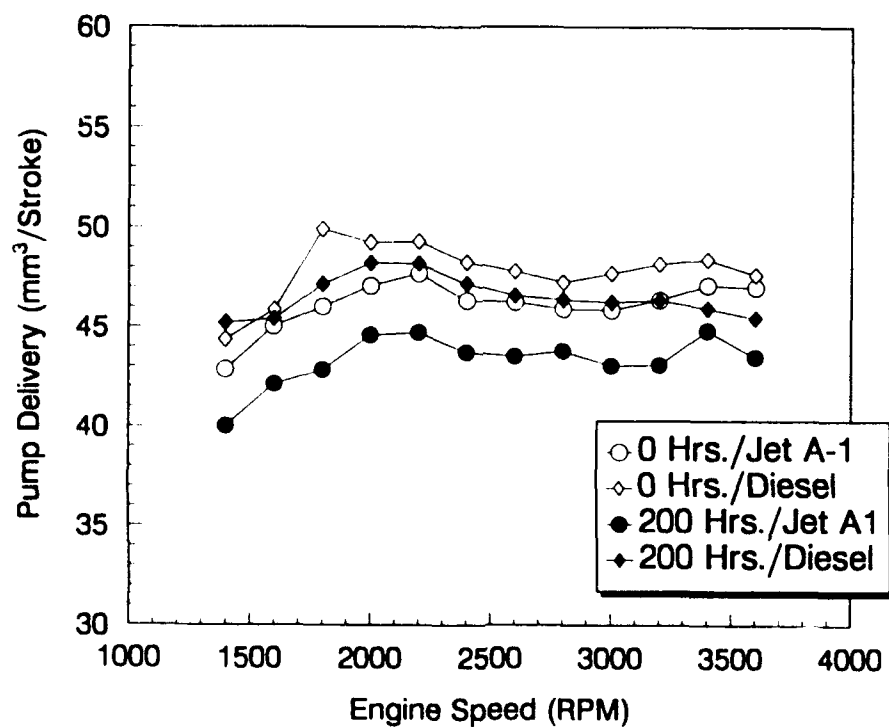
(Arctic pump - tested for 200 hours on Jet A-1 + BIOBOR-JF/FOA-15)

Figure C-24. __Fuel delivery during engine tests with Pump No. 6__
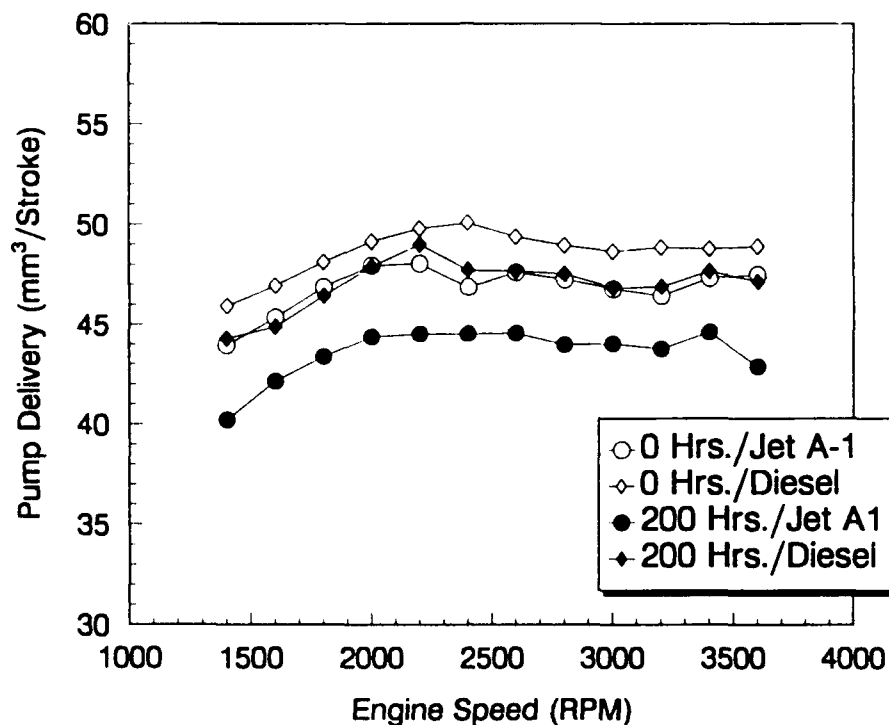
(Standard pump - tested for 200 hours on diesel)

Figure C-25. Fuel delivery during engine tests with Pump No. 7
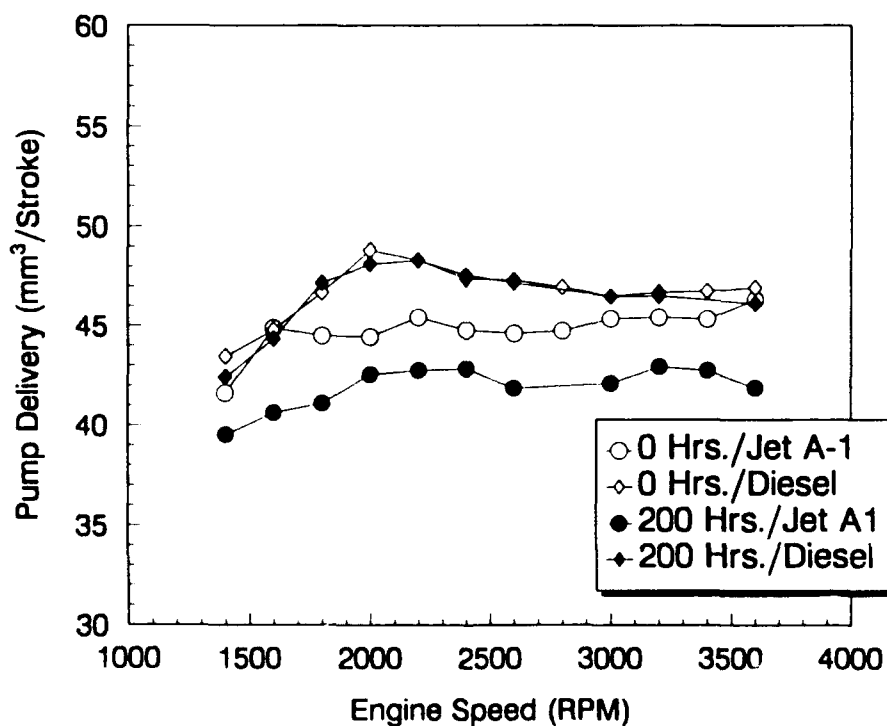
(Arctic pump - tested for 200 hours on diesel)

Figure C-26. Fuel delivery during engine tests with Pump No. 8
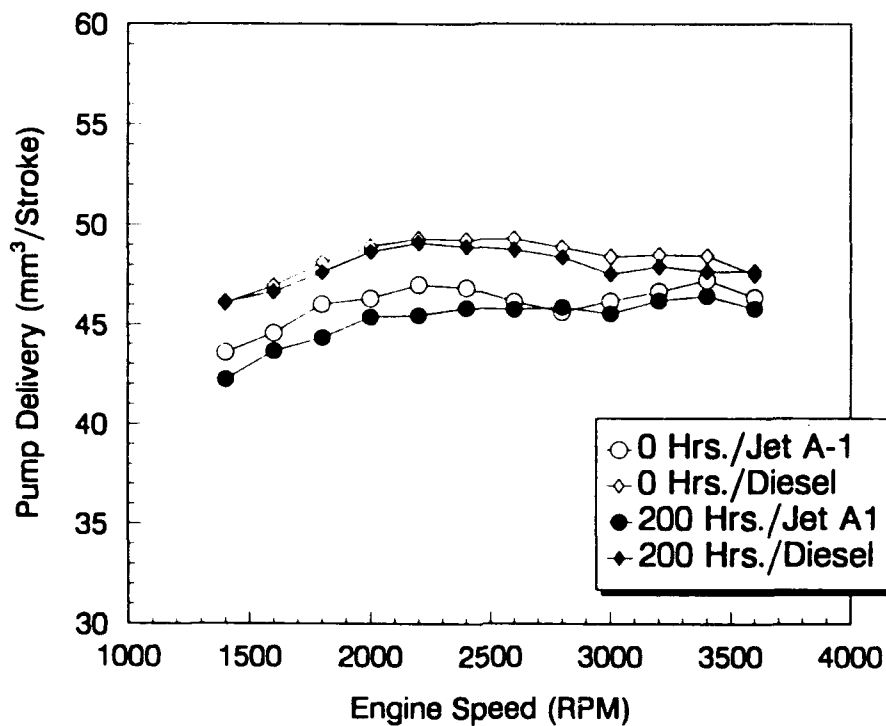
(Reference pump - arctic unit, not tested on pump stand)

Figure C-27. **Fuel delivery during engine tests with Pump No. 9**
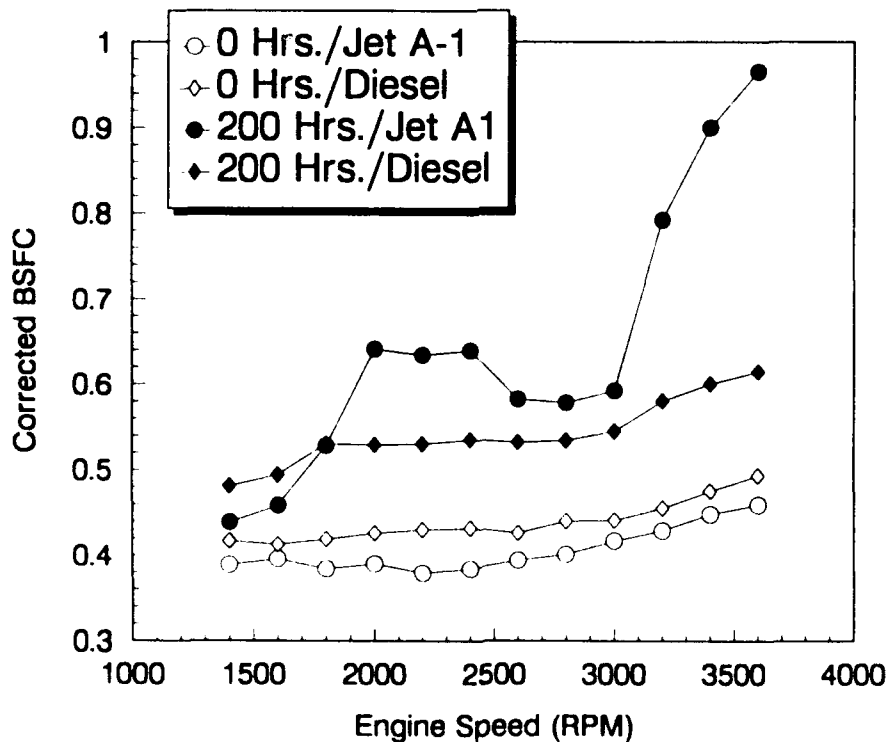
(Standard pump - tested for 200 hours on neat Jet A-1)

Figure C-28. **Brake specific fuel consumption for Pump No. 1 at STP**

99
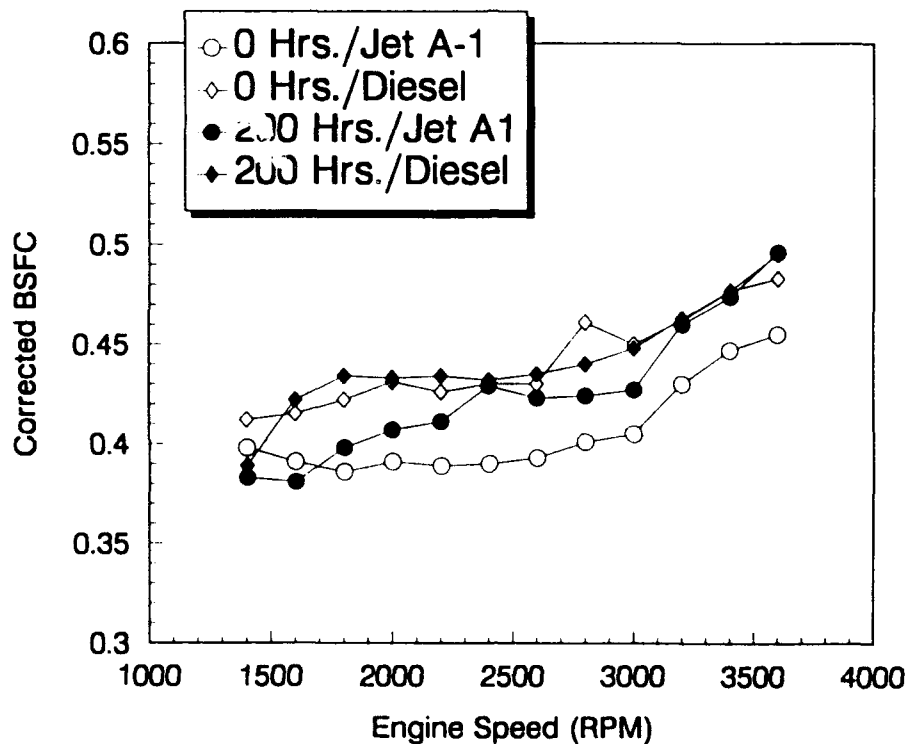
(Arctic pump - tested for 200 hours on neat Jet A-1)

Figure C-29. <u>Brake specific fuel consumption for Pump No. 2 at STP</u>
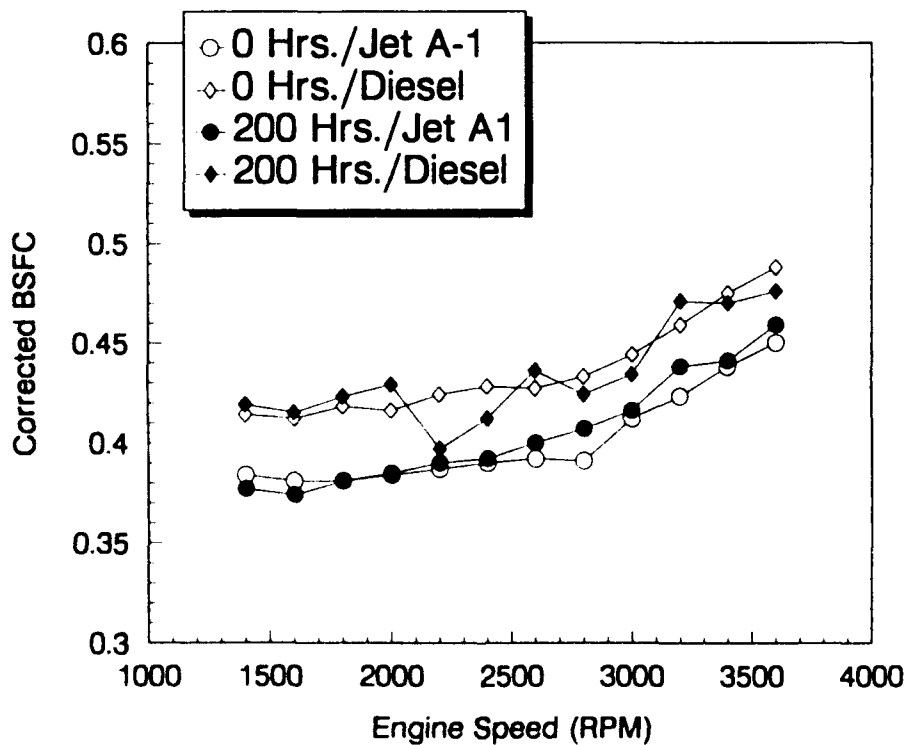
(Standard pump - tested for 200 hours on Jet A-1 + DCI-4A)

Figure C-30. <u>Brake specific fuel consumption for Pump No. 3 at STP</u>

100
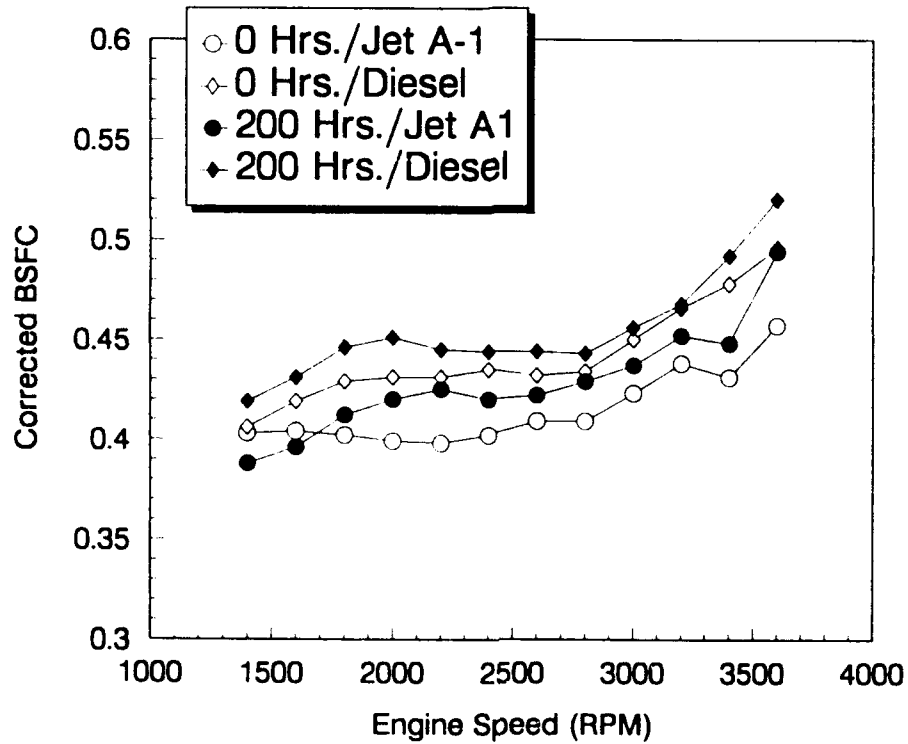
(Arctic pump - tested for 200 hours on Jet A-1 + DCI-4A)

Figure C-31. **Brake specific fuel consumption for Pump No. 4 at STP**
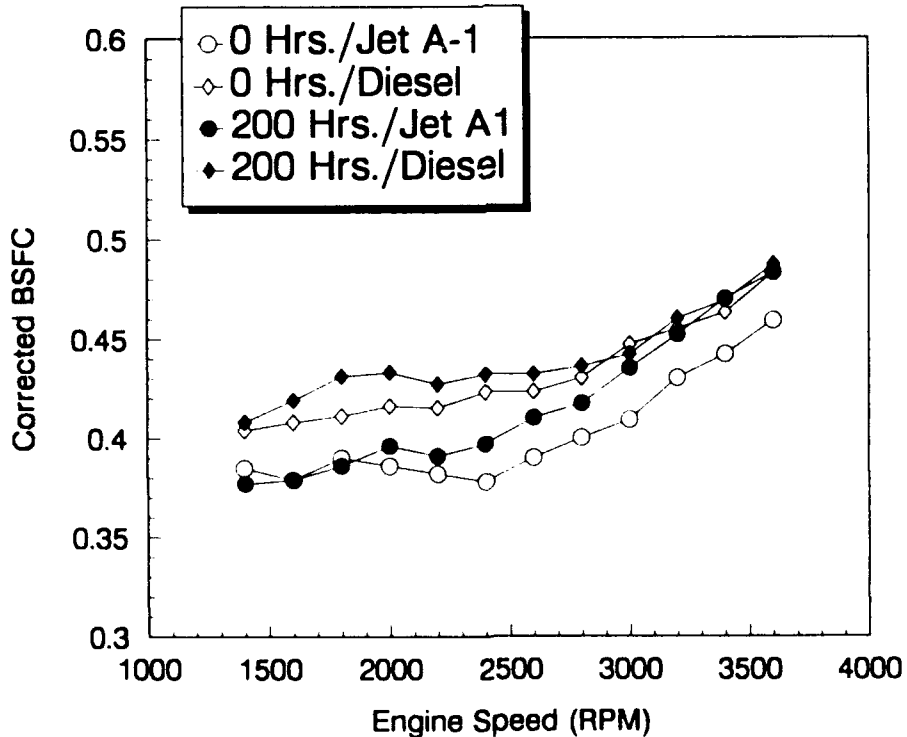
(Standard pump - tested for 200 hours on Jet A-1 + BIOBOR-JF/FOA-15)

Figure C-32. **Brake specific fuel consumption for Pump No. 5 at STP**

101
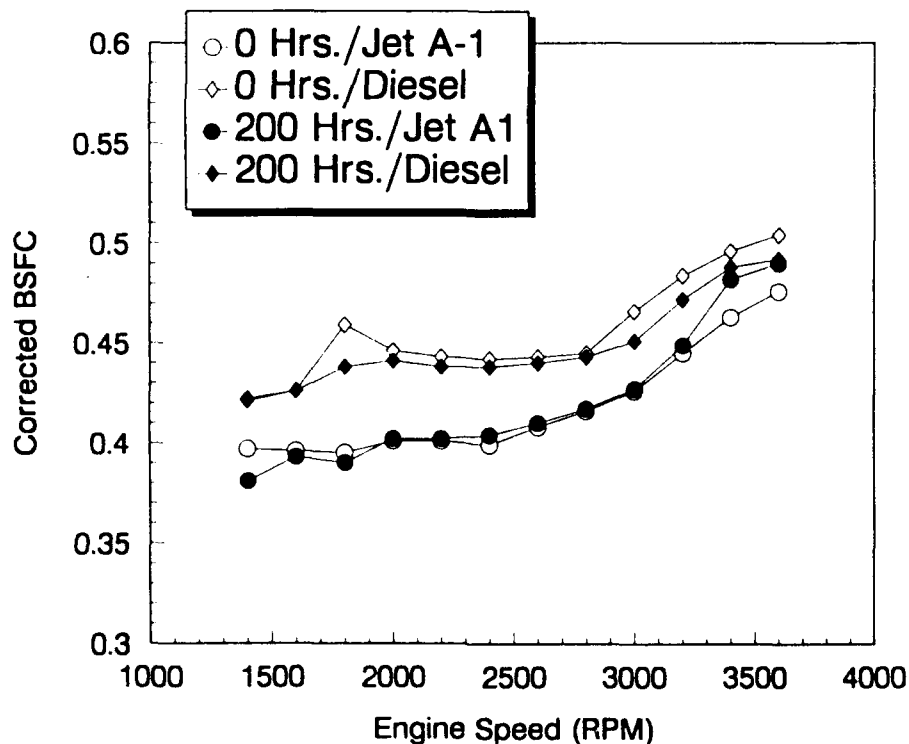
(Arctic pump - tested for 200 hours on Jet A-1 + BIOBOR-JF/FOA-15)

Figure C-33. Brake specific fuel consumption for Pump No. 6 at STP
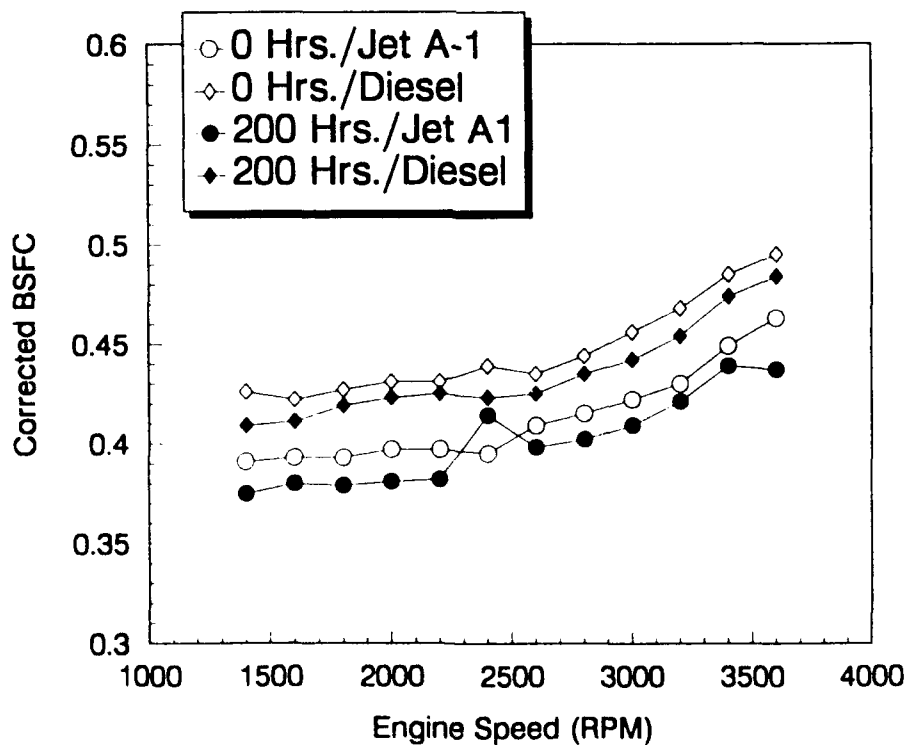
(Standard pump - tested for 200 hours on diesel)

Figure C-34. Brake specific fuel consumption for Pump No. 7 at STP
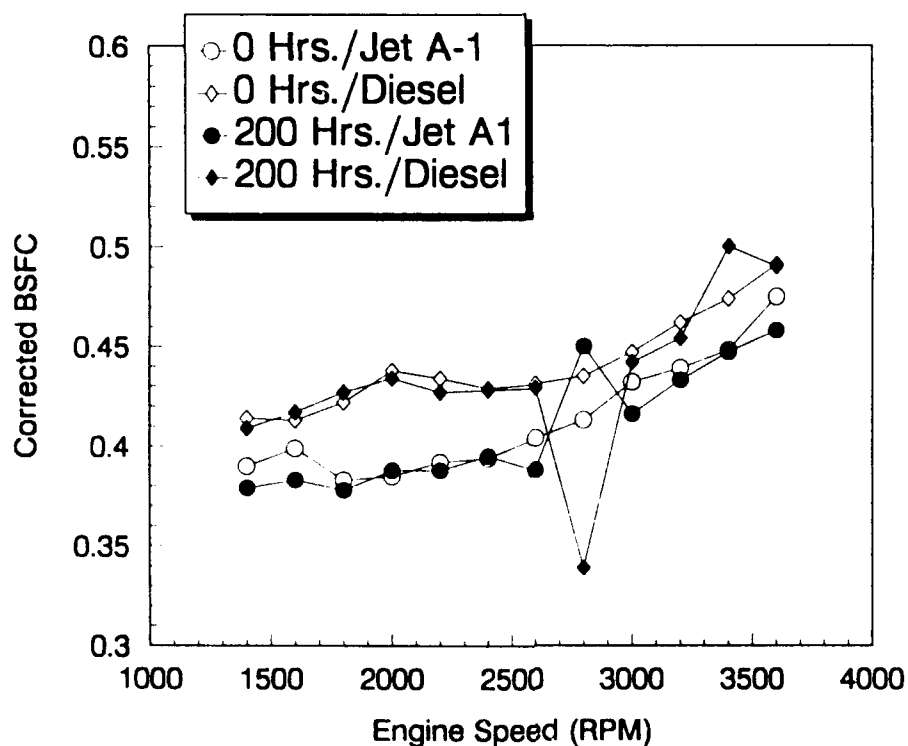
(Arctic pump - tested for 200 hours on diesel)

Figure C-35. Brake specific fuel consumption for Pump No. 8 at STP
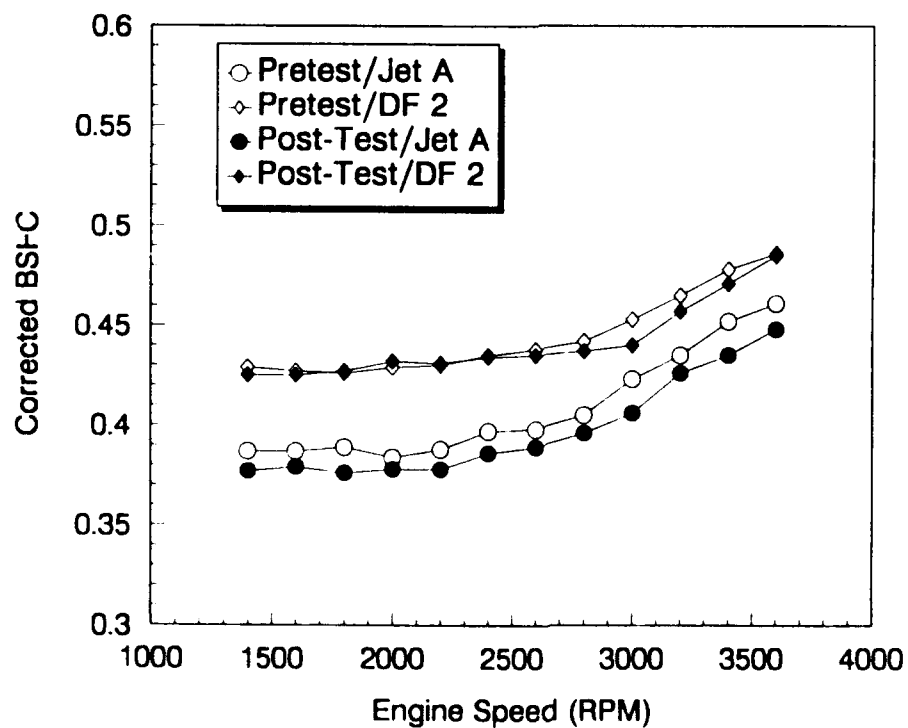
(Reference pump - standard unit, never tested on pump stand)

Figure C-36. Brake specific fuel consumption for Pump No. 9 at STP

APPENDIX D

Fuel Properties

TABLE D-1. U.S. Jet A-1 Turbine Fuel
Batch No.: 90-2B   Date: November 3, 1990
AL-19546-F

Test	Specifications		Result
	Minimum	Maximum	
Gravity, °API	37.0	51.0	49.5
Density, kg/m	0.775	0.840	0.782
Color		Report	+25
Distillation, °C			
Initial Boiling Point			160
5%			165
10%		204	167
20%			169
30%			170
40%			172
50%			175
60%			178
70%			182
80%			187
90%			195
95%			207
End Point		300	218
Recovery, vol%			99.1
Residue, vol%		1.5	0.9
Loss, vol%		1.5	0.0
Sulfur, wt%		0.300	0.002
Doctor Test		Negative	Negative
Freeze Point, °C		-47.0	-59.5
Flash Point, °C	38		44
Viscosity, cSt, at -34°C		8.0	4.2
Viscosity, cSt, at 40°C			1.07
Copper Corrosion		1B	1B
Existent Gum, mg/100 mL		7.0	3.4
Particulates, mg/L		1.0	0.8
Smoke Point, mm	20.0		29.0
WSIM		Report	99
Hydrocarbon Composition, vol%			
Aromatics		20.0	8.1
Olefins		5.0	0.0
Saturates		Report	91.9
Acidity, total (mg KOH/g)		0.015	0.004
Net Heat of Combusion, MJ/kj	42.80		43.54
JFTOT, mm Hg		25.0	0.0
JFTOT, TDR		12	1
Water Reaction		1B	1A
Separation Rating, max.		2.0	0.0
Interfacing Rating, max.		1B	1A

TABLE D-2. Saudi Arabian Jet A-1 Turbine Fuel
Date: February 24, 1990
AL-19367-F

Test	Test Method	Requirements	Jeddah 02-24-90 Test Results
Visual Appearance	Clear, bright, & visually free from solid matter & undissolved water at normal, ambient temperature.		Clear/Bright
Total Acidity	ASTM D 3242	0.015, max	0.0004
Aromatics, vol%	ASTM D 1319	20.0, max	19
Olefins, vol%	ASTM D 1319	5.0, max	0.049
Total Sulfur, wt%	ASTM D 4294 or ASTM D 1266	0.30, max	0.18
Mercaptan Sulfur, wt% or Doctor Test	ASTM D 3227 ASTM D 484	0.003, max Negative	0.0017
Mercaptan Sulfur, ppm	UOP 163	30, max	--
Distillation, °C Initial Boiling Point 10% 20% 50% 90% End Point Residue, vol% Loss, vol%	ASTM D 86 or ASTM D 86 Auto Dist., or ASTM D 2887	Report 204, max Report Report Report 300, max 1.5, max 1.5, max	153 170 176 194 231 249 1.0 0
Flash Point, °C	ASTM D 56 or ASTM D 56 Auto. Flash Tester	38, min	46
Density at 60°F (15°C), kg/L	ASTM D 1298	0.775 to 0.830	0.7875
API Gravity at 60°F (16°C)	ASTM D 1298	39 to 51	47.52
Freeze Point, °C	ASTM D 2386	-50, max	-50
Viscosity, -4°F (-20°C), cSt	ASTM D 445	8.0, max	--
Hydrogen Content, mass%	ASTM D 3701	13.9, min	--
Thermal Value, Net Btu/lb (J/g)	ASTM D 2382, 240 or 1405	18,400 (42,800), min	-- --

TABLE D-3. Reference No. 2 (Cat 1-H) Diesel Fuel
Batch No.: 90-6   Date: September 26, 1990
AL-19561-F

| Test | Specifications | | Result |
	Minimum	Maximum	
Gravity, °API	33.0	35.0	34.1
Distillation, °F (°C)			
Initial Boiling Point			400 (204)
5%			449 (232)
10%			462 (239)
20%			476 (247)
30%			489 (254)
40%			501 (261)
50%	500	530	515 (268)
60%			531 (277)
70%			550 (288)
80%			573 (301)
90%	590	620	611 (322)
95%			642 (339)
End Point	650	690	669 (354)
Recovery, vol%			99.0
Residue, vol%			1.0
Loss, vol%			0.0
Cetane Number	47.0	53.0	50.0
Flash Point, °F (°C)	140 (60)		188 (87)
Cloud Point, °F (°C)			24 (-4)
Pour Point, °F (°C)		20 (-7)	15 (-9)
Water and Sediment, vol%		0.05	<0.05
Sulfur, wt%	0.38	0.42	0.39
Ash, wt%		0.010	0.001
Viscosity, cSt, at 40°C	2.00	4.00	3.00
Copper Corrosion		2	1A
Neutralization No., mg KOH/g		0.15	0.07
Ramsbottom, 10% residium, wt%		0.20	0.10
Net Heat of Combustion, MJ/kj			42.41

APPENDIX E

Measurements Taken During 200-Hour Pump Stand Tests
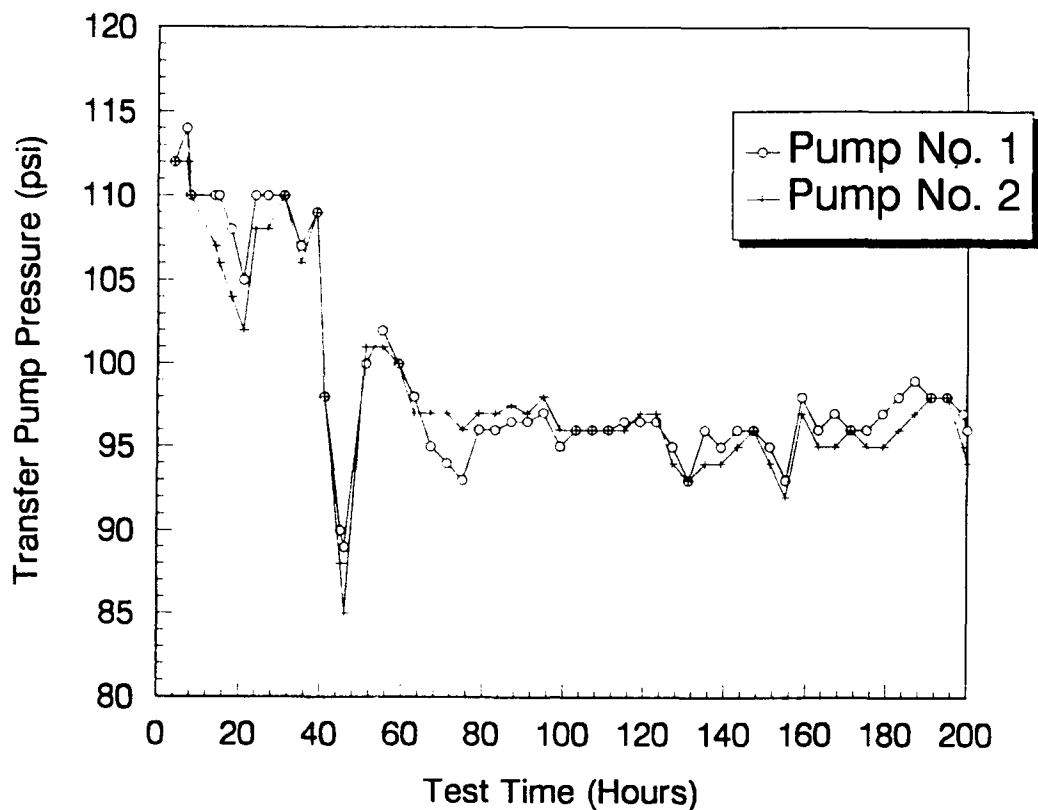
Figure E-1. Transfer pump pressure during 200-hour pump stand test with neat Jet A-1
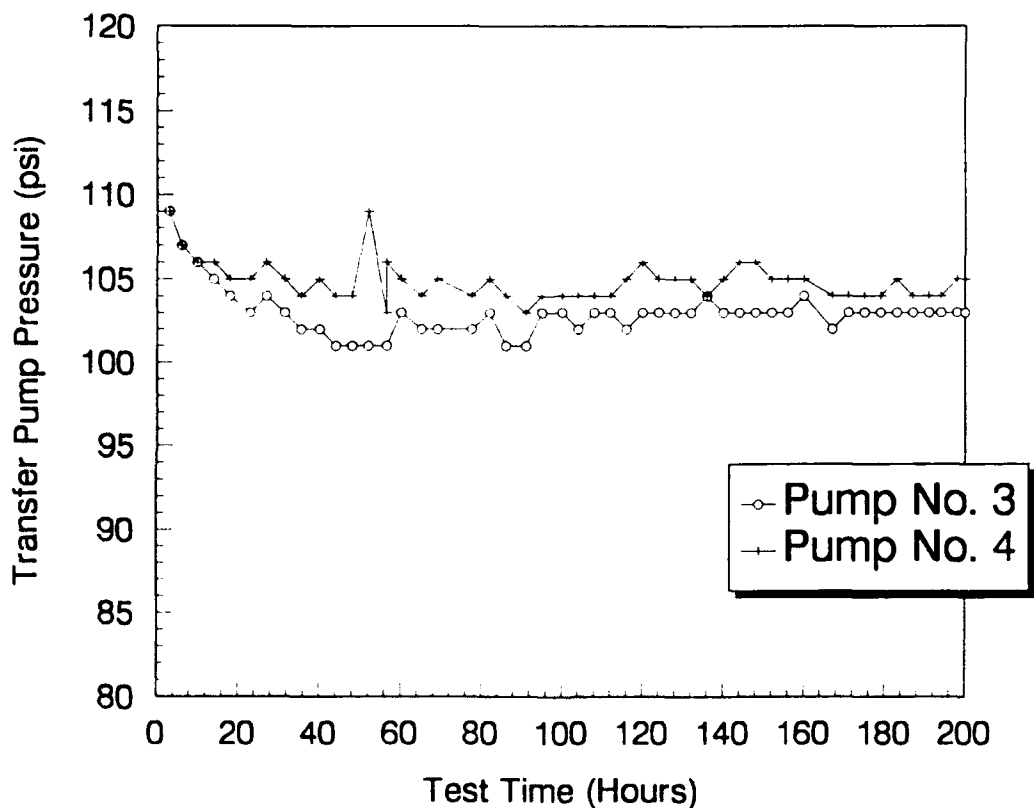
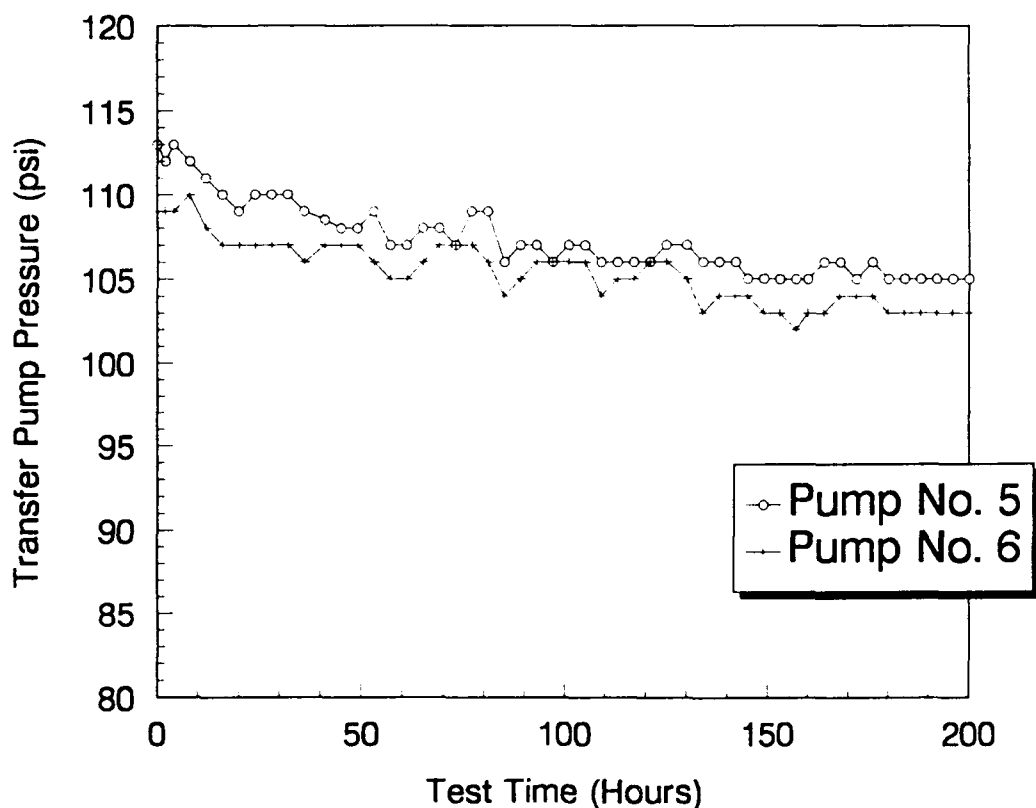**Figure E-2.** Transfer pump pressure during 200-hour pump stand test with Jet A-1 + 15 mg/L DCI-4A

113

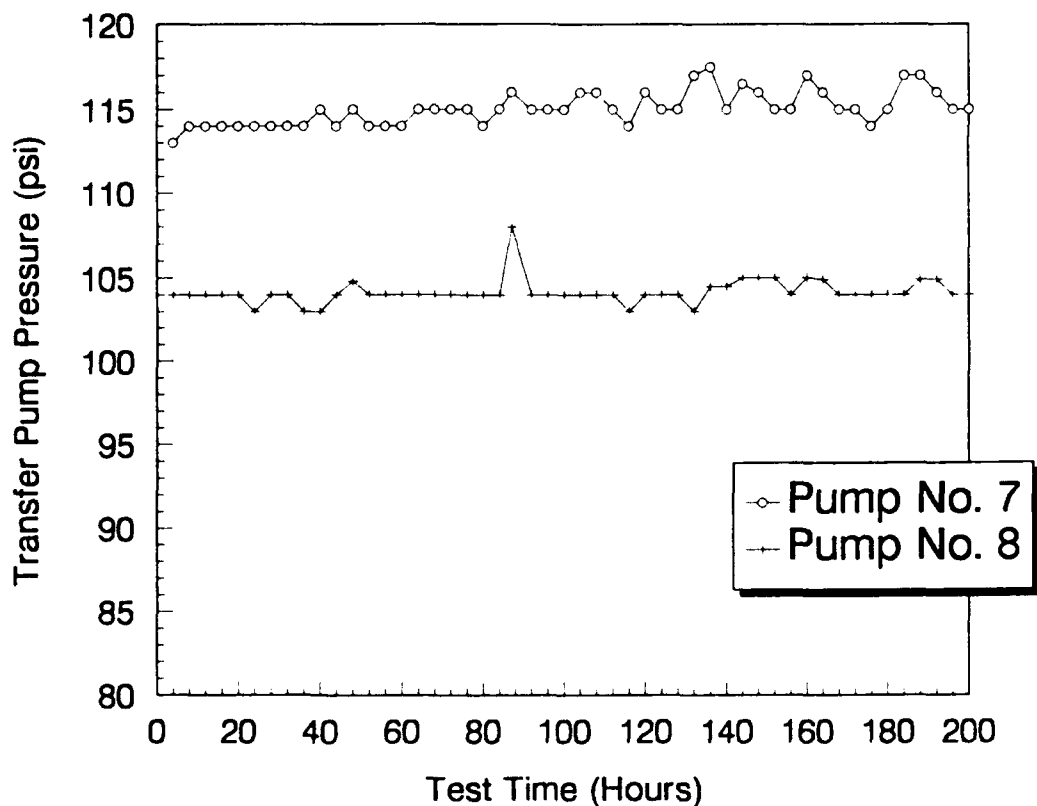**Figure E-3.** Transfer pump pressure during 200-hour pump stand test with Jet A-1 + 227 mg/L BIOBOR-JF and 71 mg/L FOA-15

Figure E-4. Transfer pump pressure during 200-hour pump stand test with diesel fuel

114

APPENDIX F

Wear Measurement and Calculation of Archards Wear Coefficient

Wear Measurements on Transfer Pump Blades

A reciprocating action is formed between the rotor and the transfer pump blade. This action forms a wear scar with a sharp step at the limit of the cycle. The depth of the wear scar was measured at this step using a Talysurf 10 profilometer. Scar depth was assumed to decrease linearly across the contact area, and the wear volume was calculated accordingly. An improved metallurgy is available in the arctic pump vanes and the appropriate indentation hardness was used in calculating Archards wear coefficient. The cumulative sliding distance was calculated for an eccentricity of 4 mm.

Note: Hardness of Arctic Pump Vanes (Hv) = 750

Hardness of Standard Pump Vanes (Hv) = 460

Sliding Distance in 200 Hours = 173 km

Approximate Contact Load = 0.36 kg

TABLE F-1. Wear Measurements on Transfer Pump Blades

	Wear Scar Dimensions			
	Max Depth, $mm \times 10^{-3}$	Final Area, mm^2	Volume, $mm^3 \times 10^{-3}$	Wear Coefficient, $K \times 10^{-9}$
Pump No. 1	4.60	11.6	26.6	67
Pump No. 2	0.73	4.7	1.7	7
Pump No. 3	2.30	4.3	4.9	12
Pump No. 4	1.25	4.7	2.9	12
Pump No. 5	2.60	4.4	5.7	14
Pump No. 6	0.90	4.0	1.8	8
Pump No. 7	2.90	4.9	7.1	17
Pump No. 8	1.20	4.1	2.4	10

Wear Measurements on Governor Thrust Washer

This is a wear ring formed by the action of the six governor weights on the governor thrust washer. The average depth of the wear scar was measured using a Talysurf profilometer and was found to be approximately constant around the complete circumference. The applied load was derived from the thrust required to counteract centripetal force on each governor weight at 1800 rpm. The indentation hardness of both the arctic and standard components were similar.

Note: Hardness of Both Arctic and Standard Parts (Hv) = 670

Cumulative Sliding Distance	= 388 km
Approximate Contact Load	= 2 kg
Circumference of Contact	= 83.2 mm

TABLE F-2. Wear Measurements on Governor Thrust Washer

	Scar Depth, $mm \times 10^{-3}$	Scar Width, mm	Volume, $mm^3 \times 10^{-3}$	Wear Coefficient, $K \times 10^{-9}$
Pump No. 1	1.6	2.8	372	107
Pump No. 2	1.1	3.0	274	79
Pump No. 3	0.7	2.5	145	41
Pump No. 4	1.1	2.1	192	55
Pump No. 5	0.3	2.0	50	14
Pump No. 6	0.4	2.8	93	26
Pump No. 7	0	--	--	--
Pump No. 8	0.6	2.7	135	39

Wear Measurements on Governor Weights

The six governor weights mate with the thrust washer described in the previous section. A narrow wear scar is formed across the 12-mm width of each weight. The wear scar is triangular in cross section and was measured using a Talysurf surface profilometer. The tabulated results are the average derived from three individual traces along each wear scar.

Note: Approximate Contact Load = 2 kg

Vickers Hardness   = 410

TABLE F-3. Wear Measurements on Governor Weights

| | Wear Scar Dimensions | | | |
	Max Depth, $mm \times 10^{-3}$	Width, mm	Volume, $mm^3 \times 10^{-3}$	Wear Coefficient, $K \times 10^{-9}$
Pump No. 1	68	1.0	408	15
Pump No. 2	50	0.90	264	10
Pump No. 3	36	0.60	132	5
Pump No. 4	28	0.62	96	4
Pump No. 5	15	0.31	36	1
Pump No. 6	23	0.50	72	3
Pump No. 7	18	0.33	36	1
Pump No. 8	15	0.34	36	1

Wear Measurements on Cam Roller Shoe

This wear scar is formed by a counterformal contact between the cam roller shoe and the pumping plunger. Little relative motion should occur other than due to vibration. The approximate sliding distance was calculated by assuming that the shoe vibrated once each time the roller strikes the cam ring. The amplitude of the movement is equal to the tolerance between the shoe and the slot in the hydraulic head after testing. The wear volume was approximated by assuming that pumping plunger is cone-shaped close to the area of contact. The tabulated result is an average value derived from both shoes on each pump. It should be noted that considerable variation existed between the two shoes on many of the pumps.

Note: Vickers Hardness   = 730

       Approximate Sliding Distance   = 8.5 km

       Total Contact Load During Injection = 57 kg

TABLE F-4. Wear Measurements on Cam Roller Shoe

	Scar Depth, $mm \times 10^{-3}$	Scar Diameter, mm	Volume, $mm^3 \times 10^{-3}$	Wear Coefficient, $K \times 10^{-9}$
Pump No. 1	54	5.8	470	236
Pump No. 2	120	6.1	1160	582
Pump No. 3	8	3.05	19	9
Pump No. 4	15	2.75	30	15
Pump No. 5	7	2.25	9	5
Pump No. 6	28	3.25	77	38
Pump No. 7	17	2.95	38	19
Pump No. 8	19	2.21	24	12

Wear Measurements on Rotor Retainers

The wear scar is a circular ring and was formed by the motion of the pump rotor. The depth of the wear scar was measured using the Talysurf profilometer and the tabulated result is the average of four individual measurements. The depth of the wear scar was relatively constant in each measurement. The radial width of the wear scar was normally 2 mm, corresponding to the overlap between the pump rotor and the washers. However, only a portion of the apparent contact area was worn in the two pumps that operated with diesel fuel. The applied load was approximated from the end loading on the shaft due to the transfer pump pressure and opposing reaction force from the governor weights. End loading from the drive shaft will also be a contributing factor.

Note: Sliding Distance   = 1425 km

   Approximate Applied Load = 4 kg

   Vickers Hardness   = 560

   Average Circumference   = 66 mm

TABLE F-5. Wear Measurements on Rotor Retainers

	Max Depth, $mm \times 10^{-3}$	Width, mm	Volume, $mm^3 \times 10^{-3}$	Wear Coefficient, $K \times 10^{-9}$
Pump No. 1	16	2	2112	69
Pump No. 2	25	2	3300	107
Pump No. 3	9	2	1188	38
Pump No. 4	9	2	1188	38
Pump No. 5	4	2	528	17
Pump No. 6	7	2	924	30
Pump No. 7	2	0.75	99	3
Pump No. 8	2	1	132	4

Wear Measurements on Drive Tang

A wedge-shaped wear scar is formed where the drive tang mates with the pump rotor. The maximum wear scar depth (at the deepest portion of the wedge) was measured using a micrometer and compared with unworn portions of the drive tang. The depth of the wear scar was then assumed to decrease linearly to zero at the opposite edge of the scar. The tabulated value is an average calculated from measurements taken from each side of the drive tang.

A single deviation of 0.1 mm is assumed to occur at the drive tang for each injection cycle, i.e., eight times per revolution. The contact load is calculated for an average radius of 0.25 inches at a torque of 250-inch pounds.*

Note: Approximate Applied Load = 250 kg

Sliding Distance = 17.2 km

Vickers Hardness = 650

TABLE F-6. Wear Measurements on Drive Tang

	Max Depth, $mm \times 10^{-3}$	Cont. Area, mm^2	Volume, $mm^3 \times 10^{-3}$	Wear Coefficient, $K \times 10^{-9}$
Pump No. 1	314	70	11000	503
Pump No. 2	21	4	43	2
Pump No. 3	21	14	147	7
Pump No. 4	7	8	28	1.5
Pump No. 5	100	31	3100	156
Pump No. 6	11	7	38	2
Pump No. 7	29	7	101	5
Pump No. 8	5	6	15	8

* Hess, T. and Salzgeber, D., "The Stanadyne DB2 Distributor Pump for Medium Duty Diesels," Off-Highway Vehicle Meeting and Exposition MECCA, Milwaukee, WI, 10-13 September 1979.

Wear Measurements on Drive Slot

The drive slot mates with the drive tang, the wear measurements for which are described in TABLE F-7. The maximum depth of each wear scar was measured using a Talysurf surface profilometer. The tabulated result is an average value derived from readings obtained on both sides of the slot. The contact area in each instance was taken from TABLE F-6. The depth of the wear scar was then assumed to decrease linearly to zero at the opposite edge of the scar and the wear volume calculated accordingly.

TABLE F-7. Wear Measurements on Drive Slot

	Max Depth, $mm \times 10^{-3}$	Cont. Area, mm^2	Volume, $mm^3 \times 10^{-3}$	Wear Coefficient, $K \times 10^{-9}$
Pump No. 1	401	70	14000	705
Pump No. 2	24	4	48	2
Pump No. 3	16	14	112	6
Pump No. ~	15	8	60	3
Pump No. 5	32	31	496	25
Pump No. 6	17	7	59	3
Pump No. 7	9	7	31	2
Pump No. 8	12	6	36	2

DISTRIBUTION LIST

Department of Defense

DEFENSE TECHNICAL INFORMATION CTR
CAMERON STATION 12
ALEXANDRIA VA 22314

DEPT OF DEFENSE
OASD/P&L
ATTN: L/EP 1
WASHINGTON DC 20301-8000

DEPT OF DEFENSE
OASD/R&E
ATTN: DUSDRE (RAT) (DR DIX) 1
WASHINGTON DC 20301-8000

DEFENSE ADVANCED RES PROJECTS AGY
DEFENSE SCIENCES OFFICE 1
1400 WILSON BLVD
ARLINGTON VA 22209

CDR
DEFENSE FUEL SPLY CTR
ATTN: DFSC-Q (MR MARTIN) 1
CAMERON STATION
ALEXANDRIA VA 22304-6160

DEFENSE STNDZ OFFICE
ATTN: DR S MILLER 1
5203 LEESBURG PIKE, SUITE 1403
FALLS CHURCH VA 22041

CDR
DEFENSE LOGISTICS AGY
ATTN: DLA-SE 1
CAMERON STATION
ALEXANDRIA VA 22304-6179

Department of the Army

CDR
US ARMY BELVOIR RESEARCH,
    DEVELOPMENT AND ENGINEERING CTR
ATTN: STRBE-F 1
        STRBE-FL (MR LEPERA) 10
        STRBE-FG 1
        STRBE-BT 2
        STRBE-TQ 1
        AMSTR-ABCE (MR COOK) 1
FORT BELVOIR VA 22060-5606

HQ, DEPT OF ARMY
ATTN: DALO-TSE (COL HOLLEY) 1
        SARD-TT (MR APPEL) 1
        SARD-TC (DR CHURCH) 1
WASHINGTON DC 20310-0561

CDR
US ARMY MATERIEL COMMAND
ATTN: AMCDE-SS 1
        AMCLG-SS (MR CUPURDIJA) 1
5001 EISENHOWER AVE
ALEXANDRIA VA 22333-0001

DIRECTOR
AVIATION APPLIED TECH DIR
US ARMY R&T ACTIVITY (AVSCOM)
ATTN: SAVRT-TY-ATP (MR MORROW) 1
FORT EUSTIS VA 23604-5577

CDR
US ARMY TANK-AUTOMOTIVE COMMAND
ATTN: AMSTA-RG (DR McCLELLAND) 1
        AMSTA-RGD 1
        AMSTA-RGP (MR HNATCZUK) 1
        AMSTA-RGR (DR BRYZIK) 1
        AMSTA-MTC (MR GAGLIO) 1
        AMSTA-MT (MR GLADIEUX) 1
        AMSTA-MC (MR POTTER) 1
        AMSTA-MV (MR ROBERTS) 1
WARREN MI 48397-5000

DIRECTOR
US ARMY MATERIEL SYSTEMS ANALYSIS
    ACTIVITY
ATTN: AMXSY-CM (MR NIEMEYER) 1
ABERDEEN PROVING GROUND MD
21005-5006

CDR
THEATER ARMY MATERIAL MGMT
    CENTER (200TH)-DPGM
DIRECTORATE FOR PETROL MGMT
ATTN: AEAGD-MMC-PT-Q 1
APO NY 09052

DOD PROJ MGR, MOBILE ELECTRIC POWER
US ARMY TROOP SUPPORT COMMAND
ATTN: AMCPM-MEP-TM (COL BECKER)   2
7500 BACKLICK ROAD
SPRINGFIELD VA 22150

CDR
US ARMY PETROLEUM CENTER
ATTN: STRGP·F (MR ASHBROOK)   1
    STRGP-FE. BLDG 85-3
      (MR GARY SMITH)   1
    STRGP-FT   1
NEW CUMBERLAND PA 17070-5008

CDR
US ARMY FORCES COMMAND
ATTN: FCSJ-TRS   1
FORT MCPHERSON GA 30330-6000

CDR. US ARMY TROOP SUPPORT COMMAND
ATTN: AMSTR-M   1
    AMSTR-S   1
    AMSTR-MEB (MR BRIGHT)   1
4300 GOODFELLOW BLVD
ST LOUIS MO 63120-1798

CDR
US ARMY LABORATORY COMMAND
ATTN: AMSLC-TP-PB (MR GAUL)   1
ADELPHI MD 20783-1145

CDR
US ARMY TANK-AUTOMOTIVE CMD
PROGM EXEC OFF, CLOSE COMBAT
APEO SYSTEMS. ATTN: AMCPEO-CCV-S   1
PM ABRAMS, ATTN: AMCPM-ABMS   1
PM BFVS. ATTN: AMCPM-BFVS   1
PM 113 FOV. ATTN: AMCPM-M113   1
PM M9 ACE. ATTN: AMCPM-MA   1
PM IMP REC VEH. ATTN: AMCPM-IRV   1
WARREN MI 48397-5000

CDR
US ARMY RESEARCH OFFICE
ATTN: SLCRO-EG (DR MANN)   1
RSCH TRIANGLE PARK NC 27709-2211

CDR
US ARMY LEA
ATTN: LOEA-PL (MR LeVAN)   1
NEW CUMBERLAND ARMY DEPOT
NEW CUMBERLAND PA 17070

CDR
US ARMY TANK-AUTOMOTIVE CMD
PROGM EXEC OFF, COMBAT SUPPORT
PM LIGHT TACTICAL VEHICLES,
   ATTN: AMCPM-TVL   3
PM MEDIUM TACTICAL VEHICLES,
   ATTN: AMCPM-TVM   1
PM HEAVY TACTICAL VEHICLES,
   ATTN: AMCPM-TVH   1
WARREN MI 48397-5000

PETROLEUM FIELD OFFICE WEST.
  MR. ECCLESTON   1
DDRW, BLDG 247, TRACEY LOCATION
P O BOX 96001
STOCKTON CA 95296-0960

CDR
US ARMY SAFETY CENTER
ATTN: CSSC-S   1
FORT RUCKER AL 36362

CDR
US ARMY ORDNANCE CENTER & SCHOOL
ATTN: ATSL-CD-CS   1
ABERDEEN PROVING GROUND MD
21005-5006

CDR
US ARMY ENGINEER SCHOOL
ATTN: ATSE-CD   1
FORT LEONARD WOOD MO 65473-5000

HQ, US ARMY T&E COMMAND
ATTN: AMSTE-TE-T (MR RITONDO)   1
ABERDEEN PROVING GROUND MD
21005-5006

HQ, US ARMY ARMOR CENTER
ATTN: ATSB-CD-ML   1
    ATSB-TSM-T   1
FORT KNOX KY 40121

CDR
US ARMY EUROPE & SEVENTH ARMY
ATTN: AEAGD-TE (MAJ CURLEY)   1
APO NEW YORK 09403

CDR
US ARMY QUARTERMASTER SCHOOL
ATTN: ATSM-CDM   1
    ATSM-PWD (LTC GIBBONS)   1
FORT LEE VA 23801

PROJECT MANAGER
PETROLEUM & WATER LOGISTICS
ATTN: AMCPM-PWL   1
4300 GOODFELLOW BLVD
ST LOUIS MO 63120-1798

HQ
US ARMY TRAINING & DOCTRINE CMD
ATTN: ATCD-SL   1
FORT MONROE VA 23651-5000

CDR
US ARMY TRANSPORTATION SCHOOL
ATTN: ATSP-CD-MS   1
FORT EUSTIS VA 23604-5000

CDR
US ARMY INFANTRY SCHOOL
ATTN: ATSH-CD-MS-M   1
FORT BENNING GA 31905-5400

HQ, 172D INFANTRY BDE (ALASKA)
ATTN: AFZT-DI-L   1
DIR OF IND OPER
FORT RICHARDSON AK 99505

CDR
101ST AIRBORNE DIV (AASLT)
ATTN: AFZB-KE-J   1
        AFSB-KE-DMMC   1
FORT CAMPBELL KY 42223

CDR
US ARMY COMBINED ARMS & SUPPT CMD
    AND FT LEE
ATTN: ATCL-CD   1
        ATCL-MS   1
FORT LEE VA 23801-6000

CDR
US ARMY TANK-AUTOMOTIVE CMD
PROD MGR
CCE/SMHE
ATTN: AMCPM-TVC   1
WARREN MI 48397-5000

HQ, EUROPEAN CMD
ATTN: J4/7-LJPO   1
VAIHINGEN, GE
APO NEW YORK 09128

Department of the Navy

CDR
NAVAL AIR PROPULSION CENTER
ATTN: PE-33 (MR D'ORAZIO)   1
P O BOX 7176
TRENTON NJ 08828-0176

CDR
DAVID TAYLOR RESEARCH CENTER
ATTN: CODE 2759 (MR STRUCKO)   1
ANNAPOLIS MD 21402-5067

PROJ MGR, M60 TANK DEVELOPMENT
ATTN: USMC-LNO   1
US ARMY TANK-AUTOMOTIVE COMMAND
    (TACOM)
WARREN MI 48397-5000

CDR
NAVAL PETROLEUM OFFICE
ATTN: CODE 40 (MR LONG)   1
CAMERON STATION
ALEXANDRIA VA 22304-6180

OFFICE OF CHIEF OF NAVAL RESEARCH
ATTN: OCNR-126 (DR ROBERTS)   1
ARLINGTON VA 22217-5000

DEPARTMENT OF THE NAVY
HQ, US MARINE CORPS
ATTN: LMM/2 (MAJ PATTERSON)   1
WASHINGTON DC 20380

CDR
NAVAL AIR SYSTEMS COMMAND
ATTN: CODE 53632F (MR MEARNS)   1
WASHINGTON DC 20361-5360

DEPUTY CG
USMC RD&A COMMAND
ATTN: PM GND WEAPONS (CB6T),
        LTC VARELLA   1
        SSEA (LTC PHILLIPS)   1
QUANTICO VA 22134-5080

CG
USMC RD&A CMD
ATTN: CODE SSCMT   1
WASHINGTON DC 20380-0001

Department of the Air Force

CDR
US AIR FORCE WRIGHT AERO LAB
ATTN: POSF (MR DELANEY)   1
WRIGHT-PATTERSON AFB OH 45433-6563

CDR
SAN ANTONIO AIR LOGISTICS CTR
ATTN: SAALC/SFT (MR MAKRIS)   1
         SAALC/LDPE (MR ELLIOT)   1
KELLY AIR FORCE BASE TX 78241

CDR
WARNER ROBINS AIR LOGISTIC CTR
ATTN: WRALC/LVR-1 (MR PERAZZOLA)   1
ROBINS AFB GA 31098

HQ US AIR FORCE
ATTN: LEYSF   1
WASHINGTON DC 20330

CDR
DET 29
ATTN: SA-ALC/SFM   1
CAMERON STATION
ALEXANDRIA VA 22304-6179

Other Organizations

NATIONAL AERONAUTICS AND SPACE
     ADMINISTRATION   1
LEWIS RESEARCH CENTER
CLEVELAND OH 44135

US DEPARTMENT OF ENERGY
ATTN: MR JOHN RUSSELL   1
MAIL CODE CE-151
FORRESTAL BLDG
1000 INDEPENDENCE AVE. SW
WASHINGTON DC 20585

ENVIRONMENTAL PROTECTION AGY
AIR POLLUTION CONTROL   1
2565 PLYMOUTH ROAD
ANN ARBOR MI 48105

MAJOR J P XHAUFLAIR   1
PHQ/JSO-G/POL
ETAT-MAJOR GENERAL
QUARTIER REINE ELISABETH
RUE D'EVERE 1
B-1140 BRUSSELS BELGIUM

PROFESSOR M CAMPINNE   1
ECOLE ROYAL MILITAIRE
LABORATOIRE
MECANIQUE - TRANSPORT
AVENUE DE LA RENAISSANCE 30
B-1040 BRUSSELS BELGIUM

CAPT M P TURINGIA   1
NDHQ/DCGEM 3-2-2
MGEN GEORGE R PEARKES BUILDING
OTTAWA K1A OK2 CANADA

LT COL M HOLTZE   1
DANISH ARMY MATERIAL COMMAND
ARSENALVEJ 55
DK-9800 HJORRING DENMARK

MR K LAURIDSEN   1
POL-AFDELING
GADHOLTVEJ 11
DK-9900 FREDERIKSHAVN DENMARK

COLONEL Y CABANEL   1
DIRECTION REGIONALE DU SERVICE
DES ESSENCES DES ARMEES
6 RUE DU DOCTEUR ACQUAVIVA
F-13998 MARSEILLES - ARMEES FRANCE

COLONEL BERGERET   1
LABORATOIRE CENTRALE DU SERVICE
DES ESSENCES DES ARMEES
280 CHEMIN DE SAINT MARTHE
F-13998 MARSEILLES - ARMEES FRANCE

MR I P RIO   1
DIRECTION CENTRALE DU SERVICE
DES ESSENCES DES ARMEES
FORTE DE VANNES
27 BOULEVARD DE STALINGRAD
BP 163
F-92240 MALAKOFF FRANCE

CDT M CAMBEFORT   1
LABORATOIRE DU SERVICE
DES ESSENCES DES ARMEES
280 CHEMIN SAINT MARTHE
F-13998 MARSEILLES - ARMEES FRANCE

MR W H KNECHT   1
BUNDESAMT FUR WEHRTECHNIK
UND BESCHAFFUNG - BAI6
KONRAD ADENAUER UFER 2-6
POB 67
D-5400 KOBLENZ GERMANY

LT COL E A SCHIESER   1
GERMAN ARMY MATERIAL COMMAND
VC-530
HAUPTSTRASSE 129
D-5483 BAD NEUENAHR-AHRWEILER
GERMANY

LT COL N DIAMANDIS   1
HELLENIC ARMY GENERAL STAFF
SUPPLY AND TRANSPORT SERVICE
STRATOPEDO PAPAGOU
HOLARGOS ATHENS GREECE

MR N SAMANIDIS   1
HELLENIC AIR FORCE
GENERAL STAFF BRANCH C-5
HOLARGOS ATHENS GREECE

LT COL A GUCCIARDINO   1
CENTRO TECNICO MOTORIZZAZIONE
I-00010 MONTELIBRETTI (ROMA)
ITALY

CAPT E LUMACA   1
CENTRO TECNICO MOTORIZZAZIONE
I-00010 MONTELIBRETTI (ROMA)
ITALY

MR G J R VAN DEN BOVENKAMP   1
DIRECTIE MATERIEEL KL
BVC/SECTIE BOSCO
VAN DER BURCHLAAN 31
POSTBUS 90822
NL-2509 LV 'S-GRAVENHAGE
NETHERLANDS

MR E HORVE   1
ARMY MATERIAL COMMAND HFK V
OSLO MIL/LOREN
N-0018 OSLO 1 NORWAY

LT COL D BUDDING   1
DIRECTIE MATERIEEL KL
BVC/SECTIE BOSCO
VAN DER BURCHLAAN 31
POSTBUS 90822
NL-2509 LV 'S-GRAVENHAGE
NETHERLANDS

LT COL N C S VROOM   1
NL MEMBER ARMY BOARD MAS
ARMY STAFF BLDG 32 RM 904
POSTBUS 90822
NL-2509 LV 'S-GRAVENHAGE
NETHERLANDS

MR P A OPPEGAARD   1
MATERIAL COMMAND
POB 10
N-2007 KJELLER NORWAY

MAJOR J A ESTEVES DA SILVA   1
DIRECCAO DO SERVICO DE INTENDENCIA
TRAVESSA ST ANTONIO DA
SE CATEDRAL NO 21
P-1100 LISBON PORTUGAL

CAPT G VIEIRA   1
DIRECCAO DO SERVICO DE MATERIAL
AV INFANTE SANTO 49
P-1300 LISBON PORTUGAL

MAJOR M ENGO NOGUES   1
CUARTEL GENERAL DEL EJERCITO
DIAM/LABCAMVE
PRIM 10 MADRID SPAIN

CAPT H ORUK   1
GENELKURMAY BASKANLIGI
ANDLASMALAR DAIRE BASKANLIGI
MAS S ANKARA TURKEY

MR R G GOMES   1
200TH TAMMC
DIRECTORATE OF BULK FUELS
KRENZBURG KASERNE
D-ZWIEBRUEKEN
APO NY 09052-5356

MAJ R D JANKE   1
PETROLEUM STAFF OFFICER
US MISSION TO NATO - NATO HQ
B-1110 BRUSSELS
APO NY 09667-5029

LT COL T R MURRAY   1
HQ US EUROPEAN COMMAND
ATTN: ECJ4-LUPO, BUILDING 2304
PATCH KASERNE
D-7000 STUTTGART 80
APO NY 09128

MR A D MARCHIOLI   1
CHAIRMAN AC/112 (WG4)
INFRASTRUCTURE LOGISTICS AND
    CIVIL EMERGENCY PLANNING DIVISION
NATO HQ
B-1110 BRUSSELS BELGIUM

MR K COWEY   1
PETROLEUM LABORATORY
DQA/TS (F&L) - BUILDING E23
ROYAL ARSENAL EAST
WOOLWICH SE18 6TD
UNITED KINGDOM

MR R F ROBERTSON   1
PETROLEUM STAFF OFFICER
INFRASTRUCTURE LOGISTICS AND
    CIVIL EMERGENCY PLANNING DIVISION
NATO HQ
B-1110 BRUSSELS BELGIUM

LT COL MIKE ROBERTS (CHAIRMAN)   1
ORD 2D
LOGISTIC EXECUTIVE (ARMY)
PORTWAY - MONXTON ROAD
ANDOVER HANTS SP11 8HT
UNITED KINGDOM

SECRETARY AC/112 (WG4)   1
INFRASTRUCTURE LOGISTICS AND
    CIVIL EMERGENCY PLANNING DIVISION
NATO HQ
B-1110 BRUSSELS BELGIUM

MAJOR P GOSLING, SECRETARY   1
FUELS AND LUBRICANTS WORKING
    PARTY MAS ARMY BOARD
NATO HQ
B-1110 BRUSSELS BELGIUM

MR A B PEACOCK (SECRETARY)   1
ORD 2D
LOGISTIC EXECUTIVE (ARMY)
PORTWAY - MONXTON ROAD
ANDOVER HANTS SP11 8HT
UNITED KINGDOM

MR N H J CHORLEY   1
CENTRAL EUROPE OPERATING AGENCY

PROF R S FLETCHER   1
CRANFIELD INSTITUTE OF TECHNOLOGY
CRANFIELD
BEDFORDSHORE MK43 OAL
UNITED KINGDOM

BP 552
11 BIS RUE DE GENERAL PERSHING
F-78005 VERSAILLES CEDEX FRANCE